*Democratic and Popular Republic of Algeria*

*Ministry of Higher Education and Scientific Research*

*University of Echahid Hamma Lakhdar-El OUED*

*Faculty of Natural and Life Sciences*

*Department of Cellular and Molecular Biology*

# *END OF STUDY Thesis*

***In order to obtaining the Academic Master's degree***

***Subject: Biological Sciences***

***Specialty: Applied biochemistry***

# *THEME*

***Exploration of Diverse Biological Activities in Medicinal Plants: In Vitro Investigations, ADMET Prediction, Molecular Docking Analysis, and Molecular Dynamics Simulation for Varied Therapeutic Properties.***

**Presented by:**

- ***Aissaoui Ichraak***
- ***Leddai Belkis***
- ***Mereghni Sacia***

**Supervisor:**

| | | | |
|---|---|---|---|
| **Chairperson** | ***Dr.Ghania Ahmed*** | **M.A.A.** | ***University of El Oued*** |
| **Supervisor:** | ***Dr. LANEZ Elhafnaoui*** | ***M.C.A,*** | ***University of El Oued*** |
| **Examiner:** | ***Dr.Kiram Abderrazak*** | ***M.A.A,*** | ***University of El Oued*** |

***Academic Year: 2023 / 2024***

# Acknowledgment and Appreciation

*And their final prayer is, 'Praise be to Allah, Lord of the Worlds.' Praise be to Allah abundantly, blessedly, and wholesomely for His guidance and facilitation in completing this work after much effort and hardship. Moreover:*

*We extend our sincere thanks to* ***the faculty lab at the college of technology*** *for hosting us, and specifically to* ***Pr. LANEZ TOUHAMI****, the director of the research lab at University of El Oued, for providing us with all the necessary means and equipment and for welcoming us into his lab .*

*We also extend our profound thanks and gratitude to our esteemed supervisor* ***Dr. LANEZ ELHAFNAOUI****, for all the support and assistance he provided in our thesis. Your help has had a significant impact on achieving the success we are proud of today. We greatly appreciate your dedication and commitment*

*We also thank laboratory engineer* ***TELIBA ALI and ADAIKA Aicha****, for their and patience with us, and for their endless advice throughout the completing of this work. May God reward them on our behalf?*

*And we must not forget the honorable* ***Pr. BEN AMOR MOHAMMED LARBI****, who had a significant hand and merit in our work, and his constant smile—may God preserve it for him. Thank you.*

*To the doctoral student* ***Djarallah Marwa****, who was a great help to us and never hesitated for a moment to assist us. May God bless her and guide her to what He loves and is pleased with.*

# إهداء

*من قال أنا لها "نالها"*

*لم تكن الرحلة قصيرة ولا ينبغي لها أن تكون،*

*لم يكن الحلم قريبا ولا الطريق كان محفوفا بالتسهيلات،*

*لكنني فعلتها ونلتها.*

*الحمدلله حبا وشكرا وامتنانا، الذي بفضله ها أنا اليوم أنظر إلى حلما طال إنتظاره وقد أصبح واقعا أفتخر به.*

*إلى ملاكي الطاهر، وقوتي بعد الله، داعمتي الأولى والأبدية"أمي غاليتي "*

*أهديك هذا الإنجاز الذي لولا تضحياتك لما كان له وجود، ممتنة لأن الله قد اصطفاك لي من البشر أما يا خير سند وعوض .إلى من دعمني بلا حدود وأعطاني بلا مقابل*

*"أبي مسعود"*

*إلى من قيل فيهم :{ سَنَشُدُّ عَضُدَكَ بِأَخِيكَ } إلى من مد يده دون كلل ولا ملل وقت ضعفي*

*" أخي شمس الدين" أدامك الله ضلعا ثابتا لي وإلى إخوتي" ياسر و أسامة"*

*إلى من تذكرني بقوتي وتقف خلفي كظلي "أختي الصغرى شيماء "*

*كما أتوجه بخالص الشكر والتقدير إلى مشرفي الفاضل {العانز الحفناوي } على جهوده الكبيرة*

*والمتفانية في توجيهي ومساعدتي خلال عملية إعداد مذكرة البحث إذ أن توجيهاتك القيمة ونصائحك السديدة كانت لي عوناً كبيراً في فهم الموضوع وتوجيهي نحو الطريق الصحيح لإتمام البحث بنجاح، أدرك تماماً أن هذا الإنجاز لم يكن ليتحقق بدون دعمك وتوجيهاتك القيمة، فشكراً لك من القلب على تفانيك واهتمامك في إرشادي خلال هذه الرحلة البحثية.*

*"أنا لا أنسى من جعلني يوما أضيء في عتمتي، أو أضحك بالرغم من سُحبِ وجهي. حتى ولو فرقتنا الأيام والأماكن؛ فالقلوب شواهد لا تنسى يدًا مُدّت لها حين شارفت على سقوطها من الحافة"*

*ممتنة للطيبين الذين أوقعوا بقلبي أثراً يُروى بالدعوات والذِكر الحَسن*

*ممتنة لمن حل فأمطر فأزهر فأسكن بخافقي جِناناً...*

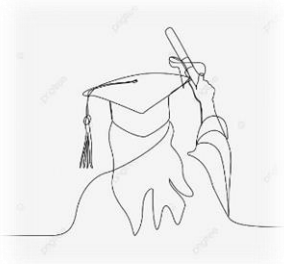

***Leddai Belkis***

# إهداء

*الحمدلله حبا وشكراً وامتنانا على البدء والختام*

*{ وَآخِرُ دَعْوَاهُمْ أَنِ الْحَمْدُ لِلَّهِ رَبِّ الْعَالَمِينَ }*

*أرى مرحلة التخرج قد شارفت على الإنتهاء بالفعل، بعد تعب ومشقة دامت*

*خمسة سنوات في سبيل الحلم والعلم حلمت في طياتها أمنيات الليالي، وأصبح عنائي*

*اليوم للعين قرة، ها انا اليوم أقف على عتبة التخرج أقطف ثمار تعبي وأرفع قبعتي بكل فخر، فاللهم لك الحمد قبل أن ترضى ولك الحمد إذا رضيت ولك الحمد بعد الرضاء.*

*وبكل حب أهدي ثمرة نجاحي وتخرجي:*

*إلى الذي زين إسمي بأجمل الألقاب، ومن دعمني بلا حدود وأعطاني بلا مقابل إلى من علمني أن الدنيا كفاح وسلاحها العلم والمعرفة : " والدي عيسى عيساوي "*

*إلى من جعل الله الجنة تحت أقدامها، وإحتضنتني قلبها قبل يديها وسهلت لي الشدائد بدعائها، إلى القلب الحنون والشمعة التي كانت لي في الليالي المظلمات سر قوتي ونجاحي وجنتي،و داعتمي الأولى في مسيرتي*

*وسندتي وقوتي وملاذي بعد الله فخري وإعتزازي: " والدتي "*

*كما أتقدم بأعمق الشكر والتقدير لأستاذي المشرف {العانز الحفناوي} على الجهود الكبيرة التي بذلتها كمشرف على مذكرتي*

*لقد كان لطيفًا جدًا العمل تحت إشرافك الفعّال والملهم ، شكرًا لك على الإرشاد القيم والملاحظات البناءة التي ساهمت في تطوير مذكرتي وجعلها أفضل. تقديري لجهودك اللافتة وتفانيك في دعمي خلال هذه الرحلة.*

*وأخيرا من قال لها أنا لها "نالها" وأنا لها إن أبت رغما عنها أَتَيْتُ بها، ماكنت لأفعل لولا توفيق من الله، هاهو اليوم العظيم هنا اليوم الذي أجريت سنوات دراستي حالمة بها حتى توالت بمنه وكرمه لفرحة التمام، فالحمدلله الذي ما تيقنت*

*به خيراً وأملاً إلا أغرقني سروراً وفرحا.*

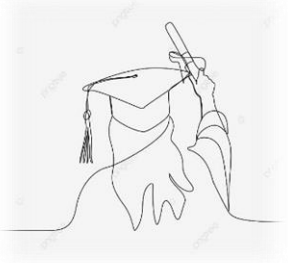

***Aissaoui Ichrak***

# إهداء

*من قال أنا لها "نالها"*

*لم يكن الحلم قريبا ولا الطريق كان محفوفا بالتسهيلات,*

*. لكننا فعلناها ونلناها*

*الحمد لله حبا وشكرا و امتنانا, الذي بفضله ها أنا اليوم أ نظر*

*. إلى حلم طال إنتظاره وقد أصبح واقعا أفتخر به*

*إلى قوتي بعد الله, داعمتي الاولى والابدية "أمي" أهديك هذا الانجاز*

*الذي لولا تضحياتك لما كان له وجود,ممتنة لان الله قد اصطفاك لي من البشرأما ياخير سند وعوض .*

*إلى من دعمني بلا حدود وأعطاني بلا مقابل*

*"أبي محمد الخليل "*

*إلى من قيل فيهم : {سَنَشُدُّ عَضُدَكَ بِأَخِيكَ}*

*إلى من مد يده دون كلل ولا ملل وقت ضعفي "أخي محي الدين " أدامك الله ضلعا ثابتا لي*

*و إلى أستاذي ومشرفي الفاضل,{ الحفناوي العانز } , الذي لم يبخل بجهده ووقته لإرشادنا ومساعدتنا طوال مدة البحث تعلمنا منك الكثير ,ونحن ممتنين لصبرك ومعرفتك الواسعة*

*كما لا أنسى صديقاتي العزيزات بلقيس وإشراق لقد كنا خير داعم لبعضنا بمثابة أخوات ، كلماتنا التشجيعية والمواساة وقت ضعفنا مزاحنا المتواصل وضحكاتنا التي لا تنتهي*

*وشجاراتنا لقد كنا حقا جزءا لا يتجزأ من حياتنا أنا محظوظة بصداقتكن*

*فالحمد لله دائما وأبدا وأ سأل الله أن يجمعني بكن في جنات النعيم مع النبيين والشهداء آمين آمين .*

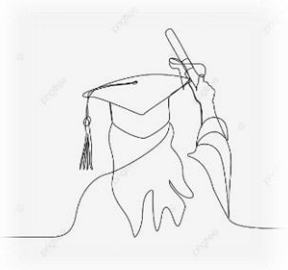

***Mereghni sacia***

**Abstract:**

This research presents a comprehensive investigation into the potential therapeutic properties of essential oils extracted from *Ammudoucus leucotrichus* and *Mentha piperita* plants, sourced from the El Oued region. Through a multi-faceted approach encompassing cyclic voltammetry (CV), ultraviolet-visible spectroscopy (UV), molecular docking, and molecular dynamics simulations, we aimed to elucidate their interactions with biomolecules and assess their efficacy against cancer and bacterial pathogens.

Gas chromatography-mass spectrometry analysis revealed the chemical composition of the oils, with particular emphasis on compounds exceeding 1% yield. For *Ammudoucus leucotrichus* oil, major components included Perilla aldehyde (64.66%), D-limonene (26.99%), and Alpha-pinene (5.8%), while *Mentha piperita* oil comprised 1, 8-Cineole (16.08%), trans-Sabinene hydrate (27.51%), and Pulegone (20.77%), among others.

Furthermore, our study focused on elucidating the interaction between DNA and BSA with these essential oils using CV and UV techniques. The obtained values of free energy changes of binding for *Ammudoucus leucotrichus* oil with DNA (-35.06 kJ/mol) and BSA (-29.56 kJ/mol), as well as for *Mentha piperita* oil with DNA (-29.14 kJ/mol) and BSA (-35.40 kJ/mol), were found to be in good agreement with molecular docking results.

Antibacterial assays demonstrated substantial inhibition zones against *Escherichia coli* (18.5 mm for *Ammudoucus leucotrichus* and 20.2 mm for *Mentha piperita*), *Bacillus subtilis* (20.1 mm for *Ammudoucus leucotrichus* and 21.6 mm for *Mentha piperita*), and *Staphylococcus aureus* (10.9 mm for *Ammudoucus leucotrichus* and 13.8 mm for *Mentha piperita*). Evaluation of IC50 values using UV spectroscopy provided insights into the oils' antibacterial activity. For instance, *Ammudoucus leucotrichus* oil displayed IC50 values of 2.935 mg/ml against *E. coli*, 0.641 mg/ml against *B. subtilis*, and 3.895 mg/ml against *S. aureus*, while *Mentha piperita* oil showed values of 1.500 mg/ml against *E. coli*, 1.477 mg/ml against *B. subtilis*, and 2.412 mg/ml against *S. aureus*. In comparison, Amoxicillin exhibited IC50 values of 3.961 mg/ml against *E. coli*, 8.154 mg/ml against *B. subtilis*, and 4.712 mg/ml against *S. aureus*. Additionally, molecular docking was performed for compounds with significant yields, revealing Pulegone as the best candidate, particularly effective against *E. coli*.

Additionally, molecular dynamics simulations were conducted to assess the stability of the Pulegone-*E. Coli* complex over 100 ns. The root-mean-square deviation (RMSD) remained below 1.5 angstroms, indicating the stability of the complex. Furthermore, RMSF analysis highlighted the interactions of Pulegone with amino acids in the active site, confirming its potential as a therapeutic agent.

**Keywords:** *Ammodaucus leucotrichus, Mentha piperita*, Amoxicillin, molecular dynamics, DNA, BSA, IC50, UV, CV, ΔG.

**Résumé :**

Cette recherche présente une enquête exhaustive sur les propriétés thérapeutiques potentielles des huiles essentielles extraites des plantes *Ammudoucus leucotrichus* et *Mentha piperita*, provenant de la région d'El Oued. À travers une approche multi-facettes englobant la voltamétrie cyclique (CV), la spectroscopie ultraviolet-visible (UV), le docking moléculaire et les simulations de dynamique moléculaire, nous avons cherché à élucider leurs interactions avec les biomolécules et évaluer leur efficacité contre le cancer et les agents pathogènes bactériens.

L'analyse par chromatographie en phase gazeuse-spectrométrie de masse a révélé la composition chimique des huiles, en mettant l'accent sur les composés dépassant un rendement de 1%. Pour l'huile d'*Ammudoucus leucotrichus*, les composants principaux comprenaient l'aldéhyde de Perilla (64,66%), le D-limonène (26,99%) et l'Alpha-pinène (5,8%), tandis que l'huile de *Mentha piperita* comprenait le 1,8-Cinéole (16,08%), le trans-Sabinène hydrate (27,51%) et la Pulegone (20,77%), entre autres.

De plus, notre étude s'est concentrée sur l'élucidation de l'interaction entre l'ADN et l'BSA avec ces huiles essentielles en utilisant des techniques de CV et d'UV. Les valeurs obtenues des changements d'énergie libre de liaison pour l'huile d'*Ammudoucus leucotrichus* avec l'ADN (-35,06 kJ/mol) et l'BSA (-29,56 kJ/mol), ainsi que pour l'huile de *Mentha piperita* avec l'ADN (-29,14 kJ/mol) et l'BSA (-35,40 kJ/mol), se sont révélées être en bon accord avec les résultats de docking moléculaire.

Des tests antibactériens ont montré des zones d'inhibition substantielles contre *Escherichia coli* (18,5 mm pour *Ammudoucus leucotrichus* et 20,2 mm pour *Mentha piperita*), Bacillus subtilis (20,1 mm pour *Ammudoucus leucotrichus* et 21,6 mm pour *Mentha piperita*), et Staphylococcus aureus (10,9 mm pour *Ammudoucus leucotrichus* et 13,8 mm pour *Mentha piperita*). L'évaluation des valeurs de CI50 à l'aide de la spectroscopie UV a fourni des informations sur l'activité antibactérienne des huiles. Par exemple, l'huile d'*Ammudoucus leucotrichus* a affiché des valeurs de CI50 de 2,935 mg/ml contre *E. coli*, 0,641 mg/ml contre *B. subtilis*, et 3,895 mg/ml contre *S. aureus*, tandis que l'huile de *Mentha piperita* a montré des valeurs de 1,500 mg/ml contre *E. coli*, 1,477 mg/ml contre *B. subtilis*, et 2,412 mg/ml contre *S. aureus*. En comparaison, l'amoxicilline a présenté des valeurs de CI50 de 3,961 mg/ml contre *E. coli*, 8,154 mg/ml contre *B. subtilis*, et 4,712 mg/ml contre *S. aureus*. De plus, le docking moléculaire a été réalisé pour les composés avec des rendements significatifs, révélant la Pulegone comme le meilleur candidat, particulièrement efficace contre *E. coli*.

De plus, des simulations de dynamique moléculaire ont été réalisées pour évaluer la stabilité du complexe Pulegone-*E. coli* sur 100 ns. Le déplacement quadratique moyen (RMSD) est resté en dessous de 1,5 angström, indiquant la stabilité du complexe. De plus, l'analyse RMSF a mis en évidence les interactions de la Pulegone avec les acides aminés dans le site actif, confirmant son potentiel en tant qu'agent thérapeutique.

**Mots-clés**: *Ammodaucus leucotrichus, Mentha piperita,* amoxicillin, dynamique moléculaire, ADN, BSA, IC50, UV, CV

**ملخص :**

تقدم هذه الدراسة تحقيقًا شاملاً في الخصائص العلاجية المحتملة للزيوت الأساسية المستخلصة من نباتي أم دريقة والنعناع الفلفلي من منطقة الوادي الأوسط في الجزائر. من خلال نهج متعدد الوجوه يضم الترسيب الدوري الكهربائي (CV)، وطيف فوق البنفسجي المرئي (UV)، والربط الجزيئي، ومحاكاة الديناميكا الجزيئية، هدفنا هو توضيح تفاعلها مع الجزيئات الحيوية وتقييم فعاليتها ضد السرطان والجراثيم البكتيرية.

أظهر تحليل الكروماتوغرافيا الغازية - الكتلة تركيب المواد الكيميائية للزيوت، مع التركيز بشكل خاص على المركبات التي تزيد نسبتها عن 1%. لزيت أم دريقة، كانت المكونات الرئيسية تشمل البيريلا ألدهيد (64.66%)، ودي ليمونين (26.99%)، وألفا-بينين (5.8%)، بينما كان زيت النعناع الفلفلي يحتوي على 1،8-سينيول (16.08%)، وترانس-سابينين هيدرات (27.51%)، وبوليجون (20.77%)، وغيرها.

بالإضافة إلى ذلك، ركزت دراستنا على توضيح التفاعل بين الحمض النووي وبروتين المصل البشري مع هذه الزيوت الأساسية باستخدام تقنيات CV و UV. أظهرت القيم المتحصل عليها لتغييرات الطاقة الحرة للربط لزيت أم دريقة مع الحمض النووي ( 35.06kJ/mol -) و (BSA (-29.56 kJ/mol، وأيضًا لزيت النعناع الفلفلي مع الحمض النووي (29.14kJ/mol-) و BSA (35.40 kJ/mol-) تطابقًا جيدًا مع نتائج الربط الجزيئي.

أظهرت التجارب البكتيرية مناطق تثبيط كبيرة ضد البكتيريا الإشريكية (18.5mm أم دريقة و20.2mm للنعناع الفلفلي)، والباسيليس الإشريكية (20.1mm أم دريقة و 21.6mm للنعناع الفلفلي )، والعنقودية الذهبية ( 10.9mm أم دريقة و 13.8mm للنعناع الفلفلي ). قدم تقييم قيم IC50 باستخدام طيف UV تحليلاً لفعالية الزيوت المضادة للبكتيريا.

بالمقارنة، كانت قيم IC50 للأموكسيسيلين 3.961 mg/ml ضد الإشريكية، 154.mg/ml ضد الباسيليس الإشريكية، و 4.712mg/ml ضد العنقودية الذهبية. أُجري الربط الجزيئي للمركبات ذات العائدات الكبيرة، مما كشف عن بوليجون كأفضل مرشح، خاصة فعال ضد الإشريكية.

أُجريت أيضًا محاكاة الديناميكا الجزيئية لتقييم استقرار تكوين مركب بوليجون-الإشريكية على مدى 100 نانوثانية. بقي التحليل الجذري لمتوسط المربعات (RMSD) دون 1.5 أنجستروم، مما يشير إلى استقرار التكوين. بالإضافة، أبرز تحليل RMSF تفاعل بوليجون مع الأحماض الأمينية في الموقع النشط، مؤكداً إمكانية استخدامه كعامل علاجي.

**الكلمات المفتاحية**: أم دريقة ، نعناع الفلفلي ، الحمض النووي، بروتين البومين المصلي البقري ، الأموكسيسيلين ، الديناميكا الجزيئية، IC50 ، UV، CV

## *List of Abreviations*

**α :** Alpha

**β:** Beta

**λ :** gamma

**ΔG:** free energy of binding

**A:** Absoption

**A°:** Angstrom

**ADMET**: Absorption, Distribution, metabolism, Excretion, and Toxicity

**AFNOR**: the French Association for Standardization

**BSA :** Bovine Serum Albumin

**C :** Concentration

**C° :** degrees celsius

**CPU:** Central Processing Unit

**CRAPC :** the Centre de Recherche Scientifique et Technique en Analyses Physico-Chimique

**CV :** Cyclic Voltammetry

**DMSO :** Diméthylsulfoxide

**DNA:** Deoxyribonucleic Acid

**EDTA :** Ethylene diaminetetraacetic acid

**Eos:** Essential oils

**g:** gramme

**GC/MS:** Gas Chromatography-Mass Spectrometry

**GHz:** Gigahertz

**Hbond:** hydrogen-bonding

**HCl:** Hydrochloric acid

**$IC_{50}$:** Concentration causing 50 % inhibition of an activi

**IFD:** Induced Fit Docking

**IUPAC:** International Union of Pure and Applied chemistry

**IV:** In vitro

**K :** Potassium

**$K_2HPO_4$:** Potassium hydrogen phosphate

**KcaL:** kilo calorie

**KCl:** Potassium chloride

**Kg :** Kilogram

**$KH_2PO_4$:** Potassium Dihydrogen Phosphate

**Kj:** Kilo joule

**KOH :** potassium hydroxide

**$LD_{50}$ :** Lethal Dose 50%

**Lipo:** lipophilic

**M:** Molarity

**m:** the mass

**MDS:** Molecular Dynamics Simulation

**mg:** Miligram

**ml:** Mililiter

**Mm:** Milimeter

**Ms:** mass spectrometer

**NaHCO3:** baking soda

**Ph:** Potential of Hydrogen

**RMSF:** Root Mean Square Fluctuation

**SDS:** Sodium Dodecyl Sulfate

**SIB:** Swiss Institute of Bioinformatics

**Solv GB:** Generalized Born electrostatic solvation

**TLB:** White Blood Cell Lysis Solution

**TLR:** Red Blood Cell Lysis Solution

**UV:** Ultra-violet

**V:** the volume

**Vdw :** encompassing van der Waals

**VTRS:** the Valorisation and Technology of the Saharian Resources Laboratory

**E :** energy

**µM:** Micromollaire

**:** Microlitre

# *List of figures*

## *List of tables*

# Summary

## Chapter II :Anticancer activit

**Chapter III :Antibcterail activity**



**Part II : Experimental**

**Chapter I : Materials and Methods**

## Chapter II :Results and Discussion

# Introduction

Medicinal plants have been integral to various cultures from ancient times to the present, often based on traditional knowledge that has occasionally been substantiated through modern scientific studies for integration into contemporary medical practices. The prudent use of these plants is essential due to potential interactions with pharmaceuticals and possible side effects. Ensuring the continuous study of their efficacy and safety is crucial, as is efforts to preserve their biodiversity and the traditional knowledge that accompanies them. Building on the foundation of traditional uses of plants, essential oils represent a significant area of interest. These natural extracts, known for their aromatic properties and complex chemical makeup, are obtained from different parts of plants and extensively utilized in skincare, haircare, aromatherapy, and healthcare sectors. Given their potent concentration, it is advisable to dilute essential oils with carrier oils to prevent adverse skin reactions, ensuring safe and effective application.

In the realm of disease prevention, anti-cancer activities are particularly noteworthy. These activities encompass mechanisms or substances that inhibit the proliferation or initiate the destruction of cancer cells, including slowing cell growth, inducing apoptosis, preventing tumour development, and reducing inflammation. The ongoing scientific exploration into the potential of anti-cancer agents is pivotal in enhancing the effectiveness of treatments and advancing cancer prevention strategies. Similarly, antibacterial activities are essential in controlling bacterial growth and preventing infections, which are critical for maintaining public health. These activities involve various mechanisms that target bacteria, underscoring the importance of ongoing research in developing new, effective antibacterial treatments that improve health outcomes and enhance public health standards.

Our current study aims to bridge traditional knowledge and modern science by investigating the active compounds and chemical compositions of two plants found in EL Oued, southeast Algeria. The focus on, *Mentha Piperita* and *Ammudaucus Leucotrichus* was chosen due to the limited existing research, despite their widespread availability in many Algerian regions and their frequent use in traditional medicine. The study commenced with a thorough theoretical analysis, followed by the extraction of essential oils using hydro distillation. Subsequent analyses of these oils' chemical components aimed to assess their inhibitory effects on bacterial activity and cancer cell growth, exploring their potential as anti-cancer and antibacterial agents.

# *Part I : Bibliographic*

# *Chapter I : Generalities of Essential oils*

# 1. Essential oils:

## 1.1. Definition:

Several available definitions of an essential oil converge on the fact that essential oils, commonly referred to as 'essences,' are products of generally quite complex composition, containing the volatile odoriferous principles contained in plants. They differ from fixed oils (olive oil, etc.) and vegetable fats by their volatile nature as well as their chemical composition.

AFNOR (Association Francoise de la normalisation) defines essential oil as a product obtained from a plant raw material, either by steam distillation or by mechanical processes, the oil is then separated from the aqueous phase by physical processes (Afnor, 2000; Afnor, 1986).

## 1.2. Localization of essential oils:

Essential oils can be found in all plant organs: flowering tops (mint), bark (cinnamon), roots (vetiver), and rhizomes (ginger), fruits (anise). (Brueton, 1999) In principle, all parts of a plant contain essential oils, but they are often predominantly found in one of them.

Essential oils in many aromatic plants are primarily located in the glandular trichrome that develop on the surface of leaves and other plant organs (Werker, 1985).

## 1.3. The chemical composition of essential oils:

Essential oils are highly complex mixtures of organic compounds with diverse chemical structures and functions. They are characterized by two or three major components present at relatively high concentrations (20-70%) compared to others (Bakkalia et al., 2008).

The composition of an essential oil varies within the same genus, as well as within the same species. This is referred to as chemo types. The chemo type indicates the major or distinctive biochemical component of essential oils extracted from the same botanical variety. This crucial classification allows for the selection of essential oils for more precise, safer, and more effective use (Gildmeister, 1919).

## 1.4. Physical and Chemical Properties of Essential Oils:

Essential oils are liquids at room temperature and volatile, which distinguishes them from vegetable oils. They are lip soluble and soluble in usual organic solvents as well as in alcohol, steam-distillable but very sparingly soluble in water. Therefore, a surfactant is required to suspend them in water. They generally have a density lower than that of water and a high

refractive index. They are susceptible to alteration and sensitive to oxidation (El kalamouni, 2010). Essential oils are colourless or pale yellow in liquid state and at room temperature.

**1.5. Benefits and uses of essential oils:**

Since ancient times, aromatic oils have been used in Chinese and Egyptian civilizations, and their use was also common in our Arab and Islamic civilization. The use of aromatic oils evolved over time, becoming widely used in beauty institutes and centres. They were used in treating illnesses as a therapeutic system aimed at maintaining human health.

The main benefit of essential oils for plants is their ability to attract pollinating insects, thus increasing pollination. Additionally, some oils act as insect repellents or are toxic to animals, serving a protective role for plants against these harmful insects that may prey on them (Seguin et al., 2001) .ore over, essential oils remove metabolic by-products and excrete them outside the plant. There are several other benefits and uses that apply to all living organisms. Essential oils work to strengthen most body systems, including the immune system. They also aid in promoting blood circulation and energizing the body. There are some essential oils that have the ability to help with hair growth, and these properties are found in lavender. It also increases the absorption of oxygen and ATP (adenosine triphosphate).

**1.6. Techniques for analysing essential oils:**

**1.6.1. Gas chromatography coupled with mass spectrometry (GC/MS):**

The GC/MS technique is the most commonly used in the field of essential oils. In the vast majority of cases, it allows for determining the molecular mass of a compound and obtaining structural information about a molecule from its fragmentation (Carvalli, 2002).

The GC/MS coupling has several advantages: the gas chromatogram separates the components of a mixture, and the associated mass spectrometer provides the mass spectrum of each component, often allowing for their identification (Hoffmann, 2005) .

**1.6.2 Principle:**

This technique involves ionizing molecules through electron bombardment, resulting in the formation of ions in the gas phase. The ions are then directed towards the analytical part of the apparatus. The ion beam then passes through the mass analyser Detected and transformed into a signal. To achieve this, there are different types of detectors capable of converting a weak ionic current into a measurable signal.

## 2. Presentation of the plant *Ammodaucus leucotrichus:*

### 2.1. Definition:

*Ammodaucus leucotrichus* is a medicinal plant belonging to the *Apiaceae* family, formerly known as *Ombelliferae* (Velasco-Negueruela et al., 2006).

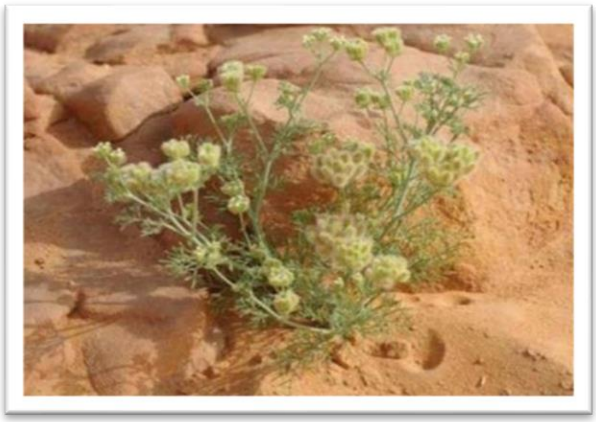

**Figure 1** : *Ammodaucus Leucotrichus* (El-haci, 2015)

### 2.2. Botanical description:

This description outlines *Ammodaucus leucotrichus* as a small annual plant, measuring 10 to 12 cm tall, with a globous (hairless) stem that is erect, branching, and finely striated. Its leaves are finely dissected and slightly fleshy. The flowers are clustered in umbels with 2 to 4 branches; they are small, with five free petals. The fruit is a diachene, 6 to 10 mm long, covered with long, very dense, silky, and crisped hairs, yellowish-brown at the base and then white (Benhouhou, 2005). This plant is highly valued and collected, which tends to make it scarce. It has a very strong anise-like odour (Quezel & Santa, 1963) it usually blooms in early spring (February to April).

### 2.3. Geographical distribution of *Ammodaucus Leukotrichus*:

The geographical area of this so-called Saharan species goes from the Atlantic to Egypt. Its entire distribution is based in northern Africa (Algeria, Morocco, Tunisia, Libya) it extends to Egypt and Tropical Africa (Manssouri et al., 2020).

### 2.4. Classification:

The systematic classification of *A.leucotrichus* is the following (Quezel & Santa, 1963):

- **Kingdom:** Planta

- **Phylum**: Spermatophytes
- **Subphylum**: Angiosperms
- **Class**: Eudicots
- **Subclass**: Asterids
- **Order**: Apiales
- **Family**: Apiaceae
- **Genus**: *Ammodaucus*
- **Species**: *Ammodaucus Leukotrichus Coss. & Hard*

**Figure 2** *:* Present photo the general appearance of *Ammodaucus leucotrichus* (Benhouhou, 2005)

### 2.5. Chemical Composition:

Chemical studies conducted by (Dahmane et al., 2017; Manssouri et al., 2020) on the separation and identification of the chemical compounds of the plant *A. Leucotrichus,* reported the presence of terpenes (perilladehyde, limonene, myrcene, the α-pinene, the β-pinene), coumarins and saponins, as well as other components such as: thymol, tannins, carvacrol, glycoside flavone and shybunol.

### 2.6. Traditional use of *Ammodaucus Leukotrichu*:

The fruits of *Ammodaucus Leukotrichus* This crunch and perfume breath, perfumes the third tea. In North Africa, fruits are used as a condiment and traditional medicine. They are used in the treatment of cold shots, fever and digestive disorders especially for children. The plant is also used, in the form of fruit decoction, for the treatment of diabetes (Adams, 1995). The fruits in infusion or in the form of powder are used against vomiting. This plant has aphrodisiac properties (Hammiche & Maiza, 2006)

### 2.7. Therapeeutic effects of *Ammodaucus Leucotrichus:*

*Ammodaucus Leucotrichus* is a plant for medicinal use used in the Sahara populations. The main uses are against: stomach ache, indigestion, diarrhoea, vomiting, spasms and colic, intestinal worms and constipation. The plant is also used for the treatment of allergy symptoms (Hammiche & Maiza, 2006). In North Africa, fruits are used as a condiment and traditional medicine. They are used in the treatment of cold shots, fever and digestive disorders especially for children (Adams, 1995). Reports that some indigenous populations in Morocco use the fruits of *Ammodaucus Leukotrichus* for the treatment of lung cancer in the form of mixed powder with honey and administered orally, it is also used against coughing, as Emmenagogue and against anorexia (Hammiche & Maiza, 2006). *Ammodaucus Leucotrichus* are used for the treatment of cardiac palpitations (Jouad et al., 2001).

The genus Ammodaucus is among the most used kinds in traditional pharmacopoeia (Fleurentin et al., 2002). And it is considered spice or condiment (Bellakhdar & Younos, 1993). Thus different parts of the leaves, flowers and crushed fruits in the form of powder are added in meals for flavouring (Hellis, 2005). The fruits in infusion or in the form of powder are used against vomiting. This plant has aphrodisiac properties (Hammiche & Maiza, 2006).

## 3. Presentation of the plant Menthe *piperita*:

### 3.1. Definition:

According to Paris and Moyse (1971), mints belong to the Menthe genus of the Lamiaceae family. This genus comprises about twenty species and a large number of subspecies and varieties that readily hybridize, making the taxonomy of the genus particularly challenging (Leung & Foster, 1996). Also known as peppermint, they are perennial stoloniferous herbs native to temperate regions, namely Europe and North Africa. They have square stems and opposite leaves. The inflorescences vary among species, appearing as rounded heads, dense spikes, or axillary pseudo-whorls. As for the flowers, they have a nearly regular corolla and four almost equal stamens.

### 3.2. Botanical description:

*Mentha piperita* is a hybrid resulting from a spontaneous cross between *Mentha aquatic* (water mint) and *Mentha spicata* (spearmint) (Baudoux, 2002). Mint grows on cool, moist, and organic-rich soil, typically at elevations up to 1800 meters. It is a common plant in temperate

regions worldwide, particularly in central and southern Europe where it is abundant and extensively cultivated (Benayad, 2008). Its Latin name (piperita) comes from its very characteristic scent, strongly peppery and cool, due to the essential oil contained in its leaves. It is a wild, perennial herbaceous plant belonging to the Lamiaceae family, a large family of plants often producing essential oils that are widely distributed around the world.

The mint plant is creeping, with square, ascending stems that can reach up to 1.20 meters in height. Its leaves are opposite, oval, acute, and toothed, usually of a beautiful green color, often wrinkled, sometimes fuzzy, emitting a strong characteristic odour easily recognizable. The flowers, which grow in clusters in the leaf axils, are pink in colour, and the stems are purple (Morigane, 2007).

**Figure 3 :** Description of the plant *Mentha piperita* (Teuscher et al., 2005)

### 3.3. Geographical distribution of *Mentha piperita:*

*Mentha piperita* has naturalized in many countries in Europe, including the United Kingdom, Denmark, Ireland, Belgium, the Netherlands, Germany, Austria, Poland, Ukraine, Bulgaria, former Yugoslavia, Greece, Italy, Romania, France, Portugal, and Spain. It has also spread to the Azores, Siberia (Russia), Australia, New Zealand, and North America (Canada, United States). The United States is the largest producer of mint globally, with production also occurring in China, India, Australia, some European countries (such as France and Italy), and Canada (Lachance, 2001). In North Africa, the species is commonly found in many gardens and cultivated for culinary purposes (Perrot, 1928).

### 3.4. Classification:

According to Quezel and Santa, the classification of mint is as follows:

- **Kingdom:** Planta

- **Subkingdom:** Vascular plants
- **Phylum:** Spermatophytes
- **Subphylum:** Angiosperms
- **Class:** Magnoliopsida (Dicotyledons)
- **Subclass:** Dilleniidae
- **Ordre:** Labiales (Labiatae)
- **Family:** Lamiaceae
- **Tribe:** Mentheae
- **Genus:** *Mentha*

**Figure 4** : *Mentha piperita* leaves (Khireddine, 2013)

### 3.5. Chemical Composition:

The essential oil of spearmint is mainly rich in (-)-carvone (content between 40 to 80%) and dihydrocuminyl acetate (10 to 12%). These two major constituents are responsible for the plant's odour. Additionally, limonene is present (5 to 15%). They are accompanied by dihydrocarvone, dihydrocarveol, carvyl acetate, and β-caryophyllene. In other chemical varieties, carvone is accompanied by 1, 8 cineole (up to 20%), pulegone (up to 50%), or terpinol-4 (up to 18%) (Avato et al., 1995).

### 3.6. Traditional use of *Mentha piperita:*

Mint has been a part of Mediterranean culture for millennia. Easily recognizable by its distinctive aroma, spearmint is commonly used in tea preparation. However, it is also utilized in phytotherapy, aromatherapy, perfumery, and cosmetics (Baba aissa, 1999).

Moreover, mint possesses numerous medicinal virtues. It is recommended as an antispasmodic, aphrodisiac, analgesic, as it helps to calm and relieve pain, and as a flavoring

agent. Pharmacological studies have shown that this essential oil is primarily used to treat digestive disorders, spasms, inflammation, colitis, nauseous states, and against certain parasites. It presents an expectorant effect in cases of bronchitis or flu. It is worth mentioning that it is refreshing and analgesic at the same time (Leung, 1996). Additionally, it has healing activity, accelerating and promoting skin healing.

Mint is used to flavour certain products, including toothpaste, chewing gum, confectionery, and refreshing beverages, among others. However, mint can have undesirable effects in some cases. Therefore, it is generally not recommended for pregnant women. However, it is recommended in case of menstrual delay (Cretti, 1981).

Mint has stomachic properties that aid digestion and digestive function, thus helping to combat certain gastrointestinal disorders. It also acts as a nerve tonic, providing a beneficial and soothing effect on the nervous system. Additionally, its stimulating and exciting action gives mint aphrodisiac virtues. It also helps eliminate stagnant gas in the intestines thanks to its carminative effect. These oils are considered to be anti-catarrhal and expectorant, reducing mucolytic secretions and facilitating their expulsion. They also act on the bile ducts by releasing them and increasing their secretion, thanks to their cholagogue and choleric properties. It is worth noting that they are highly valued for facilitating menstruation due to their emmenagogue properties. In summary, the properties of mint oil include a diverse range of beneficial health effects. The essential oil of mint is febrifuge, meaning it helps fight fever. This oil is also considered an excellent stimulant that promotes physiological activity in the body. It's important to note that this natural substance possesses anti-infectious properties (Leung, 1996).

# *Chapter II:*
# *Anticancer activity*

# 1. Study of anticancer activity:

## 1.1. Definition of cancer:

Cancer can be defined as one or more clones of cells whose multiplication within an organ or tissue does not follow the laws of normal tissue development (Banlard, 1987). The anarchic development of cells leads to the formation of a new neoplastic tissue that does not have a normal architecture. When this neoplasm is localized and does not possess the characteristics of invasiveness or metastasis, it is called benign; otherwise, it is called malignant (Lechat, 2006). This disease is "wild" because it destroys the tissue it invades. Metastases, in turn, destroy distant tissues. Cancer alters the functions of organs and eventually leads to death (Yaker, 1985).

## 1.2. Type of cancer:

### 1.2.1. Breast cancer:

In women, the breast is a hypertrophied secretory gland. During lactation, clusters of grape-like lobes (mammary gland or acini) produce milk that fills and swells a particularly branched system of ducts. About 90% of breast cancers originate from epithelial cells lining the lactiferous ducts (Lecarpentier, 2012). Breast cancers are defined as malignant proliferation of epithelial cells lining the ducts or lobules of the breast, referred to as ductal or lobular carcinomas, respectively. If there is a breach of the basement membrane separating the epithelium from the connective tissue, these carcinomas are termed invasive. Otherwise, they are termed in situ or intra-ductal carcinomas. They may or may not possess metastatic potential (Musgrove et al., 2009).

#### 1.2.1.1. Breast metastases:

Many different specialized cells, including fibroblasts, immune cells, endothelial cells, and mural cells of blood and lymphatic vessels, along with the extracellular matrix, must form an appropriate microenvironment necessary for tumor growth and metastatic progression. The metastatic spread of breast cancer primarily occurs via neo-lymphatic vessels, with rapid invasion of lymph node chains including axillary, internal mammary, supraclavicular, and cervical nodes. Regional invasion can lead to involvement of the chest wall. This can result in secondary foci in the bones, lungs, liver, contralateral breast, or even the brain (Iwatsuki et al., 2010).

### 1.2.2. Prostate cancer:

Prostate cancer is the most common neoplasm in men in the Western world. It rarely manifests before the age of 50. Its incidence has been steadily increasing in recent decades, a trend attributed to the aging population (Ndoye et al., 2014).

This type of cancer is often characterized by uncontrolled proliferation of epithelial cells in the prostate gland, which multiply haphazardly to form a malignant tumour. This tumour can spread locally, referred to as localized or intracapsular cancer. These cells can eventually migrate out of the prostate, primarily to lymph nodes and bones, resulting in metastases. This stage is termed non-localized or extracapsular cancer.

The disease often progresses slowly over several years. For most affected men, the slow progression of the tumour does not lead to clinical signs or symptoms during their lifetime (Has, 2012).

### 1.2.3. Lung cancer:

Bronchopulmonary cancers are malignant tumours that develop from bronchial structures and/or, more rarely, from lung parenchyma. They can be primary or secondary (Ouedraogo, 2003).

According to (Frusch et al., 2007), lung cancer is the leading cause of cancer-related deaths worldwide. Despite therapeutic advances, the prognosis for this condition remains grim. Across all stages, the five-year survival rate is 15%. Tobacco is by far the leading risk factor for this disease. Recent progress has been made in identifying the cellular mechanisms and genetic factors that promote the emergence of lung cancer.

#### 1.2.3.1. The types of lung cancer:

More than 90% of lung cancers are due to the following four histological types: adenocarcinoma, squamous cell carcinoma, large cell carcinoma, and small cell carcinoma (Frusch et al., 2007).

### 1.2.4. Thyroid cancer :

Thyroid cancers are malignant tumours that develop from the epithelial cells of the thyroid gland (El-Jai, 2009). They typically manifest as a thyroid nodule, often associated with a "multi-nodular" goiter. This raises the issue of toxic nodules, which are always associated with low TSH levels, and thyroid cancer, which warrants the systematic practice of fine-needle aspiration biopsy (Bouklikha, 2014). They are mostly cancers with a favourable prognosis, predominantly affecting women (76%), with an average age at diagnosis of around 50 years (Inc, 2020).

**Table 1 :** Main Histological types of thyroid cancer (Inc, 2020)

| Histological types | Frequency |
|---|---|
| Differentiated follicular/vesicular stem cancers<br>( 80% papillary carcinomas<br>10% follicular carcinomas<br>and 10% poorly differentiated cancers) | >90 |
| Medullary or C-cell cancers | 5% |
| Anaplastic cancers | Rare |

According to El-Jai (2009), differentiated thyroid cancers are the first malignant endocrine cancers but remain rare, accounting for only 1% of neoplastic pathologies. They include:

- ✓ Papillary carcinomas: the most common (80% of all thyroid carcinomas) and have a good prognosis if well managed early.
- ✓ Follicular or vesicular carcinomas: much less common (5% of thyroid cancers).

### 1.3. The role of DNA in cancer and its relation:

The use of ferrocene derivatives as bioactive molecules has recently been established. Several reports demonstrate that many compounds containing ferrocene exhibit interesting cytotoxic and DNA cleavage activities, which have been proven to be potential therapeutic agents against major diseases (Nafees & Zijian, 2014; Muhammad et al., 2011). Indeed, some compounds synthesized from organometallic sandwich fragments have been studied for their various biological properties, including antimalarial, antimicrobial, and anticancer properties (Sara et al., 2016; Ayyavoo & Rajakumar, 2017; Pier, 2000). However, the drug-DNA interaction in vivo involves concurrent interactions with DNA topoisomerase I or II enzymes to form a ternary complex (Hurley & Boyd, 1988). These interactions can lead to lethal double-strand DNA breaks and ultimately selective death of tumour cells. However, cytotoxic drugs generally have high toxicity for both normal and cancer cells, and their therapeutic index is usually low. Additionally, if DNA represents the blueprint of life, then proteins are defined as the molecular machines carrying out this blueprint. Therefore, the objective was to study newly

synthesized derivatives and understand their mode of action towards biological macromolecules in order to improve their efficacy.

DNA is the primary intracellular target of anticancer drugs. The study of small molecule interaction with DNA has been the subject of research for decades as it provides insight into preclinical examination design (Muhammad et al., 2013). New, more effective drugs targeting DNA cause damage to cancer cells, block their division, and even induce cell death, accelerating drug discovery and development processes (Maolin et al., 2017). Thus, studying the interaction of metal-based compounds with DNA has been deemed useful for better understanding their pharmacological properties. Today, complex mechanisms explaining processes from DNA damage production to cell death are being explored, opening promising avenues for the development of more selective and effective anticancer agents. Oncological processes are characterized by uncontrolled cellular proliferation; therefore, DNA is the biological target of many antitumor drugs (Baguley, 1991).

### 1.4. The role of BSA in cancer and its relation:

Albumin is the most abundant protein in plasma and, as a carrier protein, it is responsible for transporting a variety of compounds, including vitamins, fatty acids, and pharmaceutical products (S. Howard, 1976). Indeed, the interaction of small molecules with bovine serum albumin is an important aspect of drug development. Serum albumins increase the solubility of hydrophobic ligands in plasma, modulate their release by acting as drug reservoirs, and affect their bioavailability. An overview of HSA and the interaction between anticancer ligands is currently needed, as these drugs represent more than half of the total drug consumption worldwide (Nab, 2012). This study not only provides a brief overview of BSA properties (similar to HSA), but also insights into the binding and anticancer capabilities of ferrocene compounds that can guide the rational design and development of metal-based drugs and BSA-based carriers for clinical applications (Geisow & Beaven, 1977). Indeed, this part will help better understand the importance of binding anticancer compounds to plasma proteins and the effect of this binding on their overall distribution and pharmacological activities (Hong et al., 2004).

### 1.5. Mechanisms the anticancer:

Anticancer drugs are medications designed to kill or halt the growth of cancer cells. They work by targeting various mechanisms involved in cell division, proliferation, and survival of cancer cells (Hanahan & Weinberg, 2011). The main mechanisms of action of anticancer drugs include:

- ✓ Cell Division Inhibition: Certain anticancer drugs, such as taxes and vinca alkaloids, function by blocking cell division through interfering with the formation of microtubules, which are essential structures for the proper separation of chromosomes during cell division (Aslam et al., 2014).
- ✓ Inhibition of DNA synthesis: Alkylating agents, such as cyclophosphamide, cisplatin, and busulfan, work by adding alkyl groups to DNA, which disrupts the DNA structure and prevents DNA replication.
- ✓ Inhibition of protein synthesis: Protein synthesis inhibitors, such as antimetabolite agents like 5-fluorouracil and methotrexate, disrupt the synthesis of proteins necessary for cell growth and.
- ✓ Inhibition of receptor signalling: Monoclonal antibodies, such as trastuzumab and rituximab, act by binding to cell surface receptors, preventing signalling that promotes cell growth.
- ✓ Induction of apoptosis: Apoptosis-inducing agents, such as kinase inhibitors, trigger programmed cell death, which is an essential process for eliminating damaged or abnormal cells.

These mechanisms of action are often combined to achieve a maximal effect on cancer cell growth and survival. However, it's important to note that anticancer drugs can also have adverse effects on healthy cells, leading to side effects such as hematologic toxicity and peripheral neuropathy (Longley & Johnston, 2005).

### 1.6. Anticancer Activity of Natural Substances:

It should be noted that cancer is a major cause of death worldwide. Indeed, of the total global deaths, 15% were attributable to cancer, which is more than the proportion of deaths caused by HIV/AIDS, tuberculosis, and malaria combined. In industrialized countries, it is the second leading cause of mortality after cardiovascular diseases (Oms, 2006). According to projections by the World Health Organization (WHO), by 2020 the number of deaths due to cancer will see a considerable increase in developing countries, in Asia, Africa, and Latin America, primarily due to the continuous aging of the human population and the increase in pollution (Rastogi et al., 2004). In developing countries, traditional medicine is sometimes the only affordable and accessible source of care, especially for the poorest patients. This traditional medicine primarily uses plant-based therapies. Indeed, several anticancer molecules come from medicinal plants. Taxol is a famous anticancer molecule that was first isolated from the Pacific yew Taxus brevifolia in the 1960s, and it came from a screening (testing of many molecules) at the National Cancer Institute, which had set up a major program to search for anticancer molecules from plant species. Thus, 108,000 extracts had been prepared from 35,000 plant species and

then evaluated for their cytotoxicity on cancer cells. Among the active extracts was an extract from the bark of the Pacific yew. After purification of this extract, Taxol was found to be cytotoxic and also active in vivo, for the treatment of certain diseases like cancer. Also, with the aim of testing the anticancer effect of Saharan species, we have conducted anti-tumour trials using extracts from these species. The results of these trials will be discussed in the following chapters.

### 1.7. Anticancer medications:

Anti-cancer agents are drugs used alone or in combination in chemotherapy regimens that constitute the treatment of cancers. They aim to combat the uncontrolled proliferation of cells that differ from normal cells due to the presence of genetic and functional abnormalities. This chemotherapy is not intended to destroy the tumour locally but to prevent tumour escape secondary to the formation of distant metastases (Apretna et al., 2004; Delavigne, 2009).

#### 1.7.1. The different classes of anticancer drugs and their mechanisms of action have been classified into three categories based on their pharmacological mechanisms:

- ✓ **Cytotoxic Anticancer Drugs:**

Agents used in cytotoxic chemotherapy differ in their modes of action and their belonging to chemical families. There are six main families distinguished: alkylating agents, topoisomerase I and II inhibitors, microtubule poisons (intercalating agents), antimetabolites, and DNA cross-linking agents (Merceron et al., 2006).

**Table 2 :** Chemotherapy Agents and Their Mechanisms of Action (Merceron et al., 2006; Faure et al., 2010; Burotto et al., 2015)

| Class of anticancer drugs | Examples of anticancer drugs | Mechanism of action |
|---|---|---|
| **Alkylating agents** | Cyclophosphamide<br>Ifosfamide<br>Chlorambucil<br>Melphalan<br>Mitomycin<br>Platinum salts (cisplatin, carboplatin, and oxaliplatin) | These compounds possess one or more very nucleophilic alkyl groups capable of interacting with DNA to create covalent lesions, resulting in the inhibition of its transcription and replication. Furthermore, they are responsible for the release of free radicals leading to DNA strand breaks. |

| | | |
|---|---|---|
| **Microtubule poisons (Intercalating agents)** | Periwinkle alkaloids (vincristine, vinblastine, vinorelbine)<br>Taxanes (paclitaxel, docetaxel) | These molecules are characterized by multiple condensed aromatic nuclei. They cause a distortion of the DNA molecule, which prevents the progression of RNA and DNA polymerases, thus inhibiting replication and transcription. They also induce the generation of free radicals. |
| **Antimetabolites** | Antipyrimidines (5-fluorouracil, gemcitabine, cytarabine)<br>Ant folates (methotrexate). | They are structural analogy of purine and pyrimidine bases, as well as folinic coenzymes. They inhibit the synthesis of nucleic acids by causing a deficiency in nucleotides. |
| **Cleaving agents** | Bleomycine | They possess a molecular structure that allows them to insert themselves between the components of DNA, thus causing multiple breaks in this molecule. |
| **Inhibitors of topoisomerase I** | Camptothecin derivatives: Irinotecan and topotecan | Topoisomerases are enzymes involved in the replication, transcription, and repair of DNA by creating single or double-strand breaks. By inhibiting these enzymes, we deprive the cell of using its genetic information, thus leading to its death. |
| **Inhibitors of topoisomerase II** | Anthracyclines (adriamycine, étoposide) | |

- ✓ **Targeted therapies:**

These are medications whose action targets a specific level of functioning or development of tumour cells. Two types are distinguished:

1. Extra-cellular action medications: These are directed against a membrane receptor present on the tumor cell (such as: Avast in, Erbitux...).
2. Intra-cellular action medications: These inhibit the transmission of the cell proliferation signal by enzymatic inhibition (such as: Multikinases, Gleevec...) (Merlin, 2008; Psimaras et al., 2010).

- ✓ **Other anticancer agents:**

These are anticancer agents with modes of action different from the two groups above (Psimaras et al., 2010).

### 1.7.2. Toxicity of anticancer drugs:

The various medications used in chemotherapy protocols do not act specifically on tumour cells but can also be toxic to healthy cells, especially those with rapid proliferation (Delavigne, 2009). These toxic effects can be listed as follows: cardiotoxicity, neurotoxicity, nephrotoxicity, hepatotoxicity, alopecia, dehydration, fatigue, sterility, malnutrition, skin problems, allergies, and many others (Tacar et al., 2012; Yang et al., 2016; Mason et al., 2016).

## 1.8. Treatment of cancer:

### 1.8.1. Surgery:

Surgical treatment may aim to remove the tumour through excision. This type of treatment is curative for solid cancers in cases of early tumour diagnosis (Yaker, 1985; Banlard, 1987).

### 1.8.2. Radiotherapay:

Radiotherapy is an adjuvant treatment, always used in conjunction with ablative surgery. It involves irradiating the site of tumour resection (post-surgery) using high-energy rays (X-ray and Gamma) to eliminate residual tumour cells (Foa et al., 1985).

### 1.8.3. Chemotherapy:

Chemotherapy is the science that applies natural active principles (such as phyto-synthetic substances extracted from plants) or synthetics with a perfectly known structure to reduce the rate of multiplication of tumour cells (Privat, 1985).

### 1.8.4. Immunotherapy:

Immunotherapy is a treatment that can complement the destruction of residual cancerous tumour formation post-chemotherapy (Foa et al., 1985). It involves two mechanisms: passive and active immunotherapy.

Passive immunotherapy is represented by cellular therapy, which involves injecting the patient with cytotoxic T cells isolated from the tumour (Old, 1996).

Active immunotherapy is represented by vaccination. For example, the concept of anti-melanoma vaccination aims, after identifying specific antigens of the given tumour, to induce a specific immune response by injecting them into the patient (Carter, 2001).

### 1.8.5. Hormone therapy:

It involves the antagonistic effects on tumour growth of various types of hormones, including oestrogens in the case of breast cancer and androgens in the case of prostate cancer (Lieberman, 2002), or certain neuropeptides in a specific form of lung cancer, small cell carcinoma (Moodey, 2006).

# *Chapter III*: *Antibacterial activity*

# 1. Study of antibacterial activity:

## 1.1. Bacteria definition:

Bacteria are the smallest organisms endowed with metabolism, capable of growth and division at the expense of nutrients. They are prokaryotic cells (their DNA is not localized in a nucleus). Their usual diameter is about 1 µm, and their shape varies. They are ubiquitous, as they exhibit adaptations to extreme environments due to their highly varied metabolism. Studying bacteria is essential for combating diseases, as bacteria are the cause of some serious diseases as well as multiple benign conditions. The prevention and control of these diseases largely depend on the efforts of bacteriologists, both in human medicine and in veterinary medicine or agriculture. However important pathogenic bacteria may be, they constitute only a small part of the bacterial population as a whole. Most bacteria pose little or no danger and are undeniably useful to humans. For example, some produce antibiotics that have revolutionized therapy, while others are used in the food industry for making butter, cheese, and yogurt (Singleton, 1999).

## 1.2. Structure of a Bacterial Cell:

The bacterial cell appears to be surrounded by a rigid envelope (cell wall) that encloses a thinner and more delicate second envelope (the plasma membrane). The underlying cytoplasm is generally very homogeneous and contains primarily ribosomes, sometimes with reserve substances. It does not contain any organelles described in eukaryotic cells (endoplasmic reticulum, mitochondria, etc.). These structures (cell wall, membrane, cytoplasm, and bacterial chromosome) are essential components of the cell that are always present. Other structures may potentially be associated with it: the capsule (outermost envelope), flagella, pili or fimbriae, spores, which are resistance forms found only in certain bacterial species, and finally plasmids, which are circular extra-chromosomal DNA capable of self-replication (Prescott, 2003; Hart & Shears, 1997).

## 1.3. Types of bacteria:

### 1.3.1. Gram negative bacteria:

- ✓ ***Escherichia coli:***

*Escherichia coli* is a member of the Enterobacteriaceae family. It is a Gram-negative, facultative anaerobe bacillus that does not form spores and lacks oxidase. *E. coli* is part of the

commensal microflora of humans and many other animals. It colonizes the digestive tract of warm-blooded animals (carnivores, omnivores, herbivores, and birds), as well as reptiles. Its primary habitat is the digestive tract. The environment constitutes the secondary habitat for *E. coli*. Unlike the primary habitat, it is rather unfavourable for their survival (Merabet & Sekhsoukh, 2020).

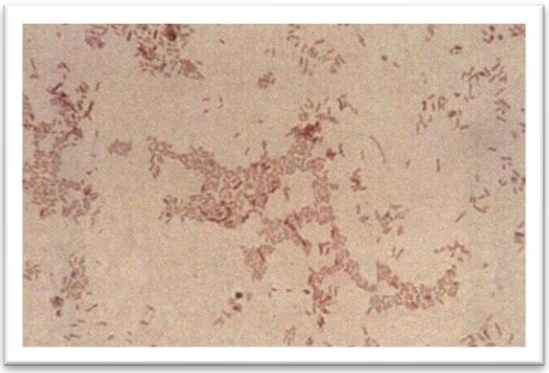

**Figure 5 :** *Escherichia coli*, Gram staining (Magnification, x100) (Hart, 1999)

✓ ***Pseudomonas:***

The bacteria of the genus *Pseudomonas* belong to the family Pseudomonadaceae. They are motile rods with polar flagella and are strictly aerobic. These bacteria readily grow on standard media at 30°C, with some species like *P. aeruginosa* capable of growing at higher temperatures, up to 41°C or even 43°C, which is used for diagnostic purposes. They often produce pigments, such as pyocyanin and pyoverdine, aiding in their identification. *Pseudomonas* can utilize various substrates as a source of carbon and energy, including carbohydrates, lipids, amino acids, and aromatic compounds. Some species, like P. aeruginosa, are opportunistic pathogens, resistant to antibiotics and antiseptics, causing nosocomial infections, especially in immunocompromised patients. They can also be phytopathogenic (Leclerc et al., 1995).

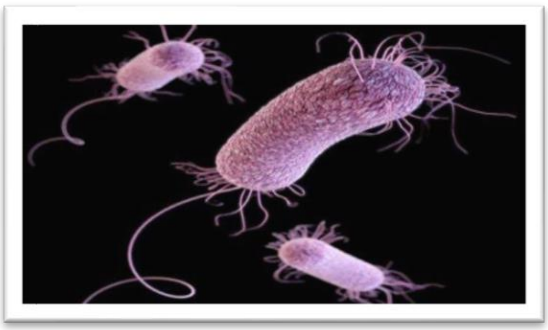

**Figure 6 :** Computer-generated three-dimensional image of *P. aeruginosa* (Green et al., 1974)

### 1.3.2. Gram positive bacteria:

- ✓ ***Staphylococcus aureus:***

Staphylococci are facultative aerobic-anaerobic, Gram-positive, spherical (cocci) bacteria, highly resistant in the environment but not demanding in culture. Staphylococcus aureus is one of the most common bacteria in human pathology. It is a commensal germ of the skin and digestive flora found in the nasal passages of about 20% of individuals and temporarily in about 30% of the general population (Merabet & Sekhsoukh, 2020).

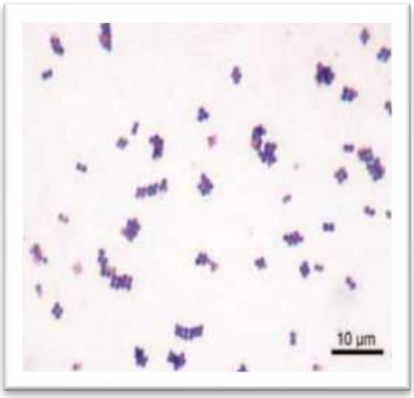


**Figure 7 :** Appearance of *Staphylococcus aureus* after Gram staining (Hennekinne, 2009)

- ✓ ***Streptococcus pneumoniae:***

S. pneumoniae belongs to the family Streptococcic. This Gram-positive coccobacillus, with the shape of an egg or a lancet, is often grouped in pairs, hence its name diplococcus, or may form short chains (Alonso Develasco, 1995). There are about 90 serotypes; the capsule surrounding the pneumococcus, which is its distinctive feature and the main virulence factor, presents a complex mosaic of monosaccharides, oligosaccharides, and other polymeric components, all of which have a high molecular weight (Ryan & Ray, 2004). The pneumococcus grows on blood agar, where it forms facultatively anaerobic round colonies surrounded by α-homolysis (Auwat et al., 1999).

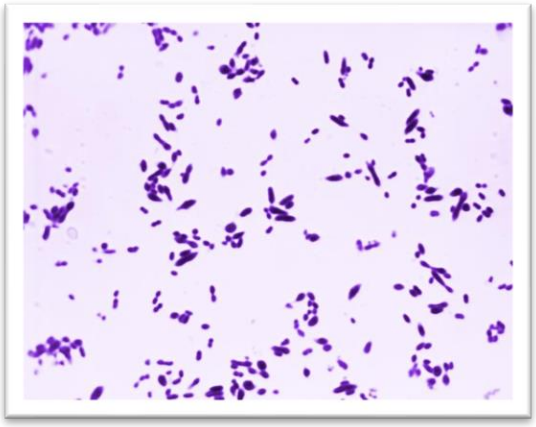

**Figure 8 :** Morphology of *Streptococcus pneumoniae*

(https://phil.cdc.gov/Details.aspx?pid=21340)

### 1.4. Bacterial Morphologies:

Bacteria have strong affinities with plants. But they are considered a separate kingdom (even two, when considering Archaea, or Archaea bacteria, as a distinct group of Prokaryotes). From a structural standpoint, these microorganisms can form small filaments, similar to a thallus, consisting of similar, very small cells, partitioned in one, two, or three directions. However, most often, bacteria appear as unicellular organisms, occasionally joined with similar organisms in the form of chains or a zoogloeal (macroscopic gelatinous mass). In their rounded cell form, they are called micrococci (*Micrococci*); if they dissociate immediately upon formation, they Are called *Bacterium*, *Diplococcus*, etc.; if they remain joined in more or less long rods, they constitute bacilli (*Bacillus*) (Jorda, 2004).

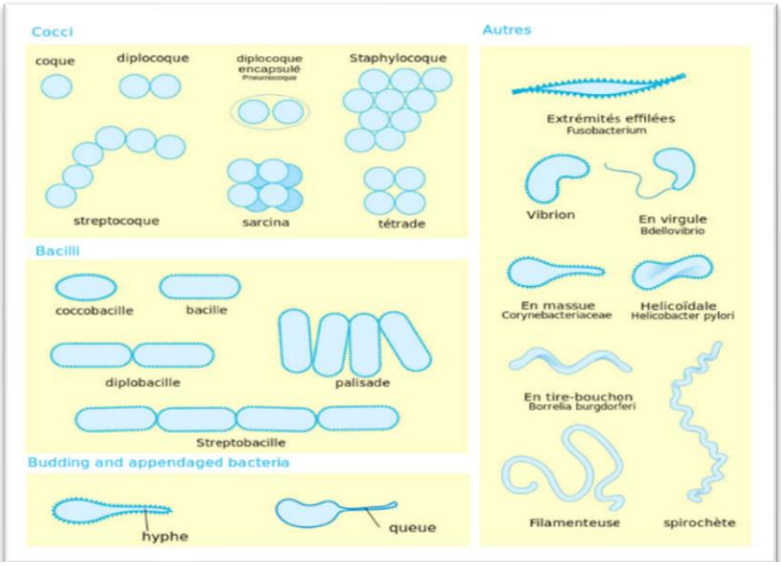


**Figure 9 :** Morphological Diversity and Cellular Arrangements of Bacteria (Villarreal, 2006)

### 1.5. Classification:

#### 1.5.1. Classification Standards:

##### 1.5.1.1. Scientific Names:

Bacteria, like other living organisms, are classified by genus (based on the presence of one or more identical characteristics) and, within the genus, by species. The scientific name consists of the genus followed by the species (for example, *Clostridium botulinum*). Within a species, there may be different types called strains. Strains differ in their genetic material and chemical components. Sometimes, certain drugs and vaccines are only effective against specific strains (Larry & Charles, 2018).

##### 1.5.1.2. Staining:

Another classification commonly used is based on their reaction to Gram staining. This method allows differentiating bacteria based on their staining ability, which varies according to the composition of their cell wall (Heart & Shears, 2006). The most commonly used stain is the Gram stain. Some bacteria stain blue, and they are called Gram-positive. Others stain red and are referred to as Gram-negative. The difference in staining between Gram-positive and Gram-negative bacteria is due to differences in their cell walls. These differences are also responsible for different types of infections, and different types of antibiotics are effective against them (Larry & Charles, 2018).

##### I.5.1.3. Shapes:

There are three basic shapes used to classify bacteria: spherical shape (cocci), rod shape (bacilli), and spiral or helical shape (spirochetes) (Larry & Charles, 2018).

##### I.5.1.4. Oxygen Requirement:

Bacteria can be classified based on their oxygen requirement for survival as aerobic bacteria or anaerobic bacteria. When the environment is favourable in terms of nutrients, temperature, pH, and oxygen, bacteria can survive and multiply. Under certain circumstances, bacteria can have significant pathogenic potential and be responsible for mild or severe diseases (Flandrois, 2000).

### 1.6. Mechanisms antibacterial activity:

#### 1.6.1 Enzymatic Inhibition, first:

- ✓ The production of beta-lactamase is the first mechanism. Beta-lactamases degrade the amide bond on the lactam ring, rendering beta-lactams inactive. Transposons carry the Bla genes, which can be chromosomal, plasmid-based, or transferable (Alioua & Bouamoucha, n.d.).
- ✓ Production of penicillinase Bacteria have inherent resistance due to the species-specific nature of chromosomal penicillinases. Bacteria acquire resistance through plasmid-based penicillinases.
- ✓ Chromosomal beta-lactamases Known as cephalosporinases, these are naturally produced by various species, including Enterobacter cloacae, Pseudomonas aeruginosa, and Acinetobacter sp.
- ✓ Enzymes that inactivate aminoglycosides Three types of enzymes- acetyltransferase, nucleotide transferase, and phosphotransferase - have been identified as capable of inactivating aminoglycosides. Often, plasmids contain the genes encoding these enzymes.
- ✓ Enzymes that inactivate chloramphenicol a plasmid-encoded chloramphenicol acetyltransferase can inactivate chloramphenicol. The antibiotic is inactivated by acyltransferase, preventing it from binding to the targeted site.

#### 1.6.2. Alteration of Binding Sites:

- ✓ Modification of Penicillin-Binding Protein (PBP) by altering chromosomal genes or adding new genes that express new PBPs, this phenomenon reduces the affinity of the target (PBP) for beta-lactams (Alioua & Bouamoucha, n.d.).
- ✓ Modification of Ribosome Binding Site the antibacterial effects of macrolides, aminoglycosides, or chloramphenicol can be diminished by intracellular modification of the targeted ribosomal subunit in the bacterial cell. Antibiotics that can no longer attach to the ribosomal site are unable to suppress protein synthesis or bacterial growth following this modification.
- ✓ Transformation of Peptidoglycan Precursor Enterococci become resistant to glycopeptides when the terminal D-Ala of the peptidoglycan precursor is transformed into a lactate group.

- ✓ Modification of DNA Topoisomerase and DNA Gyrase DNA gyrase is an enzyme necessary for the action of quinolones. Resistance is caused by accidental modifications of a single amino acid in DNA gyrase. The same applies to mutations in topoisomerase IV.
- ✓ Modifications of Target Enzymes Resistance is also caused by modifications in dihydropteroate reductase and dihydropteroate synthetase, making them resistant to binding with sulphonamides.

### 1.6.3. Decreased Cell Permeability:

By altering the permeability of the internal or external membrane of the bacterium, the admission of the antibiotic to its site is reduced. The porins of Gram-negative bacteria can be modified, which may limit or prevent the antibiotic's ability to reach its site of action (Alioua & Bouamoucha, n.d.).

### 1.6.4.Efflux Pumps :

By actively pumping the antibiotic out of the bacterium, the antibiotic cannot reach its site of action. Bacterial cells naturally contain efflux transporters for a variety of drugs, which significantly increases the natural resistance of bacteria to many antibacterial treatments. These pumps require energy.

**References :**


**A**

**Adams, R. P., (1995)**. «Identification of Essential Oils Components by Gas Chromatography-Mass Spectroscopy », Allured Publ., Illinois, and IL.

**Afnor, (2000)**. Recueil de normes : les huiles essentielles. Tome 1 .Echantillonnage et méthodes d'analyse. AFNOR, Paris, 440 p.

**Afnor, (1986)**. Recueil des Normes Françaises « huiles essentielles », AFNOR .Paris. 57 p.

**Alioua, R., & Bouamoucha, I. (n.d.).** Thème Etude de l'activité antibactérienne de l'extrait méthanolique du fruit de Zaarour rouge (Crataegus monogyna) vis-à-vis des bactéries résistantes aux antibiotiques Membres.

**AlonsoDeVelasco, E., Verheul, A. F., Verhoef, J., & Snippe, H. (1995)**. Streptococcus pneumoniae: virulence factors, pathogenesis, and vaccines. Microbiological Reviews, 59(4), 591-603.

**Aslam, M. S., Naveed, S., Ahmed, A., Abbas, Z., Gull, I., & Athar, M. A. (2014)**. Side Effects of Chemotherapy in Cancer Patients and Evaluation of Patients Opinion about Starvation Based Differential Chemotherapy. Journal of Cancer Therapy, 05(08), 817–822. https://doi.org/10.4236/jct.2014.58089.

**Auzat, I., Chapuy-Regaud, S., Le Bras, G., Dos Santos, D., Ogunniyi, A. D., Le Thomas, I., Garel, J. R., Paton, J. C., & Trombe, M. C. (1999)**. The NADH oxidase of Streptococcus pneumoniae: its involvement in competence and virulence. Molecular Microbiology, 34(5), 1018-1028.

**Azalenko k. (1995)**, Contribution à la détermination des chemotypes d'une plante à Huile essentielle du Togo : Lippiamutiflora. Mémoire d'ingénieur de travaux, ESTBA, Univ. Lomé.

**B**

**BabaAissaf., (1999)** – Encyclopédie des plantes utiles (Flore d'Algérie et du Maghreb), Librairie moderne, Rouïba, 173.

**Baguley B.C. (1991)** DNA intercalating anti-tumour agents. Anti-Cancer Drug Design 6, 1-35.

**Bakkalia. F, Averbeck. S, Averbeck. D, Idaomar.M.** Biological effects of essential oils a review. Food and Chemical Toxicology. 46, Pages 446–475 (2008).

**Banlard L. (1987)**, Anatomie, physiologie, microbiologie, dunoded, P : 320.

**Baudoux d. (2002)**. L'Aromatherapie. Se soigner par les huiles essentielles, Ed Bruxelles.

**Bellakhdar J., Younos C. (1993)**. La diététique médicale arabo-islamique à travers Les traités arabes anciens et la pratique actuelle au Maroc. Actes du 2ième Colloque Européen D'Ethnopharmacologie et de la 11e Conférence internationale d'Ethnomédecine, Heidelberg : 43–51.

**Benayad N., (2008)** – les huiles essentielles extraite par plantes médicinales Marocaine : moyen efficace de lutte contre les ravageurs des denrées alimentaires Stockées, Université Mohammed V– Agdal de Rabat, Novembre 2008, p 13-30.

**Benhouhou, S. (2005)**. A guide to medicinal plants in North Africa, p31-32.

**Bouklikha C., Sofiane D. (2014)**.Cancer de la thyroide. Université AboubakrBelkaidTlemcen.Mémoire doctorat ,39.

**Bruneton J. ; (1999)**. Pharmacognosie, phytochimie, plantes médicinales. Techniques et Documentation. 3ème Ed. Lavoisier. Paris, 199-388.

**C**

**Carter P. (2001)**. Improving the efficacy of antipody-based cancer therapie. P: 118- 129.

**Carvalli J.F (2002)**. Caractérisation par CPG/IK, CPG/SM et RMN de carbone -13 d'huile Essentielle de Madagascar. Thèse de Doctorat, Université de Corse Pascal Paoli.

**Cretti I., (1981)** – les plantes aromatiques et médicinales, comment les reconnaître et les Utilisées, Ed. Atlas, p128.

**D**

**D. Apretna, F. Thiessard, G. Miremont-Salamé, F. Haramburu. (2004)**. Pharmacovigilance, cancer et médicaments anticancéreux. Oncologie 6: 66-71.

**Dahmane D., Dob T., Krimat S., Nouasri A., Metidji H. And Ksouri A. (2017)**.Chemical composition, antioxidant and antibacterial activities of the essential oils of Medicinal plant Ammodaucus leucotrichus from Algeria. Journal of Essential oil Research, 29(1): 48-55.

**E**

**E.Seguin,** A.Ghestem and M.Paris Ovecchioni, Le préparateur en pharmacies( Botanique–Pharmacognosie-Phytotherapie). Édition Tec & Doc., 143-146 (2001).

**El jai A. (2009)**. Les cancers différenciés de la thyroïde à propos de 35 cas. Th. Doct.

**El kalamouni. (2010)**, caractérisations chmiques d'extraits de plantes, 22-38.

**El-haci. I. (2015)**. Etude phytochimique et activités biologiques de quelques plantes Médicinales : Ammodaucus leucotrichus Coss. & Dur., Anabasis aretioides Moq. & Coss. Et Limoniastrum feei (Girard). Thèse de doctorat. Université aboubekr belkaid tlemcen.154 p.

**F**

**Flandrois JP. (2000)**.Bactériologie Médicale. Coll Azay. Puf.

**Fleurentin. J., Pelt J.M., Mazars G. (2002)**. Des sources du savoir aux Médicaments du futur. 4éme congrès européen d'ethnopharmacologie, Edition IRD. 300p.

**Foa J, Bartolin R, Delboyc. (1985)**. Manuel de therapeutique medical. Ed : Masson (paris) P : 344.

**Frusch N., Bosquee L., Louis R. (2007)**. Le cancer du poumon. Epidemiologie et facteurs etiologiques. Revue Médicale de Liège, 62(9), 548-53.

**G**

**Gildmeister E.,** Hoffman FR.Les huiles essentielles. Ed Schimmel et Cie. (1919).

**Green S K., Schroth M N., Cho J., Kominos S K., Vitanza-jack V B. (1974)**. Agricultural plants and soil as a reservoir for Pseudomonas aeruginosa.

**H**

**Hammiche, V., Maiza, K. (2006)**. Traditional medicine in Central Sahara: Pharmacopoeia of Tassili N'ajjer. J. Ethnopharmacol, 105: 358–367.

**Hammiche. V., MAiza. K. (2006)**. Essential oils of Thymus broussonettii, T. zygisandT.satureioides, J Essent Oil Res, 5, 4553.

**Hanahan, D., & Weinberg, R. A. (2011)**. Hallmarks of cancer: The next generation. Cell, 144(5), 646–674. https://doi.org/10.1016/j.cell.2011.02.013.

**Hart T., Shears P. (1999)**.Atlas de poche de microbiologie. Flammarion MédecineScience. Paris. P 118.

**Hart T., Shears P., (1997)**. Atlas de poche de microbiologie. Ed. Flammarion.

**Has (Haute Autorité de Santé) Française. (2012)**. Rapport d'orientation - Cancer de la prostate.[http://www.has-sante.fr/portail/upload/docs/application/pdf/2012-04/rapport_dorientation_- _cancer_de_la_prostate_2012-04-03_16-39-9_898.pdf].

**Heart T. Shears P. (2006)**. Atlas de poche de microbiologie. Médecine-Sciences Flammarion.

**Hellis.Y .(2005).** الموسوعة النباتية لمنطقة سوف النباتات الصحراوية الشائعة في منطقة العرق الشرقي الكبير . P248.

**Hennekinne, JA. (2009).** Nouvelles approches pour la caractérisation des toxi-infections alimentaires à staphylocoques à coagulase positive, thèse de Doctorat. Université Agro Paris Tech, France. p : 16-17.

**Hoffmann E et Vincent S (2005)**.Spectrométrie de masse. 3e édition, BUNOD. http://tpe-huile-essentielle-e-monsite.com/page/i-les-differents-procedes-d-Extraction-d-unehuile-essentielle/4-extraction-par-solvant.htm/

**Hong GAO, Liandi Lei a, Jiaqin Liu, Qin Kong, Xingguo Chena, Zhide Hua (2004)** the study on the interaction between human serum albumin and a new reagent with antitumour activity by spectrophotometric methods. Journal of Photochemistry and Photobiology A: Chemistry 167, 213–221

**Hurley l. H., Boyd f. L. (1988)** DNA as target for drug action. Trends Pharmacol. *Sei*. 9, 402-407

**I**

**Inc (Institut national du cancer). (2020).** « Cancer de la thyroïde : du diagnostic au suivie » en ligne, 19p.

[https://www.ecancer.fr/content/download/291475/4150776/file/Cancer_de_la_thyroide_du_diagnostic_au_suivi _mel_20200605.pdf].

**Iwatsuki, M., Mimori, K., Yokobori, T., Ishi, H., Beppu, T., Nakamori, S., Mori, M. (2010).** Epithelial– mesenchymal transition in cancer development and its clinical significance. Cancer science, 101(2), 293-299.

**J**

**Jodra Serge, (2004 – 2014).** Les Bactéries. Imago Mundi. Encyclopédie gratuite en ligne.

**Jouad. H., Haloui. M., Rhiouani. H., El hilaly. J., Eddouks. M. (2001).** Ethnobotanical survey ofmedicinal plants used for the treatment ofdiabetes, cardiac and renal diseases in the Northcentreregion of Moroco (Fez-Boulemane), Jethnopharmacol, 77,175, 182p.

**K**

**Khireddine H., (2013)-** Comprimés de poudre de dattes comme support universel Des principes actifs de quelques plantes médicinales d'Algérie. Thése magister, Universit M'Hamed Bougara .Boumerdes, 96p.

**L**

**Lachance Y., (2001)-** Info Essence, Bulletin sur les huiles essentielles et autres extraits Végétaux. N° 17, pp.1-9.

**Larry M. Bush, Charles E. (2018).** Généralités sur les bactéries. LE MANUEL MSD. Version pour le grand public.

**Lecarpentier J., (2012).** Étude des facteurs modificateurs du risque de cancer du sein des femmes à risque génétique élevé. Th. Doct. Paris 11.

**Lechat P., (2006).** Pharmacologie DCEMl, Ed : CH4-PS. Paris. p : 353-354

**Leclerc H, Gaillard J-L,** Simonet M.Microbiologie générale, la bactérie et le monde bactérien. Doin Editeurs, Paris, 1995.

**Leung A.Y. et Foster S., (1996 )–** Encyclopedia of common naturel ingredients used in Food, drugs and cosmetics, a Wiley-Interscience Publication. 649p.

**Lieberman R. (2002).** "Chemoprevention of prostate cancer: current status and future direction" cancer and metastasis reviews 21 (3). P: 297-309.

**Longley, D. B., & Johnston, P. G.( 2005).** Molecular mechanisms of drug resistance. Journal of Pathology,205(2),275–292. https://doi.org/10.1002/path.1706.

**M**

**Manssouri M., Znini M. and Majidi L. (2020).** Studies on the antioxidant activity of essential oil and various extracts of *Ammodaucus leucotrichus* Coss. & Dur. Fruits from Morocco. Journal of Taibah University for Science, 14(1): 124-130.

**Mauricio Burotto, Vinay Prasad, Tito Fojo. (2015).** Non-inferiority trials: why oncologists must remain wary. Medical Oncology, Center for Cancer Research, National Cancer Institute, National Institutes of Health, Bethesda, MD 20892, USA.

**Merabet, S. A., Sekhsoukh, M. N. (2020).** Synthèse et évaluation in vitro du potentiel antioxydant et antimicrobien d'une série de composés 1,5 Benzodiazépines. 32–37.

**Moodey T W. (2006).** "Peptides hormones and lung Cancer" panminerva medica. P: 19-20.

**Morigane. (2007).** Grimoire des Plantes polytechnique de Toulouse, 22-38.

**Muhammad sirajuddin, Saqip Ali, Amin Badshah. (2013)** Drug-DNA interactions and their study by UV visible, fluorescence spectroscopies and cyclic voltametry. Journal of photochemistry and photo biologie b biology 124, 1-19.

**Muhammad Zaheera, Afzal Shaha, Zareen Akhtera∗, Rumana Qureshia, Bushra Mirzab,Misbah Tauseef b and Michael Boltec Synthesis, (2011).** Characterization, electrochemistry and evaluation of biological activities of some ferrocenyl Schiff bases. Appl. Organometal. Chem. 25, 61–69

**Musgrove. E. A., Sutherland, R. L. (2009).** Biological determinants of endocrine resistance in breast cancer. Nature Reviews Cancer, 9(9), 631-643.

**M. J. Geisow and G. H Beaven, (1977).** "Physical and Binding Properties of Large Fragments of Human Serum Albumin", Biochemical Journal, 163; 3. 477 - 484

**Maolin Wang 1,2,3, Yuanyuan Yu 1,2,3, Chao Liang 1,2,3, Aiping Lu 1,2,3, and Ge Zhang 1,2,3,( 2017).**ReviewRecent Advances in Developing Small MoleculesTargeting Nucleic

Acid International Journal of Molecular Sciences Medicinal Chemistry & Drug Discovery

**N**

**Nab-Paciitaxel (Abraxane®) (2012)**. Liaison à l'albumine permettant une pénétration naturelle du taxane dans la cellule tumorale, LIGUE CONTRE LE CANCER.

**Nafees Muhammad and Zijian Guo (2014).** Metal-based anticancer chemotherapeutic agents Chemical Biology 2014, 19:144–153. http://dx.doi.org/10.1016/j.cbpa.2014.02.003

**Ndoye M., Niang L., Gandaho K. I., Jalloh M., Labou I., Gueye S. (2014).** Cancer avancé de la prostate au Sénégal. Aspects diagnostiques à l'hôpital de Grand Yoff. Progrès en urologie, 24(5), 271-275.

**O**

**Old L. (1996) ;** L'immunotherapie. Les progres de la lutte contre le cancer. P: 592- 603. Overview of the pharmacokinetics and pharmacodynamics. Urology 54: P: 9-22.

**OMS, (2006).** Le cancer. Aide-mémoire. W. H. Organisation, Word Health Organisation.297: 1-4.

**Ouedraogo V G. (2003).** Les cancers broncho-pulmonaires au centre hospitalier national YalgadoOuedraogo : aspects épidémiologiques, cliniques et diagnostiques, Thèse de Médecine. Université d'Ouagadougou.

**P**

**Perrot E.M., (1928)** – Cultures des plantes médicinales. Ed. Presse universitaires de France, 294 p.

**Pier Giovanni Baraldi, Andrea Bovero, Francesca Fruttarolo, Delia Preti, Mojgan Aghazadeh Tabrizi, Maria Giovanna Pavani, Romeo Romagnoli(2000)** DNAMinor Groove Binders as Potential Antitumor and Antimicrobial Agents Dipartimento di Scienze Farmaceutiche, Universita` di Ferrara, 44100 Ferrara, Italy DOI 10.1002/med.20000

**Privat M. (1985).** Therapeutique. Encyclopedie universalis. P: 1122-1126.

**Q**

**Quezet, P., Santa, S. (1963).** Nouvelle flore de l'Algerie et des regions désertiques méridionale, Tome II, edition Centre national de la recherche scientifique, Paris, P 659.

**R**

**Rastogi, T., Hildesheim, A., Sinha, R., (2004).** « Opportunities for cancer epidemiology in developing coun- tries. » Nat Rev Cancer 4(11): 909-917.

**Ryan, K.J. and Ray, C.G. (Ed.). (2004).** Medical Microbiology (4th Ed.). United States of America: The McGraw-Hill Companies.

**S**

**S. Howard Armstrong, Jr., M.D (1976).** Mechanisms of Action of Serum Albumin Therapy in Internal Medicine? Boston, Massachusetts.

**S. V, K. Ayyavoo and P. Rajakumar, (2017)**. Synthesis, characterization, optical, electrochemical properties and antifungal, anticancer activities of ferrocenyl conjugated novel dendrimers. New J. Chem. DOI: 10.1039/C6NJ01120A

**Sara Realista,** Susana Quintal, Paulo N. Martinho, Ana I. Melato, Adrià Gil,Teresa Esteves, Maria De Deus Carvalho, Liliana P. Ferreira, Pedro D. Vaz & Maria José Calhorda (2016): Electrochemical studies and potential anticancer activity in ferrocene derivatives, Journal of Coordination Chemistry, DOI: 10.1080/00958972.2016.1257125

**Sébastien Faure. (2010).** Anticancereux cytotoxiques. Actualités pharmaceutiques n° 497.

**Singleton P., (1999).** Bactériologie. Ed. Dunod, 4ème édition.

**Sybille_Merceron (photo), Abdelmalek_Ghimouz, Philippe_Goater, Marc_Esteve. (2006).** Y a-t-il une conduite à tenir spécifique pour la gestion périopératoire des patients souschimiothérapie cytotoxique_? S._Merceron, Département d'anesthésie-réanimation-douleur, Institut Curie, 26 rue d'Ulm, 75005 Paris.

**T**

**Teuscher E., Anton R., Lobstein A., (2005)-** Plantes aromatiques : Epices, aromates, condiments et huiles essentielles .Paris: Tec &Doc ; 2005.522p.

**V**

**Valérie Delavigne. (2009).**Les cancers. Springer-Verlag France 978-2-287-85840-6.

**Velasco-Negueruela A., Pérez-Alonso M.J., De Paz P.P., Palá-Paúl J. And Sanz J. (2006).** Analysis by gas chromatography–mass spectrometry of the volatiles from the fruits of Ammodaucus leucotrichus subsp. Leucotrichus and subsp. Nanocarpus grown in North Africa And the Canary Islands, respectively. Journal of Chromatography A, 1108(2): 273-275.

**Villarreal Mariana Ruiz. (2006).** Bacterial morphology diagram fr.svg.

**W**

**Werker E., Putievsky E., Ravid U.** The essential oils and glandular hairs in different Chemotypes of Origanum vulgar L. Journal Annals of Botany. 1985, 55, 793-801.

**Y**

**Yaker. (1985).** Cancerologie generale, Ed : office des publications universitaire (Algerie). P : 20-40.

# *Part II:*

# *Experimental*

# *Chapter I:*

# *Materials and Methods*

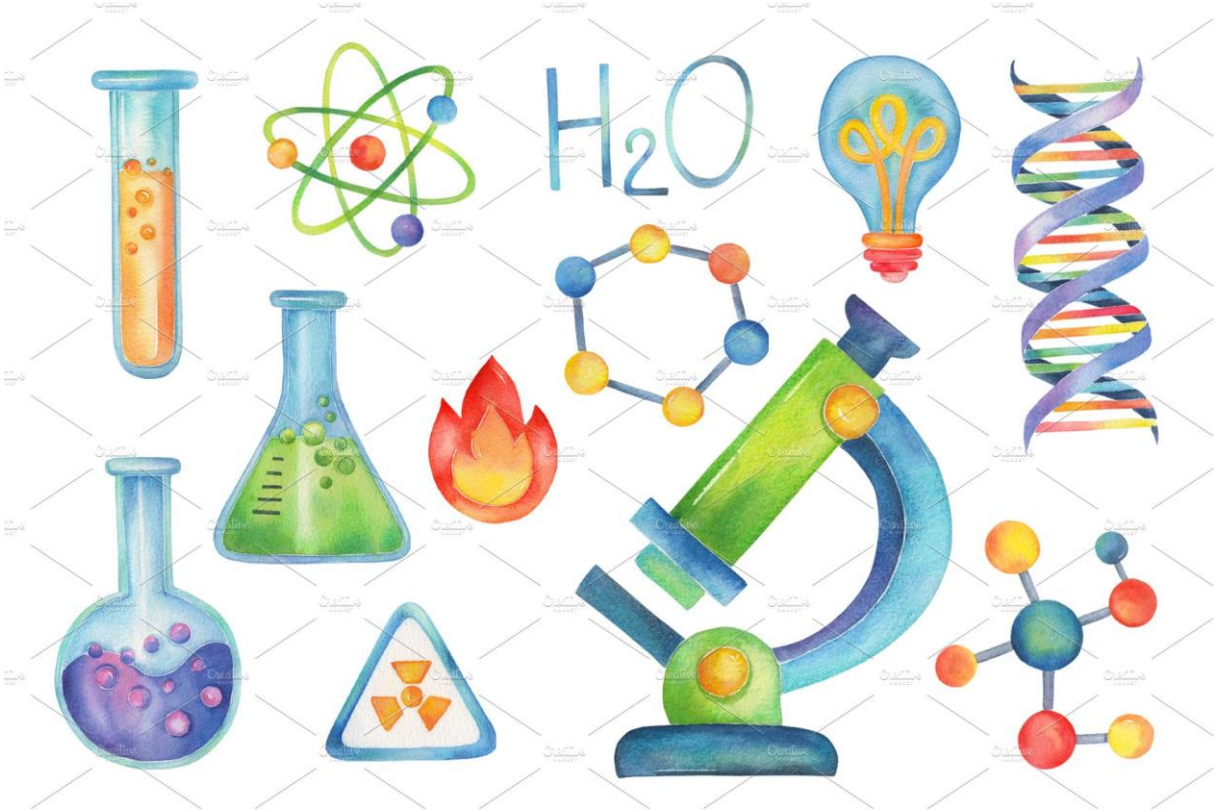

# 1. Introduction:

This study was conducted collaboratively between two specialized laboratories: the Valorisation and Technology of the Saharian Resources Laboratory (VTRS) at the Faculty of Exact Sciences, Department of Chemistry, University of El Oued, and the Centre de Recherche Scientifique et Technique en Analyses Physico-Chimique (CRAPC) in Ouargla, Algeria. The VTRS lab facilitated essential oil extraction, conducted *in vitro* and *in-silico*. Meanwhile, CRAPC handled the precise GC/MS analysis of the extracted oils. This collaborative effort ensured thorough and accurate experimentation, combining expertise and resources from both institutions.

# 2. Plant Material:

## 2.1. *Ammudaucus leucotrichus*:

The plant *Ammudoucus leucotrichus* was harvested at different time intervals during the month of June 2023 in a desertic forest region located in southeastern Algeria, specifically in the province of El Oued. The area exhibits the following specifications:

- Geographic coordinates: 33 degrees north, 6 degrees east.
- Astronomical location: Latitude 32 degrees north.
- Altitude above sea level: 82 meters.
- Distance from sea level: 230 kilometers.
- Bioclimatic character: Desertic.

## 2.2. *Mentha piperita:*

During various time intervals in May 2023, the peppermint plant (*Mentha piperita*) was harvested in a desertic woodland area located in the southeastern region of Algeria. Specifically, in Elbayadah city, which falls under the jurisdiction of the El Oued province. The region possesses the following specifications:

- Geographical coordinates: 33°N, 6°E.
- Astronomical location: Latitude 33°N.
- Elevation above sea level: 84 meters.
- Distance from sea level: 310 kilometers.
- Bioclimatic type: Desertic.

## 3. Chemicals and reagents:

### 3.1. Bovine Serum Albumin (BSA):

A solution of BSA, obtained from the educational laboratory of the biology faculty, was used as is without purification to achieve a concentration of 250 mg/50 ml in a phosphate saline buffer solution (pH = 6.33).

### 3.2. DNA Extraction Reagents:

*Blood*: Chicken blood was collected and kept directly on ice for DNA extraction.

*Red Blood Cell Lysis Buffer (TLR)*: Prepared by mixing EDTA (0.1mM), $NaHCO_3$ (12mM), $NH_4Cl$ (155mM) in distilled water.

*White Blood Cell Lysis Buffer (TLB)*: Prepared by mixing NaCl (50mM), EDTA (100mM), Tris (10mM) at pH=7.42.

*SDS Solution (20%)*: Prepared by mixing 2mg of sodium dodecyl sulphate in 10ml of distilled water.

*Saturated NaCl Solution:* Prepared by mixing 7g of sodium chloride in 10ml of distilled water.

### 3.3. Microorganisms Used:

All microorganisms used in these studies were provided by the pedagogical laboratory of the faculty of biology.

- *Escherichia coli (ATCC 25922):* Belongs to the Enterobacteriaceae family. It is non-spore forming, facultative anaerobic, and typically motile due to flagella. Its length ranges from 2 to 6 µm and its width from 1.1 to 1.5 µm.
- *Bacillus subtilis (ATCC 6051-U)*: A Gram-positive bacterium with a length ranging from 2 to 3 µm and a width from 0.3 to 0.5 µm.
- *Staphylococcus aureus (ATCC 25923)*: Is a Gram-positive spherical bacterium with a diameter ranging from 0.5 to 1.5 µm, belonging to the genus Staphylococcus.

### 3.4. Phosphate Buffer Solution:

The phosphate buffer saline solution was meticulously prepared using sodium dihydrogen phosphate and disodium hydrogen phosphate (Sigma Aldrich) in conjunction with double-distilled water and KCl. The pH was meticulously maintained at 6.4 through the utilization of this phosphate buffer.

# 4. Materials and Methods:

## 4.1. Essential Oils Extraction:

### 4.1.1. Apparatus:

The essential oil extraction process required the use of specialized equipment to ensure accuracy and efficiency. In this study, the following apparatus was utilized:

- ✓ Adventurer – Pro AV53 sensitive balance
- ✓ Heating flask
- ✓ Refrigerant
- ✓ Clevenger apparatus
- ✓ Separating funnel
- ✓ Rotary evaporator

The Clevenger apparatus, a key component in the extraction process, is depicted in Figure 10.

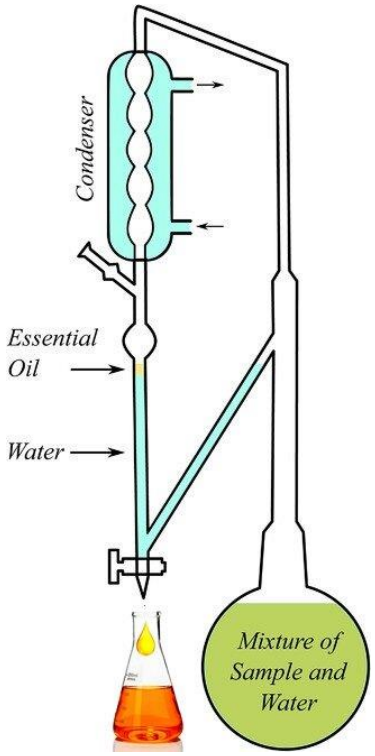


**Figure 10:** Schematic representation of the Clevenger apparatus used in the essential oil extraction process (Biswa et al., 2023)

### 4.1.2. Procedure:

The procedure for essential oil extraction involved a series of meticulous steps to ensure optimal results. The extraction process was conducted as follows:

- ✓ Cleaning of the plant sample to remove any impurities.

- ✓ Weighing the plant sample to a quantity of 100 g using a sensitive balance.
- ✓ Washing the plant sample with water to prevent burning, followed by placement in a heating flask.
- ✓ Addition of small pieces of boiling regulator to the flask.
- ✓ Direct heating of the mixture at a temperature of 100 degrees Celsius for three and a half hours.
- ✓ Conducting the steam distillation process and subsequent separation of oil and water phases using liquid-liquid separation with diethyl ether.
- ✓ Drying of the organic oily phase with anhydrous sodium sulphate.
- ✓ Filtration of the dried oil phase through filter paper to remove diethyl ether particles.
- ✓ Evaporation of the filtered oil phase using a rotary evaporator to remove any remaining organic solvent.
- ✓ Storage of the obtained essential oil in small brown bottles and refrigeration at a temperature of 5°C.

**4.2. Yield of Essential Oil Extraction:**

Two distinct methodologies are commonly employed to ascertain the yield of essential oil extraction, each offering unique perspectives on the efficiency of the process.

**4.2.1. Volumetric Yield - Mass-based:** (Naima et al., 2019)

This method entails an assessment of the mass of the utilized plant material intended for essential oil extraction, juxtaposed against the volume of the resultant oil. The yield is then computed utilizing the following Equation 1:

$$R_{EO} = \frac{V_{EO}(ml)}{m_0(g)} \times 100 \quad (1)$$

Where: $R_{EO}$: Essential oil yield, $m_0$: Mass of the utilized plant sample, $V_{EO}$: Volume of the extracted essential oil

**4.2.2. Mass-based Yield - Mass-based:** (Larbi et al., 2018)

Alternatively, the essential oil extraction yield is defined as the quotient of the mass of the extracted essential oil and the mass of the plant material utilized. This yield is calculated using Equation 2:

$$R_{EO} = \frac{m_{EO}(g)}{m_0(g)} \times 100 \quad (2)$$

Where:$R_{EO}$ Essential oil yield,$m_0$: Mass of the utilized plant sample,$m_{EO}$: Mass of the extracted essential oil

These methodologies have been systematically applied to derive essential oil yields for all examined plant specimens.

### 4.3. Characterization of Essential Oils:

The characterization of essential oils comprises two fundamental components: physicochemical properties and Gas Chromatography-Mass Spectrometry (GC/MS) analysis.

#### 4.3.1. Physicochemical Properties:

Here, we delve into the fundamental traits of essential oils, including their relative density, acidity, ester content, and refractive index. These properties offer valuable insights into the composition and behavior of essential oils, helping us understand their chemical makeup and how they interact with their environment (Atti-Santos et al., 2005).

- *Relative Density (AFNOR NF T75-111 Standard):*

At 20°C, 1 mL of the essential oil is measured using a pipette, and its mass is then determined. The procedure is repeated for distilled water, and density is calculated using the following Equation 3 (Valarezo et al., 2015):

$$d = \frac{m_{EO}}{m_{H_2O}} \tag{3}$$

Where:$m_{EO}$ Mass of the extracted essential oil,$m_{H_2O}$: Mass of the distilled water

- *Acidity Index (AFNOR NF T75-111 Standard):*

To determine the acid value, representing the concentration of free acids in 1 g of the essential oil, a titration method with potassium hydroxide (KOH) solution is employed (Sahoo et al., 2007).

Initially, a small aliquot (0.5 mL) of the essential oil is mixed with 2 to 3 drops of phenolphthalein indicator in a small vessel. Subsequently, titration is performed with 0.5 N KOH solution until the appearance of a faint pink colour, indicating complete neutralization of the acids. The acid value is then calculated using the following Equation 4.

$$I_a = \frac{56.11 \times V \times C}{m} \tag{4}$$

Where: V: the volume of the KOH solution, C: Concentration of KOH, m: the mass of the essential oil

➢ *Ester Index (AFNOR NF T75-111 Standard):*

The determination of free acids resulting from ester hydrolysis within the essential oil involves a titration process utilizing 0.5 N potassium hydroxide (KOH) solution (Alajtal et al., 2018).

- Begin by placing 0.5 mL of the essential oil into a small vessel.
- Add 1 mL of 0.5 N potassium hydroxide (KOH) solution to the vessel to initiate the titration process.
- Place the mixture in a gas-evacuated water bath for a specified duration to facilitate reaction.
- After cooling, introduce 0.5 mL of distilled water and add 3 drops of phenolphthalein indicator to the mixture.
- Titrate the excess potassium hydroxide (KOH) using 0.5 N hydrochloric acid (HCl) until a colour change is observed, indicating neutralization.
- Quantify the volume of hydrochloric acid (HCl) required to neutralize the excess potassium hydroxide (KOH).
- Calculate the ester content using the following Equation 5:

$$I_e = \frac{2805}{m}(V_0 - V_1) - I_a \quad (5)$$

Where: $V_0$ (ml): Volume of hydrochloric acid (HCl) without essential oil, $V_1$(ml): Volume of hydrochloric acid (HCl) in the presence of essential oil, $I_A$: Acid value, $I_e$: Ester value and m: Mass of the essential oil sample.

➢ *Refractive Index (AFNOR NF T75-111 Standard):*

The refractive index of an essential oil is defined as the ratio between the sine of the angle of incidence and the sine of the angle of refraction of a light ray, with a specific wavelength, transitioning from air into the essential oil, while the latter is maintained at a constant temperature (Singh, 2002)

The refractive index of the essential oil is directly measured using a refractometer at a reference temperature 20°C.

### 4.3.2. Gas Chromatography-Mass Spectrometry (GC/MS) analysis:

The coupling (GC/MS) technique stands as the most frequently employed method within the field of essential oils, facilitating the concurrent separation, identification, and quantitative measurement of the various constituents present in extracted oils.

➢ *Principle:*

The principle is founded on the varying affinities of compounds within the mixture towards two phases: a stationary phase and a mobile phase. This technique relies on the distribution of constituents between a stationary phase and a gas phase. The stationary phase comprises a silicone-based liquid that permeates an inert and granular solid material, housed within a typically coiled steel or glass column measuring 1 to 3 meters in length and 2 to 4 millimetres in diameter. The mobile phase consists of an inert carrier gas such as nitrogen, helium, or argon.

The column is maintained at a high temperature via a furnace. Under the influence of temperature, constituents vaporize and become separable. The basis of separation lies in the discrepancy of partition coefficients of volatile compounds between the stationery and gas phases. A detection system generates a signal at the exit of each molecule from the column, manifesting as the recording of peaks corresponding to each constituent.

Gas chromatography is coupled with a mass spectrometer (MS); this coupling relies on computerized comparison of the spectrum of an unknown peak with one or more reference libraries, enabling its identification.

➢ *Apparatus:*

The identification of the chemical constituents of our essential oils was performed using a gas chromatographic system (HP 5890-SERIE II) equipped with an HP5 MS capillary column (30 meters in length, 0.25 mm internal diameter, and 0.25 µm film thickness) coupled with a mass spectrometer (HP-MSD 5972).

$N_2$ was employed as the carrier gas for the analysis of the two essential oils. Spectra were recorded at an emission energy of 70 eV, and spectral analysis of the compounds was conducted by comparison with their counterparts using the WILEY275 (Chiu et al., 1982; Guinaudeau et al., 1975; Kiryakov, 1968; Shamma, 1972) spectral librairies.

➢ *Procedure:*

The carrier gas ($N_2$) is introduced at a flow rate of 1 mL/min, with the injected volume of the essential oil being 1 µL in split injection. The injector and detector temperatures are set at 250°C and 320°C, respectively. The oven temperature is programmed to initially reach 60°C and held for 8 minutes, then gradually increased to 250°C at a rate of 2°C/min, maintained isothermally at 250°C for 15 minutes, and finally elevated to 300°C at a rate of 10°C/min.

## 4.4. *In Vitro* Assessment of the Biological Activities:

### 4.4.1. Anticancer Activity:

*4.4.1.1. DNA Extraction:*

The isolation of DNA from blood can be achieved using various techniques, different protocols, and a wide range of commercially available kits (Filote et al., 2022). The chosen DNA extraction technique should be able to provide pure DNA samples ready for use in studying anticancer activity with essential oils.

In this study, we isolated DNA from chicken blood using salting-out techniques (Gaaib et al., 2011; Miller et al., 1988). The advantage of this technique is that it avoids the use of toxic and corrosive organic solvents and only utilizes standard chemicals that can be obtained from any commercial supplier, and it does not require specialized equipment or biochemical knowledge (Nasiri et al., 2005; Rivero et al., 2006). The DNA purification protocol is based on protein precipitation at high salt concentration. The traditional protocol involves initial cell disruption and digestion with sodium dodecyl sulphate, followed by the addition of high salt concentrations, typically 6 M sodium chloride. The mixture is then centrifuged to allow proteins to precipitate to the bottom, with the supernatant containing the transferred DNA into a new flask. DNA is then precipitated using cold ethanol (Howe, 1997). The steps involved in DNA extraction are summarized in Figure 11.

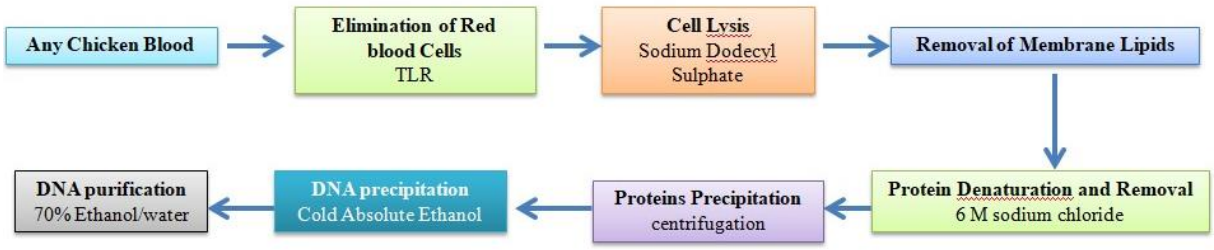


**Figure 11:** Steps Involved in DNA Extraction

✓ *Blood Sample:*

DNA is extracted from chicken blood using salting-out techniques. Chicken blood differs from human blood in that red blood cells are also nucleated and contain much more DNA than non-nucleated mammalian blood. This allows for obtaining chicken DNA in sufficient quantity and quality using relatively simple extraction techniques. Therefore, during DNA purification from chicken blood, there is more DNA material compared to working with human blood (Javanrouh & Jelokhani-niaraki, 2020).

✓ *Blood Collection:*

Samples of chicken blood were collected in blood collection tubes containing EDTA as an anticoagulant and stored at room temperature in microcentrifuge tubes, and extracted on the same working day.

✓ *Extraction Procedure:*

5 ml of whole chicken blood sample is placed in a 20 ml flask, then 10 ml of TLGR (Red Blood Cell Lysis Buffer) was added to the blood and the resulting mixture was cooled in an ice bath for 20 minutes, then centrifuged at 2500 rpm for 15 minutes at room temperature. This step was repeated 3 to 4 times until the red color of the blood disappeared, then the flask was left to dry for 5 minutes.

The white blood cells were removed by adding 2 ml of TLGB buffer and vortexed for 3 minutes. Subsequently, cell lysis was carried out by adding 150 µL of sodium dodecyl sulphate solution and centrifuged at 172 rpm for 90 minutes at 55°C. After centrifugation, 3 ml of 6 M sodium chloride solution was added, and the resulting mixture was vortexed for 6 minutes and then centrifuged at 1300 rpm for 10 minutes. The liquid phase was recovered, and 2 volumes of cold isopropanol were added, followed by centrifugation at 1300 rpm for 30 minutes at room temperature. DNA was then recovered from the isopropanol layer, washed several times with 70% ethanol, and characterized using UV-Vis spectroscopy. Figure 12 shows the UV-Vis spectrum of the isolated DNA.

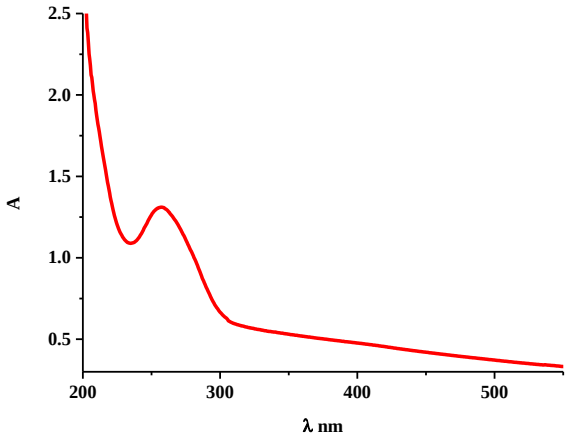


**Figure 12:** Electronic Spectrum of Extracted DNA Sample

UV-Vis spectroscopy can be used to detect protein contamination in extracted DNA (Saab et al., 2007). Proteins exhibit two absorption peaks in the UV region: the first peak is located between 190-210 nm, attributed to electronic transitions in the peptide backbone, and the

second peak is situated at 280 nm due to absorption by the aromatic amino acids tyrosine, tryptophan, and phenylalanine (Khennoufa et al., 2021).

✓ *Estimation of DNA Purity:*

The isolated DNA cannot be used without further purification as it contains contaminating RNA and proteins. Therefore, the DNA is rehydrated in distilled water, and this dissolution requires continuous agitation overnight at 42°C. The concentration and purity of the DNA can be determined by measuring ultraviolet light absorption. DNA has maximum and minimum absorption at 260 nm and 234 nm, respectively (Telfer et al., 2013). The purines and pyrimidines in the nucleic acid are responsible for these absorptions. At 260 nm, double-stranded DNA has a specific absorption coefficient of 0.02 $(\mu g/ml)^{-1}cm^{-1}$ (Griffiths & Chacon-Cortes, 2014). Additionally, the ratio of $A_{260}/A_{280}$ can detect nucleic acid purity relative to protein contamination, as proteins have maximum absorption at 280 nm. Highly purified DNA samples have a 260/280 nm ratio of (1.7-1.9), so below (1.7), a significant amount of protein impurities may be present in the sample (Whitlock et al., 2008). The $A_{260}/A_{230}$ ratio is determined to confirm that the sample is free from carbohydrates, peptides, ethanol, or any other organic compounds, and it is generally greater than 1.5 (Ning et al., 2009).

Therefore, good quality DNA should have:

$$\frac{A_{260}}{A_{280}} = 1.7 - 2 \qquad \text{and} \qquad \frac{A_{260}}{A_{230}} > 1.5$$

In our study, we used UV-Vis spectroscopy to estimate the purity of the isolated DNA. The absorbance values of the DNA solution obtained were measured at 230, 260, and 280 nm to determine the concentration and purity of the extracted DNA. The dissolved DNA can be stored at 4°C for a few days or at -20°C for longer-term storage (Heckel et al., 2017). The absorbance values were taken from Figure 12 and listed in Table 3. The values obtained for the various absorbance ratios indicate the high purity of the isolated DNA.

**Table 3 :** Absorbance Ratoi of Isolated DNA

| $A_{230}$ | $A_{260}$ | $A_{280}$ | $A_{260}/A_{230}$ | $A_{260}/A_{280}$ |
|---|---|---|---|---|
| 1.116 | 1.301 | 1.021 | 1.166 | 1.724 |

✓ *Estimation of DNA Quantity:*

The quantity of DNA was determined by absorption spectroscopy using the molar extinction coefficient value of 6600 $M^{-1}cm^{-1}$ at 260 nm (Schöppler et al., 2011).

*4.4.1.2. Cyclic Voltammetric Measurements:*

✓ Apparatus:

The apparatus used for voltammetric measurements is a Potentiostat/Galvanostat Model PGZ301 (Radiometer Analytical SAS) connected to a three-electrode electrochemical cell,

- A glassy carbon electrode with a diameter of 5.2 mm².
- A mercury/mercurous chloride/saturated KCl reference electrode.
- A platinum auxiliary electrode with a diameter of 3 mm².

All of this is controlled by a Pentium IV microcomputer (CPU 4.0 GHz and RAM 2 GB) equipped with VoltaMaster4 software, version 7.08.

✓ Reagents:

- Potassium phosphate buffer solution
- Electrolyte support (Tetra-n-butylammonium tetrafluoroborate, 99%)
- Ethanol
- Nitrogen (Gas)
- Ultra-pure water

✓ Procedure:

The reaction between the essential oils and the DNA/BSA takes place in the electrochemical cell. The reaction medium is a buffer solution consisting of a mixture of monopotassium and dipotassium phosphate ($KH_2PO_4$+$K_2HPO_4$) at 0.1 M and pH 7.2.

Before each measurement, the working electrode is polished using p4000 abrasive paper. After polishing, the electrode is washed with ultra-pure water and dried with air. The surface of the electrode thus appears mirror-like. Then, the electrochemical cell is equipped with the reference electrode and the auxiliary electrode, as well as the working electrode. The cell is filled with 10 ml of a solution consisting of 90% ethanol/buffer solution containing the essential oils under study. Nitrogen gas is bubbled through the solution for 10 to 15 minutes to remove oxygen from the cell. A variable potential is applied at a fixed scan rate and at a temperature of 28 ± 2°C. The obtained voltammogram is analysed to access the interaction parameters between the studied essential oil and the DNA/BSA.

*4.4.1.3. Spectroscopic Measurements:*

✓ Apparatus:

UV-Vis measurements were performed using a UV-Vis spectrometer (Shimadzu 1800) and a quartz cell with a volumetric capacity of 5 ml. Data acquisition was carried out with a Pentium

IV microcomputer (CPU 4.0 GHz and RAM 2 GB) equipped with UV probe software version 2.34 (Shimadzu). The data is processed using OriginLab 9.0 software.

✓ Reagents:

- Potassium phosphate buffer solution
- Ethanol
- Ultra-pure water

✓ Procedure:

The electronic spectra of essential oil in the 90% ethanol/potassium phosphate buffer solution were obtained in the absence and presence of increasing concentrations of DNA/BSA.

**4.4.2. Antibacterial Activity:**

✓ Procedure:

Antimicrobial tests were conducted to evaluate the biological activity of the studied essential oils against *Escherichia coli*, *Bacillus subtilis* and *Staphylococcus aureus*. The antimicrobial activity was assessed using the disc diffusion method as described in the literature (Klančnik et al., 2010):

- *Preparation of test products:* Dissolve EOs in DMSO to prepare solutions of different concentrations ranging from 2 to 40 mg/ml.
- *Preparation of precultures:* Cultivate the microbial strains to be tested on Petri dishes containing nutrient agar and incubate for 24 hours at 37°C to obtain a young culture of bacteria and isolated colonies.
- *Preparation of discs:* Prepare discs using 6mm diameter Whatman filter paper, followed by sterilization for 30 minutes at 120°C in the autoclave.
- *Preparation of bacterial suspensions:* Take a few well-isolated and identical colonies using a Pasteur pipette and suspend them in 10 ml of sterile physiological saline solution (0.9% NaCl). Standardize the bacterial suspension using a densitometer for seeding into the MH milieu.
- *Preparation of culture milieu:* Utilize various culture milieu including nutrient broth for isolation and maintenance of bacterial strains, nutrient agar for reactivation of the bacterial strain, and Mueller-Hinton agar for studying bacterial sensitivity to different concentrations of EO.
- *Testing antibacterial activity:* Spread the bacterial suspension over the entire surface of Mueller Hinton agar (MHA) three times using a sterile swab, then leave on the bench for 30

minutes. Assess antibacterial activity by measuring the diameter of the inhibition zone using a ruler and comparing it with that of DMSO as a negative control and antibiotics as positive controls (Amoxicillin 25 µg/disc). Measure absorbance using UV-vis spectroscopy.

The inhibitory activity of bacteria was calculated as a percentage of inhibition using the following Equation 6 (Klančnik et al., 2010):

$$\%Inhibition = \left(1 - \frac{Abs_{Essential\ oil}}{Abs_{Controle}}\right) \times 100 \quad (6)$$

**4.5. *In-Silico* analysis:**

**4.5.1. Software:**

Computational simulations, including Induced Fit Docking, molecular dynamics studies, and MM-GBSA calculations, were conducted employing the Glide module, Induced Fit Docking module, Prime module, and the Desmond module within the Maestro version 11.7 user interface of the Schrödinger suite (Small-Molecule Drug Discovery Suite 2021-4, Schrödinger, LLC, New York, NY, 2021) (Schrödinger, 2015). The simulations were executed on a DELL Intel(R) Core (TM) i9-13900HX CPU @ 2.20 GHz processor, equipped with 32.0 GB RAM, and operated on a 64-bit Linux Ubuntu 18,04.1 LTS operating system.

**4.5.2. ADMET and drug-likeness evaluation:**

Drug candidates should possess favourable ADMET properties and ideally non-toxic. Therefore, the major identified compounds from the essential oils extract were evaluated of their ADME profile, including physicochemical, lipophilicity, water solubility, pharmacokinetics, drug-like nature, medicinal chemistry, and several other parameters using SwissADME (Daina et al., 2017; Riyadi et al., 2021) module provided in SIB (Swiss Institute of Bioinformatics) webserver (https://www.sib.swiss). Furthermore, the toxicity aspect of designed compound was also predicted using ProTox (Banerjee et al., 2018) webserver (https://comptox.charite.de/protox3/).

**4.5.3. Docking setup:**

- *Ligands preparation:*

The three-dimensional configurations of the major compounds isolated from *Ammudaucus leucotrichus* and *Mentha piperita* essential oils were obtained from the National Library of

Medicine (NCBI) database (Kim et al., 2016), accessible through the NCBI website (https://pubchem.ncbi.nlm.nih.gov/).

Ligand preparation involved an energy optimization process to derive the most energetically favourable conformations for each compound. Utilizing LigPrep module within the Schrödinger suite (Schrödinger, 2024), this optimization procedure ensured the attainment of the lowest energy state for the studied drugs, including Montbretin A (a co-crystallized ligand). The ionization states were established at a pH of 7.0 ± 2.00, as computed by the Epik classic module, while maintaining specified chirality and generating relevant tautomeric forms. Furthermore, partial atomic charges were computed using Optimized Potentials for Liquid Simulations OPLS4 force field (Lu et al., 2021).

- *Receptor Preparation:*

The 3D structures of specifically selected receptors have been scrutinized, including the human DNA receptor (PDB ID: 1W0T) (Court et al., 2005), bovine serum albumin (PDB ID: 6QS9) (Castagna et al., 2019), Escherichia coli (PDB ID: 6F86) (Narramore et al., 2019), Bacillus subtilis (PDB ID: 8I2F) (Tandukar et al., 2023), and Staphylococcus aureus (PDB ID: 6LKI) (M. Wang et al., 2020). Details pertaining to these receptors, encompassing their designations and corresponding PDB IDs, are delineated within Table 4.

Processing of the proteins and DNA structures was executed through the "protein preparation Workflow" module within the Schrödinger suite (Madhavi Sastry et al., 2013), involving consecutive stages of import and processing, review and modification, and refinement.

In the initial stage, the Prime tool was employed to address missing residues and side chains, maintaining the pH of PROPKA at 7.0 ± 2.00. Subsequent steps included the optimization and assignment of hydrogen bonds, along with the removal of water molecules beyond 8 Å. Restrain minimization utilizing the Optimized Potentials for Liquid Simulations (OPLS4) force field was performed to achieve a low-energy state for the protein (Lu et al., 2021). This phase of protein preparation signifies an energy optimization methodology, presenting the protein in its energetically favourable state for subsequent *in-silico* studies.

The "Receptor grid generation" panel facilitated the creation of a grid encompassing the active site of the protein, delimited by the co-crystallized ligand Montbretin A. Default parameters were maintained, and the grid centre was generated at the coordinates X = -6.65; Y = 6.99; Z = -20.65.

**Table 4 :** Target receptors information chsen for docking studies

| | | |
|---|---|---|
|  | ***hTRF1 DNA-binding domain in complex with telomeric DNA*** | |
| | PDB ID | 1W0T |
| | Mutation | No |
| | Resolution (Å) | 2.00 |
| | R-Value Observed | 0.252 |
| | Organism | Homo sapiens |
| | Space Groupe | P $2_1$ $2_1$ $2_1$ |
| | Sequence Length | 53 |
| 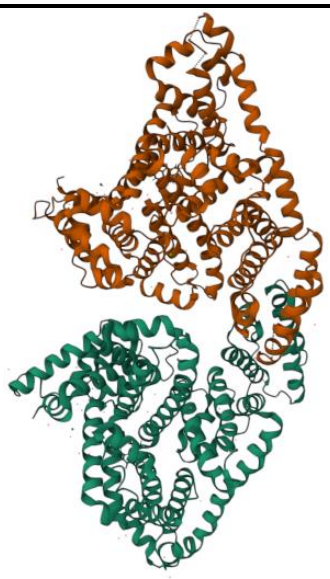 | ***Bovine Serum Albumin in complex with Ketoprofen*** | |
| | PDB ID | 6QS9 |
| | Mutation | No |
| | Resolution (Å) | 2.80 |
| | R-Value Observed | 0.218 |
| | Organism | Bos taurus |
| | Space Groupe | C 1 2 1 |
| | Sequence Length | 607 |
| 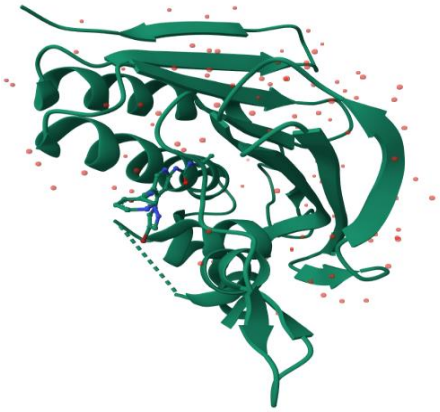 | ***Crystal Structure of E. coli GyraseB 24kDa*** | |
| | PDB ID | 6F86 |
| | Mutation | No |
| | Resolution (Å) | 1.90 |
| | R-Value Observed | 0.204 |
| | Organism | Escherichia coli |

| | | |
|---|---|---|
| | Space Groupe | P $3_2$ 2 1 |
| | Sequence Length | 206 |
| 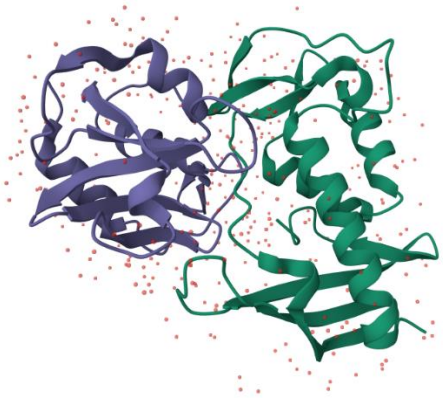 | ***Crystal structure of Bacillus subtilis LytE catalytic domain in complex with IseA*** | |
| | PDB ID | 8I2F |
| | Mutation | No |
| | Resolution (Å) | 2.03 |
| | R-Value Observed | 0.175 |
| | Organism | Bacillus subtilis |
| | Space Groupe | P $2_1$ $2_1$ $2_1$ |
| | Sequence Length | 282 |
| 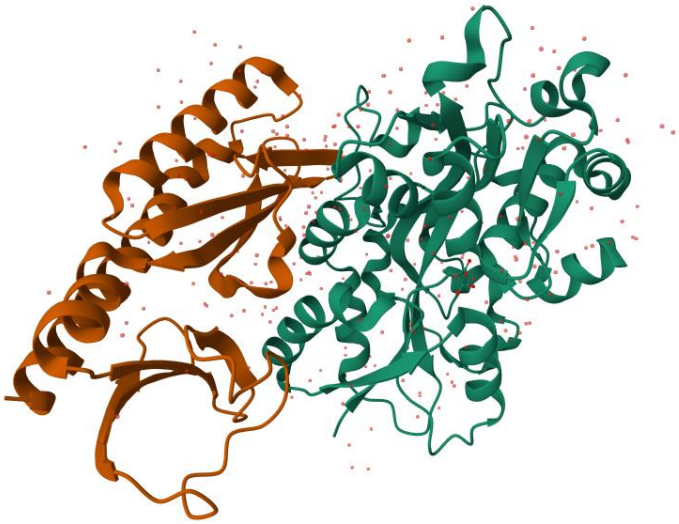 | ***Two-component system protein mediate signal transduction*** | |
| | PDB ID | 6LKI |
| | Mutation | No |
| | Resolution (Å) | 1.78 |
| | R-Value Observed | 0.210 |
| | Organism | Staphylococcus aureus |
| | Space Groupe | C 2 2 $2_1$ |
| | Sequence Length | 471 |

- *Molecular Docking:*

Computational simulations, including Induced Fit Docking, molecular dynamics studies, and MM-GBSA calculations, were conducted employing the Glide module, Induced Fit Docking module, Prime module, and the Desmond module within the Maestro version 11.7 user interface of the Schrödinger suite (Small-Molecule Drug Discovery Suite 2021-4, Schrödinger, LLC, New York, NY, 2021) (Schrödinger, 2015). The simulations were executed on a DELL Intel(R)

Core(TM) i9-13900HX CPU @ 2.20 GHz processor, equipped with 32.0 GB RAM, and operated on a 64-bit Linux Ubuntu 18,04.1 LTS operating system.

The molecular docking tool employed for all docking studies was Glide (Grid-based Ligand docking with Energetics), a module within the Schrödinger suite (Yang et al., 2021). The prepared ligands underwent docking onto the specified protein site utilizing the Glide module, in Standard Precision (SP) modes (Friesner et al., 2006).

- *Induced Fit Docking (IFD):*

The Induced Fit docking (IFD) module of the Maestro molecular modelling suite has been noted as a reliable and effective docking approach to consider flexibility in both ligands and the binding pocket residues in the binding pocket of target receptors (Khelil et al., 2020). During the IFD process, Glide/SP (Standard Precision) was performed for each ligand, the Prime refinement step specifically addressed the side chains of residues within a 5 Å radius of the ligand. Noteworthy is the retention of a maximum of 20 poses for each ligand.

- *Molecular Dynamics Simulation (MDS):*

The best compound in each plant exhibiting the highest IFD docking score was chosen for Molecular Dynamics Simulation (MDS). Recognizing the limitations of ligand docking in representing the biological system under aqueous conditions (Korb et al., 2012), a 100 ns simulation time for MDS was executed using the Desmond module within the Schrödinger suite (Bowers et al., 2006).

The MDS protocol comprised three essential steps: system builder, minimization, and MDS. In the system builder phase, the protein and ligand complex were selected and immersed in a biological environment. The transferable intermolecular potential with 3 points (TIP3P) solvent model, with the boundary condition maintained in an orthorhombic box form throughout the process with dimensions of 10 x 10 x 10 Å (Akbar et al., 2022). The OPLS-3e force field was consistently applied (Roos et al., 2019). The neutralization of model was conducted by addition of counter ions when needed and 0.15 M of NaCl salt was included to mimic the physiological state.

Subsequently, the NPT ensemble was utilized for energy minimization, maintaining pressure and temperature at 1.0132 bar and 300 K, respectively. Finally, MDS was conducted for the minimized protein-ligand complex (Halder et al., 2023).

- *Free Energy (MM-GBSA) Calculation:*

Upon completion of the dynamic simulation, an assessment of the free binding energy between the protein and the ligand was systematically undertaken utilizing the Prime MM-GBSA module within the Maestro molecular modelling suite (E. Wang et al., 2021). The calculation of ligand binding affinities was accomplished through the Molecular Mechanics/Generalized Born Surface Area ΔG (MM-GBSA ΔG) metric applied to the optimized Receptor-Ligand Complex. This computation, facilitated by the VSGB solvation model and the OPLS4 force field, stands as a methodologically rigorous approach for the comprehensive evaluation of molecular interactions and binding strengths (Gorla et al., 2021).

# *Chapter II:*

# *Results and*

# *Discussion*

## 1. Introduction:

This chapter delves into the findings regarding the extraction yield, characterization, and comprehensive exploration of the anticancer and antibacterial properties inherent in two essential oils derived from the aerial constituents of *Ammudoucus leucotrichus* and *Mentha piperita*. The overarching aim of this investigation was to assess the potential anticancer and antibacterial efficacy exhibited by essential oils as significant agents in the domain of novel pharmaceutical development.

The elucidations provided herein furnish intricate insights into the chemical constitution of the essential oils, thereby enabling their utilization in the *in-silico* study. This involved the application of advanced computational techniques such as Induced Fit Docking (IFD) and Molecular Dynamics Simulation (MDS) for each compound, capabilities not feasible in traditional *in vitro* studies.

## 2. Extraction Yield:

Figure 13 illustrates the yields of essential oils obtained through hydrodistillation of the aerial parts of *Ammudoucus leucotrichus* and *Mentha piperita*. Variety of Eloued.

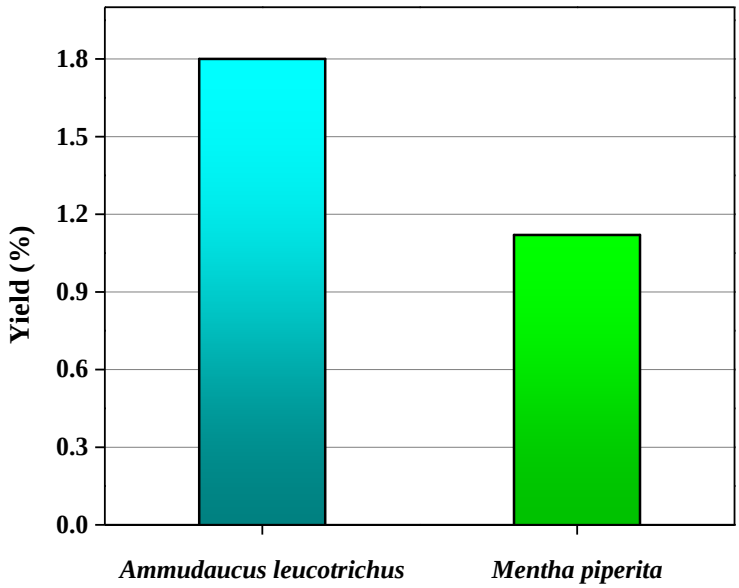


**Figure 13:** The yields of extracted essential oils

We observe that *Ammudoucus leucotrichus* exhibits a higher essential oil yield than *Mentha piperita* (1.80% and 1.12% respectively). However, the difference between the two yields is non-significant.

Nevertheless, findings reported by (Manssouri et al., 2020) indicate lower yields of essential oils extracted by hydrodistillation from *Ammudoucus leucotrichus* at ambient temperature.

Similar results to ours were, however, obtained by (Naima et al., 2019) for the essential oil extracted from the same variety using the same method.

Furthermore, significantly higher yields were achieved by (Samber et al., 2015) during the hydrodistillation of *Mentha piperita*.

These variations in results can be explained by the fact that essential oil yields are influenced by several factors during extraction: either factors related to the plant (species, variety, chemical composition, etc.) or factors associated with experimental conditions (extraction process, extraction duration, etc).

## 3. Chemical composition of essential oils:

### 3.1. Organoleptic characteristics:

Through the conducted work, it has been revealed that the essential oil extracted from the studied plants exhibits the following (Table 5) organoleptic properties:

**Table 5 :** The organolptic characteristics of essential oils

| Plant | Smell | Aspect | Colour |
|---|---|---|---|
| ***Ammudoucus leucotrichus*** | A strong smell | liquid at room temperature | Bleu |
| ***Mentha piperita*** | A pleasant fragrance | liquid at room temperature | Light-yellow |

### 3.2. Physicochemical Properties:

The physicochemical properties were meticulously determined according to the standards of the French Association for Standardization (AFNOR) using established methodologies to measure relative density, refractive index, acidity index, and ester index, as depicted in the following Table 6.

**Table 6 :** The physicochemical properties of essential oils

| Plant | Relative Density | Refractive Index | Acidity Index | Ester Index |
|---|---|---|---|---|
| ***Ammudoucus leucotrichus*** | 0.887 | 1.4268 | 4.30 | 40.91 |
| ***Mentha piperita*** | 0.933 | 1.4601 | 4.46 | 41.88 |

By comparing these results to those obtained by (Naima et al., 2019) (density 0.953, refractive index 1.474, acidity index 4.93 and ester index 45.96) and (Mimica-Dukić et al., 2003) (density: 0.834 ± 0.02, 0.835 ± 0.02, refractive index, at 25°C 1.4596 ± 0.03, 1.4622 ± 0.04), and considering that the refractive index was measured at a temperature of 23°C, we can conclude that these values are in accordance with the standards described by AFNOR (Afnor, 1982).

### 3.3. Gas Chromatography-Mass Spectrometry (GC/MS) analysis:

The analysis focused on the essential oil constituents extracted from two specific plant species using gas chromatography-mass spectrometry (GC/MS). Mass spectra corresponding to each chromatographic peak were juxtaposed with spectra from relevant scientific literature and the Weily electronic database for mass spectra (Horai et al., 2010). Retention indices were employed to ascertain compound identities. Moreover, utilizing the identical non-polar HP5 stationary phase in the gas chromatography column facilitated the preservation of consistent peak numbers and elution sequences for the compounds under investigation.

Figure 14 and Figure 15 depict the chromatograms illustrating the essential oil compositions of *Ammudoucus leucotrichus* and *Mentha piperita*, respectively, as obtained through gas chromatography-mass spectrometry (GC/MS) analysis:

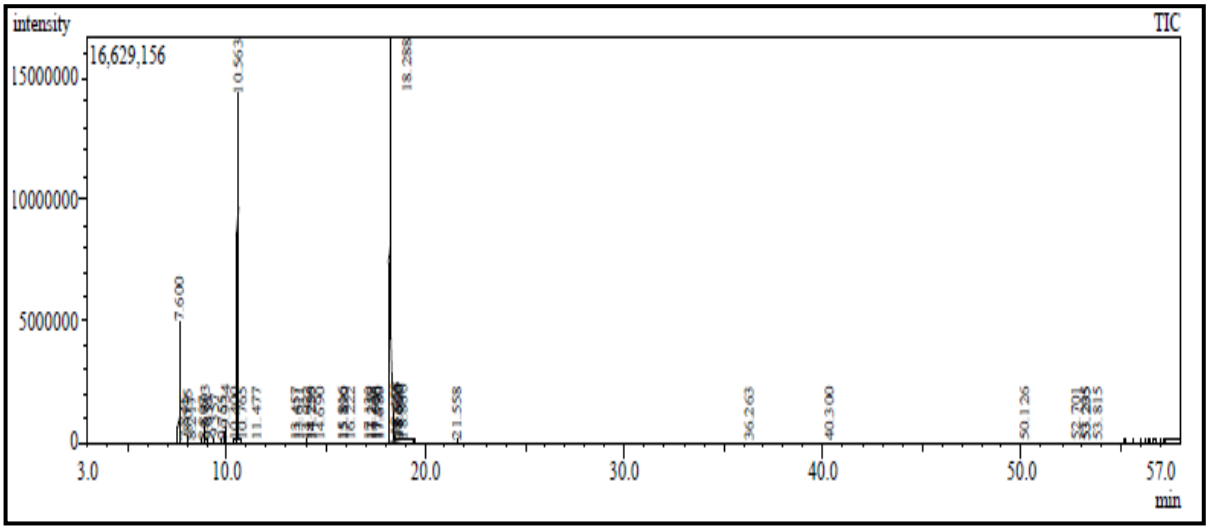


**Figure 14:** Chromatogram of the essential oil of *Ammudoucus leucotrichus* plant obtained by GC/MS

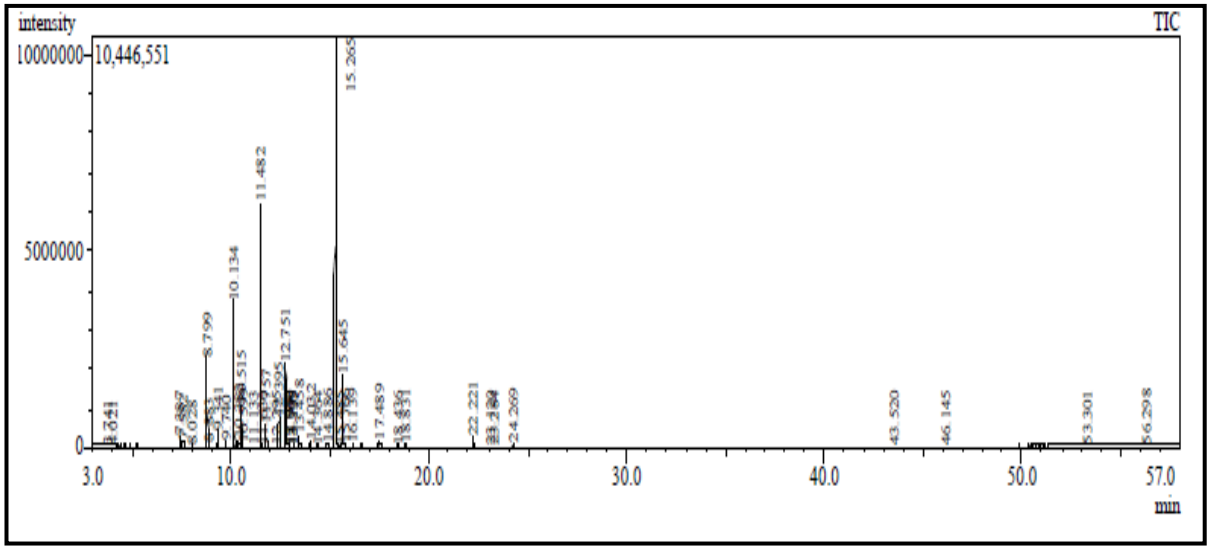


**Figure 15:** Chromatogram of the essential oil of *Mentha piperita* plant obtained by GC/MS.

Upon scrutinizing the two chromatograms, notable resemblances are evident, with discernible bands interspersed with overlapping ones. Generally, distinct regions can be identified, delineating three segments:

1. The initial segment, delimited within the time frame of (4 min to 12.4 min), hosts several bands denoting the presence of hydrocarbon monoterpenes.
2. The succeeding segment, spanning from (12.4 min to 24 min), encompasses the predominant bands, indicative of oxygenated monoterpenes prevalent in the plant's essential oil.
3. The final segment, spanning (24 min to 32.5 min), exhibits minimal banding, suggesting a negligible presence of hydrocarbon sesquiterpenes in the plant's essential oil.

The pertinent compounds in each essential oil, extracted from *Ammudoucus leucotrichus* and *Mentha piperita*, have been identified and collated as follows

### 3.3.1. *Ammudoucus leucotrichus*:

The hydrodistillation extraction of *Ammudoucus leucotrichus* yielded a Bleu oil with a yield of 1.80%. Gas chromatography-mass spectrometry (GC/MS) analysis identified 24 compounds, collectively constituting 99.91% of the oil's composition (as presented in Table 7).

The aromatic oil derived from *Ammudoucus leucotrichus* comprises 64.8% oxygenated monoterpenes and 34.86% hydrocarbon monoterpenes. Notably, perillaldehyde predominates at 64.66%, succeeded by D-Limonene at 26.99%, with a minor presence of α-pinene at 5.8%. At concentrations below 1%, additional compounds were detected, such as β-pinene at 0.66%, β-Ocimene at 0.65%, camphene at 0.4%, and minimal quantities (0.08%) of both methyl perillate and bornyl acetate.

**Table 7 :** Essential oil constituents of *Ammdoucus Leucotrichus* identified by GC/MS

| No | Compounds | $IR_{Exp}$ | $IR_{Ref}$ | (%) |
|---|---|---|---|---|
| **01** | **Alpha-Pinene** | **932** | **925** | **5.8** |
| **02** | Alpha-Fenchene | 945 | 934 | 0.02 |
| **03** | Camphene | 946 | 941 | 0.4 |
| **04** | Thuja-2,4(10)-diene | 953 | 948 | 0.04 |
| **05** | Sabinene | 969 | 969 | 0.03 |
| **06** | Beta-Pinene | 974 | 972 | 0.66 |
| **07** | Myrcene | 988 | 989 | 0.15 |
| **08** | Alpha-Phellandrene | 1002 | 1003 | 0.04 |
| **09** | Beta-Ocimene | 1009 | 1022 | 0.65 |
| **10** | para-Cymene | 1020 | 1024 | 0.06 |
| **11** | **D-Limonene** | **1024** | **1029** | **26.99** |
| **12** | 1,3,8-p-Menthatriene | 1108 | 1122 | 0.02 |
| **13** | Alpha-Campholenal | 1122 | 1127 | 0.02 |
| **14** | trans-Pinocarveol | 1135 | 1141 | 0.05 |
| **15** | Pentyl-Benzene | 1152 | 1147 | 0.03 |
| **16** | Myrtenal | 1195 | 1198 | 0.01 |
| **17** | Verbenone | 1204 | 1212 | 0.02 |
| **18** | Cumin aldehyde | 1238 | 1244 | 0.02 |
| **19** | Carvone | 1239 | 1249 | 0.02 |
| **20** | Linalool acetate | 1257 | 1257 | 0.03 |
| **21** | **Perilla aldehyde** | **1269** | **1285** | **64.66** |
| **22** | Bornyl acetate | 1287 | 1291 | 0.08 |
| **23** | Benzyl isobutanoate | 1297 | 1305 | 0.03 |
| **24** | Methyl perillate | 1392 | 1399 | 0.08 |
| **Total** | | **99.91** | | |

Our findings are consistent with those reported by (Baser et al., 1993; Louail et al., 2016; Sonboli et al., 2012). However, when comparing our results with other studies, some differences in the quantitative measurement of the main components of the essential oil and the nature of the identified components were observed. For instance, studies by (Louail et al., 2016; Moulay

et al., 2014) indicated the presence of a small quantity of α-pinene, which does not align with our results.

Additionally, (Moulay et al., 2014) mentioned that the essential oil of *Ammudoucus leucotrichus* primarily contained perillaldehyde (88.7%) and limonene (8.26%), contrasting with our findings where perillaldehyde predominates and limonene is less prominent. According to (Louail et al., 2016), the tested *Ammudoucus leucotrichus* oil contained 59.12% perillaldehyde and 23.89% limonene. Hence, the origin of the oil from Algeria (specifically Eloued region) serves as a source of the active component (perillaldehyde), commonly utilized in the fragrance and cosmetics industries due to its scent (S. Y. Wang & Chen, 2010).

For a visual representation of the top major compounds (more than 1%) and their structures, refer to Figure 16, which depicts the chemical structures and IUPAC names of the predominant constituents identified in the essential oil of *Ammudoucsus leucotrichus*.

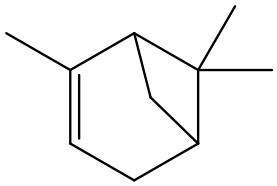

**2,6,6-trimethylbicyclo[3.1.1]hept-2-ene**
**(Alpha-Pinene)**

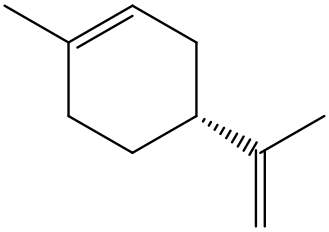

**(R)-1-methyl-4-(prop-1-en-2-yl)cyclohex-1-ene**
**(D-Limonene)**

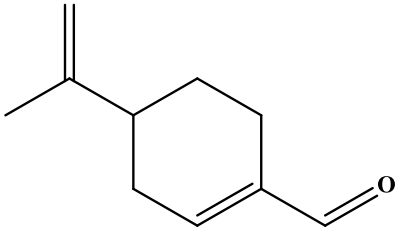


**4-(prop-1-en-2-yl)cyclohex-1-enecarbaldehyde**
**(Perilla aldehyde)**

**Figure 16:** Chemical structures and IUPAC names of the top major compounds identified in the essential oil of *Ammudoucus leucotrichus*

### *3.3.2. Mentha piperita:*

The application of hydrodistillation for extracting the essential oil from *Mentha piperita*, commonly referred to as peppermint, yielded a light-yellow oil with a 1.2% yield. Analysis revealed the presence of 34 chemical compounds (as presented in Table 8), constituting 98.24% of the total oil composition. These compounds were categorized into 70.3% oxygenated monoterpenes, 3.6% hydrocarbon monoterpenes, 0.18% oxygenated sesquiterpenes, and

22.96% other compounds. Notably, three primary compounds were identified, each exceeding 20%: trans-Sabinene hydrate (27.51%), Linalool acetate (21.90%), and Pulegone (20.77%).

**Table 8 :** Essential oil constituents of *Mentha piperita* identifued by GC/MS

| No | Compounds | $IR_{Exp}$ | $IR_{Ref}$ | (%) |
|---|---|---|---|---|
| **01** | Alpha Pinene | 924 | 932 | 0.46 |
| **02** | Camphene | 940 | 946 | 0.22 |
| **03** | Sabinene | 968 | 969 | 0.22 |
| **04** | β Pinene | 971 | 974 | 0.91 |
| **05** | Myrcene | 988 | 988 | 0.58 |
| **06** | Alpha Terpinene | 1015 | 1014 | 0.05 |
| **07** | para-Cymene | 1023 | 1020 | 0.04 |
| **08** | Limonene | 1027 | 1024 | 0.46 |
| **09** | **1,8-Cineole** | **1030** | **1026** | **16.08** |
| **10** | trans-beta-Ocimene | 1037 | 1044 | 0.41 |
| **11** | δ Terpinene | 1058 | 1054 | 0.15 |
| **12** | Terpinolene | 1088 | 1086 | 0.10 |
| **13** | **trans-Sabinene hydrate** | **1101** | **1098** | **27.51** |
| **14** | 3-Octanol, acetate | 1123 | 1120 | 0.03 |
| **15** | trans-Sabinol | 1141 | 1137 | 0.03 |
| **16** | **Menthone** | **1154** | **1148** | **1** |
| **17** | iso-Menthone | 1165 | 1158 | 0.07 |
| **18** | **Borneol** | **1167** | **1165** | **1.66** |
| **19** | l neoiso' Isopulegol | 1173 | 1167 | 0.11 |
| **20** | Terpinen-4-ol | 1178 | 1174 | 0.22 |
| **21** | **Alpha-Terpineol** | **1192** | **1186** | **2.54** |
| **22** | neoiso-Dihydrocarveol | 1230 | 1126 | 0.22 |
| **23** | **Pulegone** | **1243** | **1233** | **20.77** |
| **24** | **Linalool acetate** | **1257** | **1254** | **21.90** |
| **25** | Lavandulyl acetate | 1292 | 1288 | 0.33 |
| **26** | Piperitenone | 1347 | 1340 | 0.06 |
| **27** | Linalool isotretinoin | 1383 | :1373 | 0.48 |
| **28** | Caryophyllene (E) | 1424 | 1417 | 0.79 |
| **29** | Alpha Humulene | 1459 | 1452 | 0.12 |
| **30** | Germacrene D | 1488 | 1484 | 0.25 |
| **31** | gamma Cadinene | 1521 | 1513 | 0.04 |
| **32** | Elmole | 1555 | 1548 | 0.18 |
| **33** | Cinnamaldehyde | 1591 | 1599 | 0.19 |
| **34** | Khusimone | 1600 | 1604 | 0.06 |
| **Total** | | **98.24** | | |

Furthermore, α-Terpineol, Menthone, and Borneol were among the compounds present in concentrations exceeding 1%. Our findings are largely consistent with certain other studies,

albeit with variations observed in the proportions of major compounds. For instance, (Gavahian et al., 2015) reported significant levels of 1,8-Cineole (7.2%), Menthone (24.7%), and Pulegone (4.5%). Similarly, (Smaoui et al., 2016) obtained results in alignment with ours, revealing predominant compound percentages of 1,8-Cineole (2.8%), Menthone (33%), and Pulegone (1.6%).

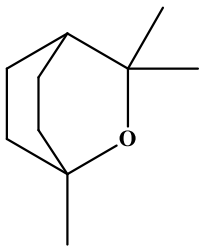

**1,3,3-trimethyl-2-oxabicyclo[2.2.2]octane (1,8-Cineole)**

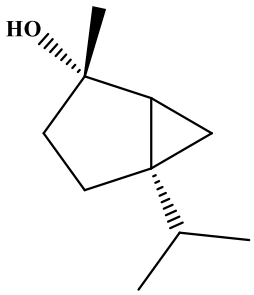

**(2*S*,5*R*)-5-isopropyl-2-methylbicyclo[3.1.0]hexan-2-ol (trans-Sabinene hydrate)**

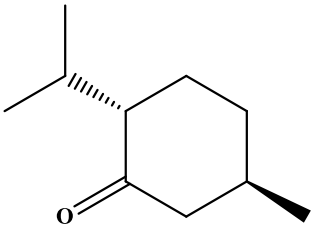

**(2*S*,5*R*)-2-isopropyl-5-methylcyclohexanone (Menthone)**

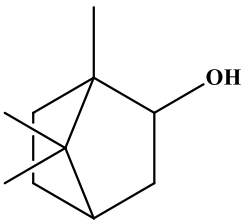

**1,7,7-trimethylbicyclo[2.2.1]heptan-2-ol (Borneol)**

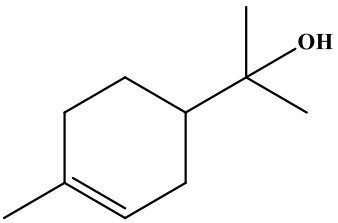

**2-(4-methylcyclohex-3-en-1-yl)propan-2-ol (alpha -Terpineol)**

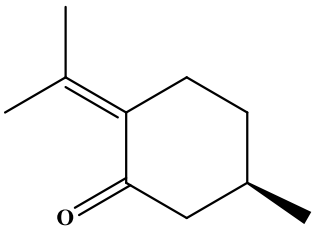

**(*R*)-5-methyl-2-(propan-2-ylidene)cyclohexanone (Pulegone)**

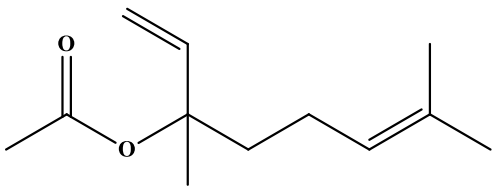

**3,7-dimethylocta-1,6-dien-3-yl acetate (Linalool acetate)**

**Figure 17:** Chemical structures and IUPAC names of the top major compounds identified in the essential oil of *Mentha piperita*

However, discrepancies were noted in the analysis conducted by (Ahmad et al., 2014), where the presence of Menthol at 34.82% differed from our findings. In a separate study by (Hossain et al., 2014) on peppermint plants cultivated in Oman, the detection of Eucalyptol, absent in our study, was noteworthy. For an illustrative overview of the major compounds identified, Figure 17, displaying the structures and IUPAC nomenclature of these constituents.

## 4. Assessment of Anticancer Activity:

### 4.1. Cyclic Voltametry interaction study:

#### 4.1.1. Binding constants:

Upon the addition of increasing concentrations of DNA or BSA to essential oil solutions, a noteworthy diminution in the anodic peak current height of the essential oil was observed. Additionally, a discernible displacement towards the negative direction in the anodic peak potential was evident during DNA or BSA addition (Figure 18). These findings strongly suggest an interaction between the essential oil under study and DNA and BSA, predominantly facilitated by electrostatic forces (E. Lanez et al., 2019; Mouada et al., 2019). Notably, voltammograms depicted that in the absence of DNA or BSA, essential oils from *Ammudoucus leucotrichus* and *Mentha piperita* exhibited anodic peak potentials at 1.251 and 1.230 V, respectively. However, in the presence of varying concentrations of BSA (from 0.04 to 0.22 µM) and DNA (from 0.81 to 3.93 µM), these potentials were observed to shift to lower values (ranging from 1.249 to 1.225 V for BSA and from 1.229 to 1.225 V for DNA), with a consistent negative shift of approximately 1 mV per unit increase in concentration. This consistent shift in peak potential suggests a pronounced interaction between the essential oil and DNA and BSA (T. Lanez et al., 2018). Furthermore, a decline in anodic peak current densities was evident in the voltammograms, attributed to the hindered diffusion of the formed DNA-EO and BSA-EO adducts.

The observed peak potential shift in the cyclic voltammetric behavior of the essential oil upon the addition of DNA or BSA can be ascribed to the electrostatic interactions between the compounds and the respective biomolecules. This phenomenon underscores the oxidizable nature of the compounds in the negative milieu provided by DNA or BSA. Such elucidation not only enriches our understanding of the electrochemical behavior of essential oils but also sheds light on the intricate interplay between these natural compounds and biomolecules (H. W. Wang et al., 2021).

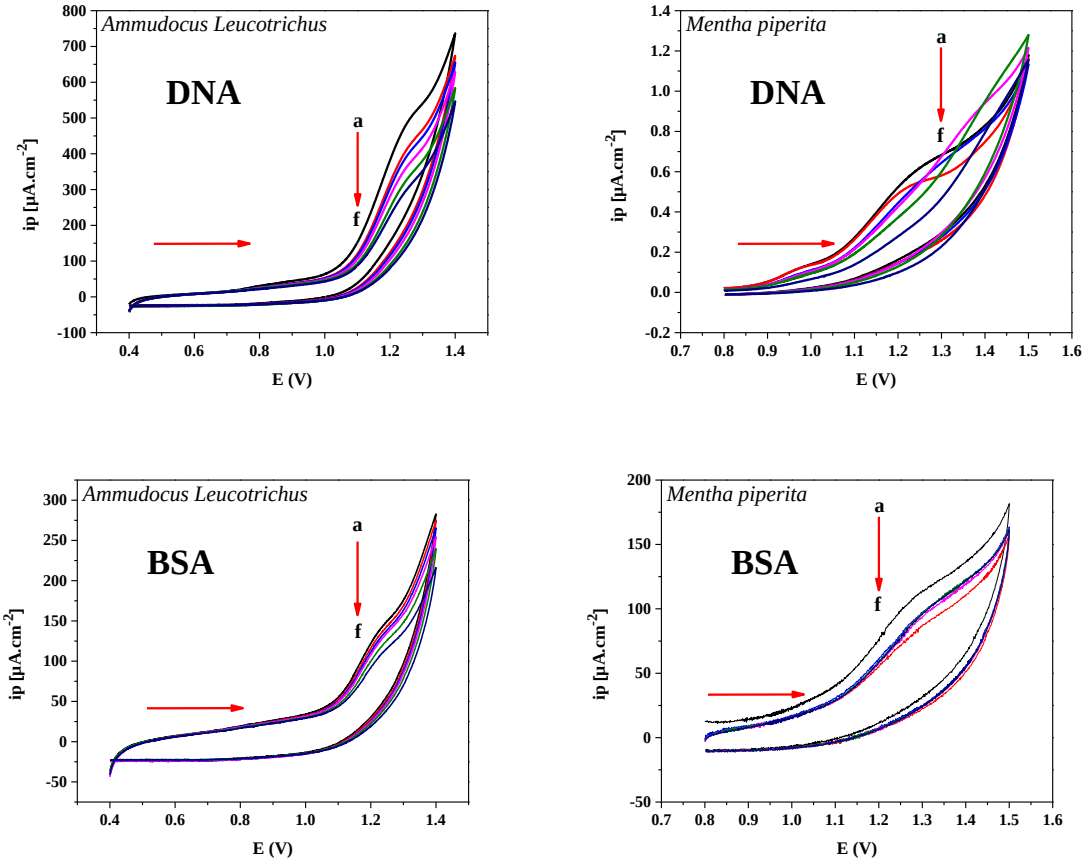


**Figure 18 :** Cyclic voltammograms of 2 mM *Ammudoucus leucotrichus* and *Mentha piperita* essential oil recorded at 0.1V $s^{-1}$ potential sweep rate on GC disk electrode at 298K in the absence and presence of increasing concentration of DNA and BSA in 0.1 M 90% ethanol/buffer phosphate solution at pH =7.2 with supporting electrolyte 0.1 M $Bu_4NBF_4$.

Typically, the negative shift in formal potential induced by the addition of a potential drug to both BSA and DNA is attributed to the electrostatic interaction between the cationic drug and the negatively charged backbone of DNA (Jamil et al., 2013; Shah et al., 2010). Therefore, the pronounced negative shift in the anodic peak potential observed in the cyclic voltammetry behavior of the essential oil upon DNA or BSA addition can be ascribed to electrostatic interactions, possibly involving hydrogen bonding, between the essential oil and the respective biomolecules. This shift in peak potential further suggests that the remaining compounds in the essential oil are more readily oxidizable in the presence of the negatively charged environment of DNA or BSA. Additionally, the progressive diminution in the oxidation peak with further addition of DNA supports the notion that the compounds in the essential oil actively participate in hydrogen bonding with DNA and BSA, thereby impeding electron transfer out of the system (Figure 9).

Furthermore, the decrease in anodic peak current density of the EO-DNA or EO-BSA adduct relative to free EO serves as a basis for calculating binding constants and binding free energies using Equation 7 (Zhao et al., 1999).

$$\log \frac{1}{[BM]} = \log K_b + \log \frac{ip}{ip_0 - ip} \quad (7)$$

Where $[BM]$ is the DNA or BSA concentration (M); $K_b$ represents the binding constant ($M^{-1}$); $ip_0$ and $ip$ denote the anodic peak current density of the free and DNA or BSA bound compound, respectively ($\mu A/cm^2$).

The plot of $\log 1/[BM]$ versus $\log 1/1-(i/i_0)$ gave a straight line (Figure 19) with a '$y$' intercept equal to the logarithm of binding constant $K_b$.

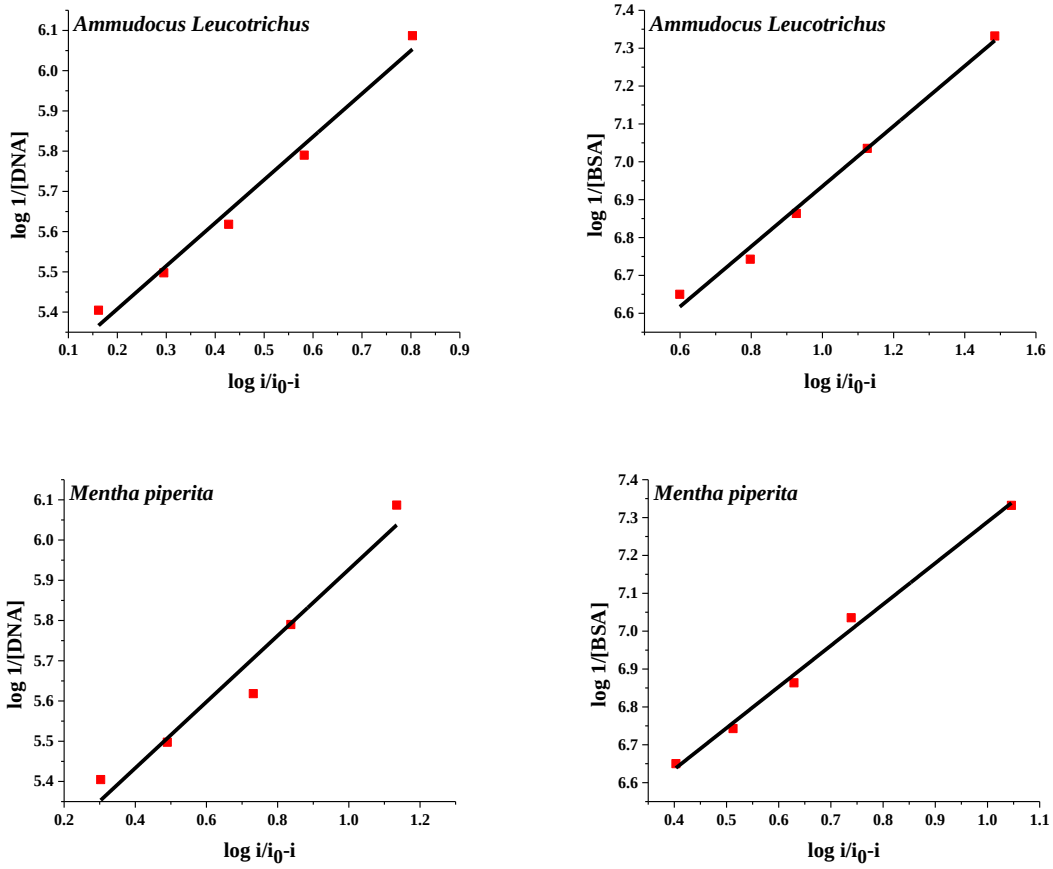


**Figure 19:** Plots of $\boldsymbol{log\left(1/1-(i_p/i_{p_0})\right)}$ versus $\boldsymbol{log\ 1/[BM]}$ used to calculate the binding constants of studied essential oil with DNA and BSA

### 4.1.2. Binding free energy:

The binding free energy change was calculated using the following Equation 8 (Atkins & De Paula, 2010)

$$\Delta G = -RT \ln K_b \quad (8)$$

Where ΔG is the binding free energy in KJ.mol$^{-1}$, R is the gas constant, 8.32 J.mol$^{-1}$K$^{-1}$ and T is the absolute temperature, 298K.

Binding parameters of the studied essential oils are listed in Table 9.

**Table 9:** Binding constants and binding free energies values for EOs with DNA and BSA from CV data

| Adduct | Equation | $R^2$ | K ($M^{-1}$) | -ΔG (KJ.mol$^{-1}$) |
|---|---|---|---|---|
| ***Ammudoucus leucotrichus _DNA*** | y = 1.070x + 5.193 | 0.979 | $1.56\times10^5$ | 35.06 |
| ***Ammudoucus leucotrichus _BSA*** | y = 0.794x + 6.141 | 0.988 | $1.38\times10^6$ | 29.56 |
| ***Mentha piperita* _DNA** | y = 0.822x + 5.104 | 0.941 | $1.27\times10^5$ | 29.14 |
| ***Mentha piperita* _BSA** | y = 1.089x + 6.199 | 0.992 | $1.58\times10^6$ | 35.40 |

### 4.2. Electronic Spectroscopy Interaction Study:

Electronic absorption spectroscopy serves as a valuable tool for investigating binding modalities. The hypochromic effect induced by DNA or BSA on the spectrum of a ligand upon binding serves as a key indicator of the binding mode. Typically, intercalator's exhibit more pronounced hyperchromic effects compared to groove binders. When essential oils bind to DNA and BSA via intercalation, the absorption spectra manifest significant hypochromic shifts and red shifts, attributable to the robust π→π* stacking interaction between the aromatic chromophore ligand and the base pairs of DNA or the amino acids of BSA (Shah et al., 2010).

In addition to voltammetry techniques, electronic spectroscopy titration was employed to investigate the interaction of essential oils with DNA and BSA in a 90% ethanol/phosphate buffer solution (KH2PO4/K2HPO4) at pH 7.2. The absorption spectra of fixed concentrations (2 mM) of *Ammudoucus leucotrichus* and *Mentha piperita* essential oils in the absence and presence of gradually increasing concentrations of DNA and BSA stock solution are depicted in Figure 20. In the UV region, *Ammudoucus leucotrichus* and *Mentha piperita* essential oils exhibit single absorption peaks at 229 and 231 nm, respectively (Figure 20). Upon addition of DNA and BSA, a considerable hyperchromic effect was observed without discernible shifts in the position of the maximum absorption peak, indicating the formation of adducts between DNA or BSA and the essential oil under investigation (Rakesh et al., 2012). This hyperchromic effect further suggests the predominantly groove binding property of EO compounds to double-stranded DNA (Shahabadi et al., 2011).

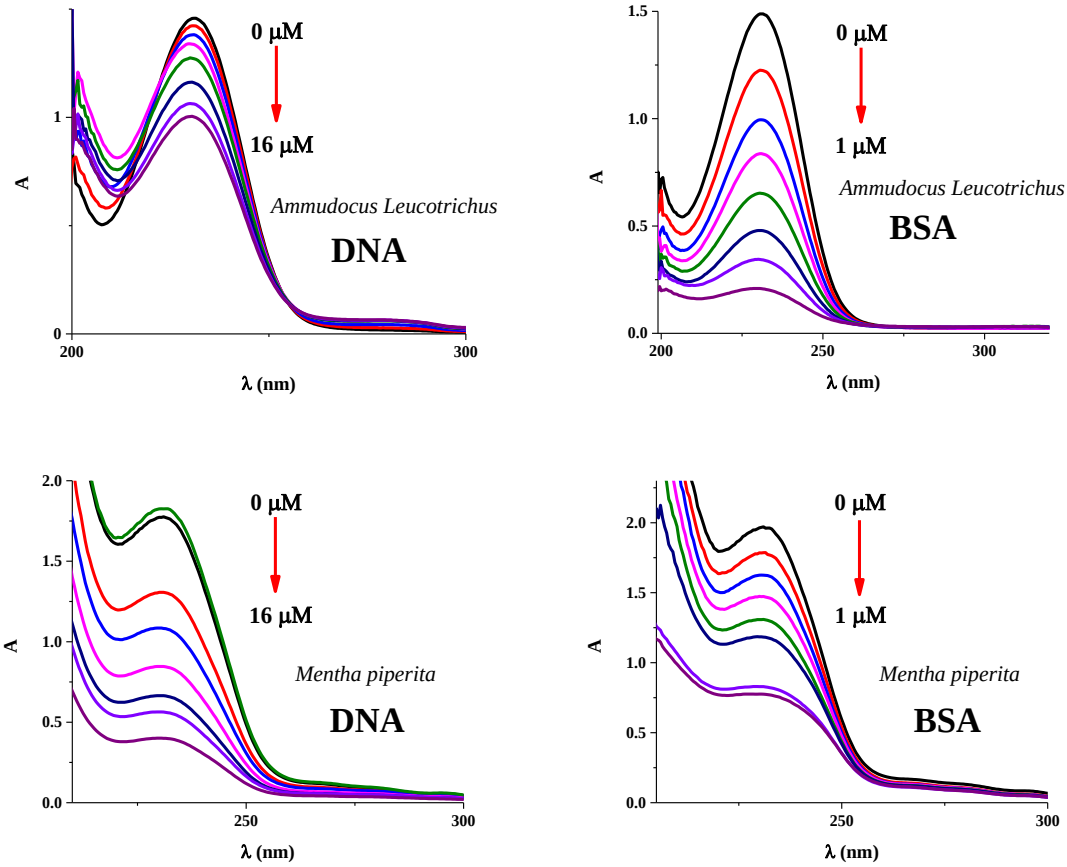


**Figure 20:** UV-visible absorption spectra of 2 mM of *Ammudoucus leucotrichus* and *Mentha piperita* essential oils in presence of increasing concentrations of DNA and BSA in 0.1 M 90% ethanol/buffer phosphate solution ($KH_2PO_4/K_2HPO_4$) at pH = 7.2 and 298K

### 4.2.1. Binding constants:

The change in absorbance values by increasing DNA and BSA concentration was used to evaluate the intrinsic binding constant employing the following Equation 9, (Isaac et al., 1999; Ni et al., 1997).

$$\frac{A_0}{A-A_0} = \frac{\varepsilon_G}{\varepsilon_{H-G}-\varepsilon_G} + \frac{\varepsilon_G}{\varepsilon_{H-G}-\varepsilon_G}\frac{1}{K_b[BM]} \qquad (9)$$

where $[BM]$ is the DNA or BSA concentration, $K_b$ is the binding constant, $A_0$and $A$ are respectively the absorbance of ligand in the absence and presence of DNA or BSA, and $\varepsilon_G$ and $\varepsilon_{H-G}$ are their extinction coefficient respectively.

The constant $K_b$ is obtained from the intercept to slope ratio of the plot of $A_0/(A-A_0)$ versus$1/[BM]$, Figure 21.

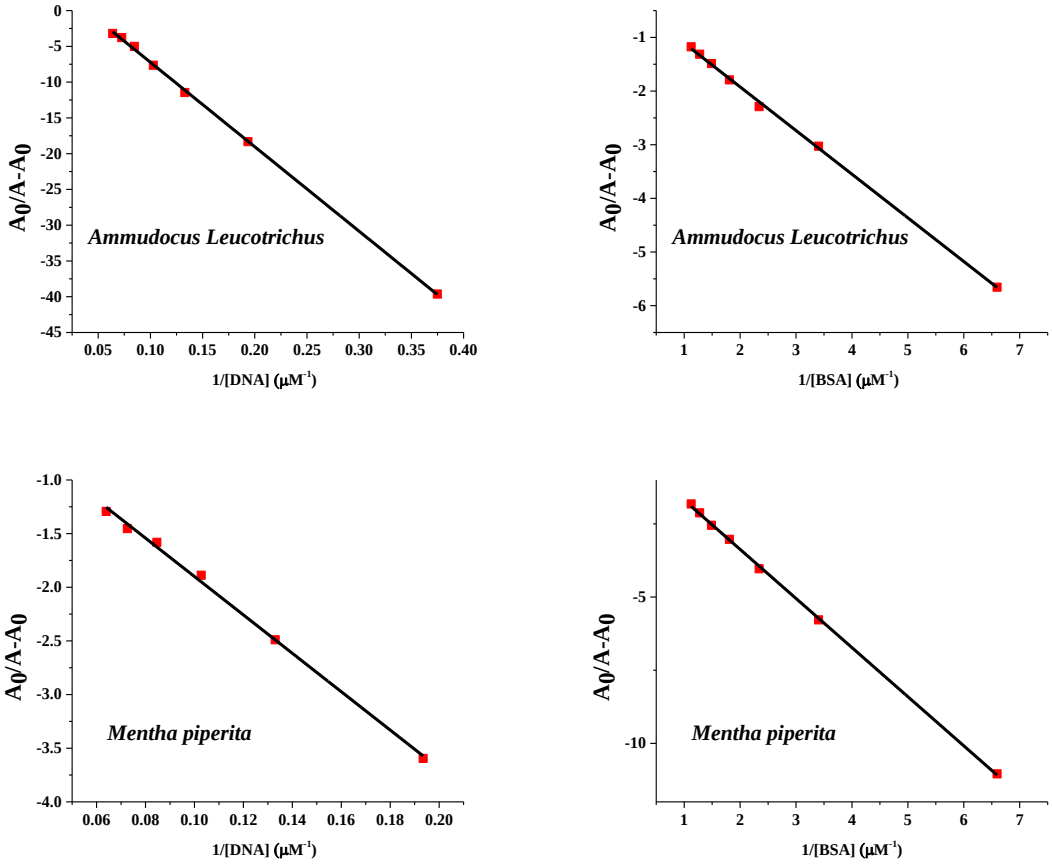


**Figure 21:** Plots of $A_0/(A-A_0)$ versus $1/[BM]$ used to calculate the binding constants of *Ammudoucus leucotrichus* and *Mentha piperita* essential oils with DNA and BSA

### 4.2.2. Binding free energy:

The binding free energy change was calculated using the following Equation 10 (W., 1998)

$$\Delta G = -RT \ln K_b \qquad (10)$$

Where ΔG is the binding free energy in KJ.mol$^{-1}$, R is the gas constant, 8.32 J.mol$^{-1}$K$^{-1}$ and T is the absolute temperature, 298K. Binding parameters are listed in Table 10.

**Table 10:** Binding constant and binding free energy values for *Ammudoucus leucotrichus* and *Mentha piperita* essential oils with DNA and BSA from UV data

| Adduct | Equation | $R^2$ | K ($M^{-1}$) | -ΔG (KJ.mol$^{-1}$) |
|---|---|---|---|---|
| ***Ammudoucus leucotrichus _DNA*** | y = -118.126x – 4.585 | 0.999 | $3.88 \times 10^4$ | 26.20 |
| ***Ammudoucus leucotrichus _BSA*** | y = -0.813x – 0.294 | 0.999 | $3.62 \times 10^5$ | 31.74 |
| ***Mentha piperita* _DNA** | y = -17.886x – 0.111 | 0.996 | $6.21 \times 10^3$ | 21.65 |
| ***Mentha piperita* _BSA** | y = -1.678x – 0.014 | 0.999 | $8.42 \times 10^4$ | 28.12 |

### 4.3. Molecular Docking Interaction Study:

In the current study, the binding interaction of all the major compounds presented in *Ammudoucus leucotrichus* and *Mentha piperita* essential oils with human DNA and BSA was further investigated by carrying out a molecular docking analysis of the binding interaction between DNA and BSA with compounds: trans thujone, alpha-Terpineol, beta-Terpineol, cis Verbenyl acetate, Camphor, Sabinene, gamma terpinene, alpha-Pinene, 1,8-Cineole, Santolina triene, alpha-Thujene and Beta Pinene oxide (the major phytochemicals present in the two plants with yield > 1) using Maestro version 11.7 user interface of the Schrödinger suite (Small-Molecule Drug Discovery Suite 2021-4, Schrödinger, LLC, New York, NY, 2021) (Schrödinger, 2015).

Each compound was docked with human DNA and BSA to understand their interactions at the enzyme's active site. Of all the major compounds present in *Ammudoucus leucotrichus* and *Mentha piperita* essential oils, the binding affinities of them for DNA and BSA were comparable to that obtained by CV and UV (Table 11). This result indicates that the plant is a rich source of compounds which, either individually or synergistically, resulted in the decrease of the activity of DNA as observed in the *in vitro* experimental anticancer interaction study. Also, the interactions were spontaneous as observed from the negative Gibb's free energy values (Avwioroko et al., 2020).

**Table 11:** Docking score of the studied compounds

| | DNA | | BSA | |
|---|---|---|---|---|
| **Compound** | **Rigid Docking Score (Kcal/mol)** | **IFD scores (Kcal/mol)** | **Rigid Docking Score (Kcal/mol)** | **IFD scores (Kcal/mol)** |
| **Perilla aldehyde** | -5.828 | -7.128 | -7.728 | -8.228 |
| **D-Limonene** | -5.794 | -7.094 | -7.694 | -8.194 |
| **alpha-Pinene** | -4.994 | -6.294 | -6.894 | -7.394 |
| **Pulegone** | -7.651 | -8.951 | -9.551 | -10.051 |
| **Menthone** | -7.069 | -8.369 | -8.969 | -9.469 |
| **trans-Sabinene hydrate** | -6.669 | -7.969 | -8.569 | -9.069 |
| **alpha-Terpineol** | -6.162 | -7.462 | -8.062 | -8.562 |
| **Borneol** | -5.636 | -6.936 | -7.536 | -8.036 |
| **Linalool acetate** | -5.094 | -6.394 | -6.994 | -7.494 |
| **1,8-Cineole** | -4.816 | -6.116 | -6.716 | -7.216 |

The results presented in Figure 22 demonstrate that the top two compounds exhibit favourable interactions with both the nucleic bases within the active site of DNA and the amino acids within the active site of BSA, primarily facilitated by electrostatic interactions. Moreover, these findings validate the potential binding interactions between both DNA and BSA with the phytoconstituents of *Ammudoucus leucotrichus* and *Mentha piperita* essential oils, as previously observed in spectroscopic and cyclic voltammetry studies. The optimal ligand-binding poses within the active sites of DNA and BSA obtained through molecular docking are depicted in Figure 22.

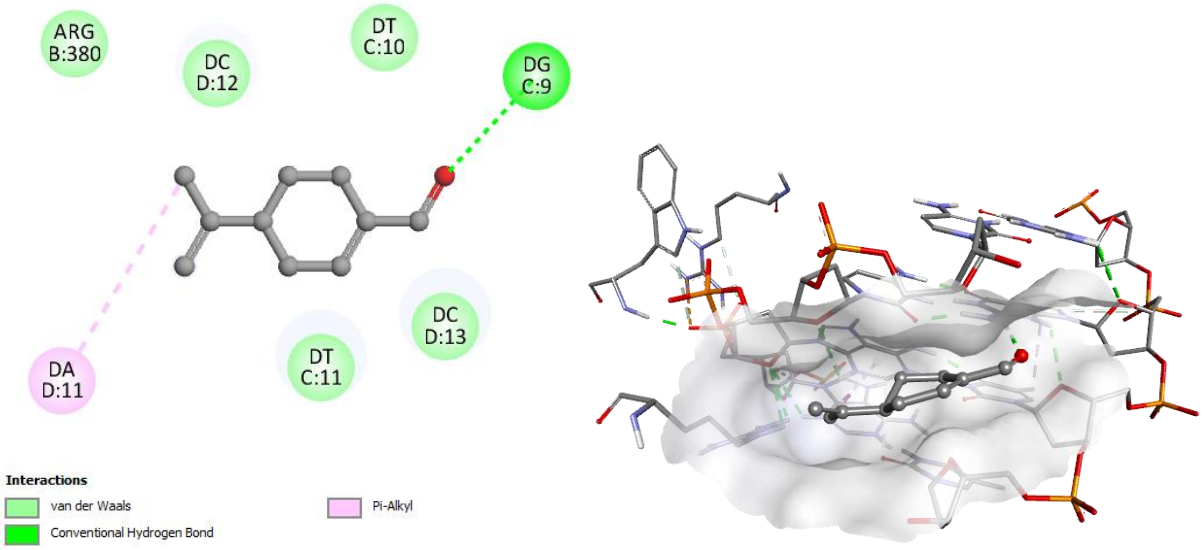


*Docking complex and interaction plot for compound Perilla aldehyde with DNA*

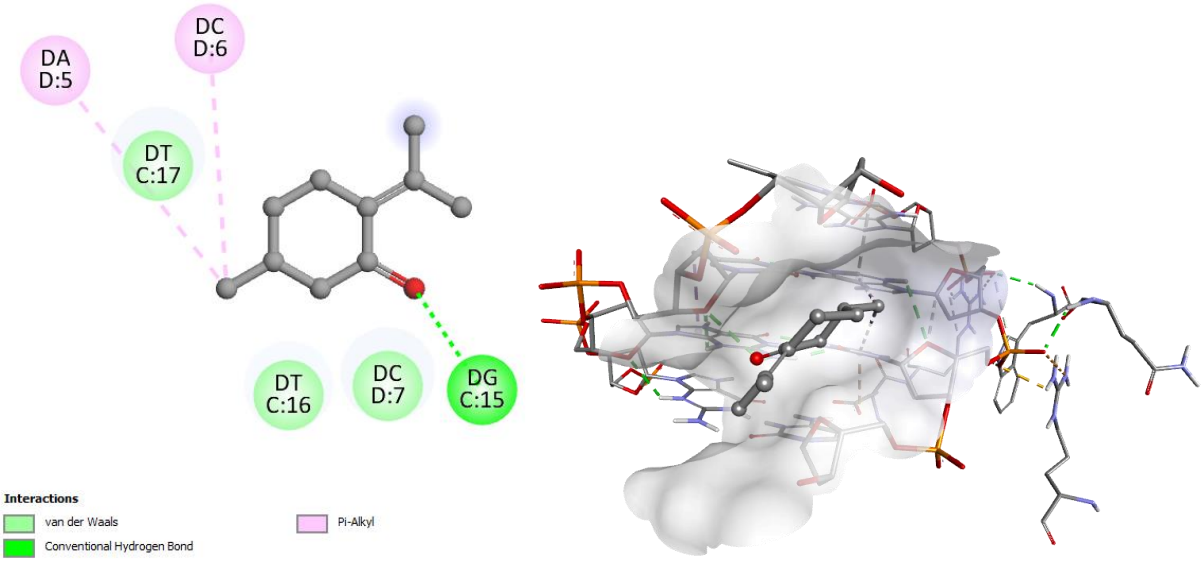


*Docking complex and interaction plot for compound Pulegone with DNA*

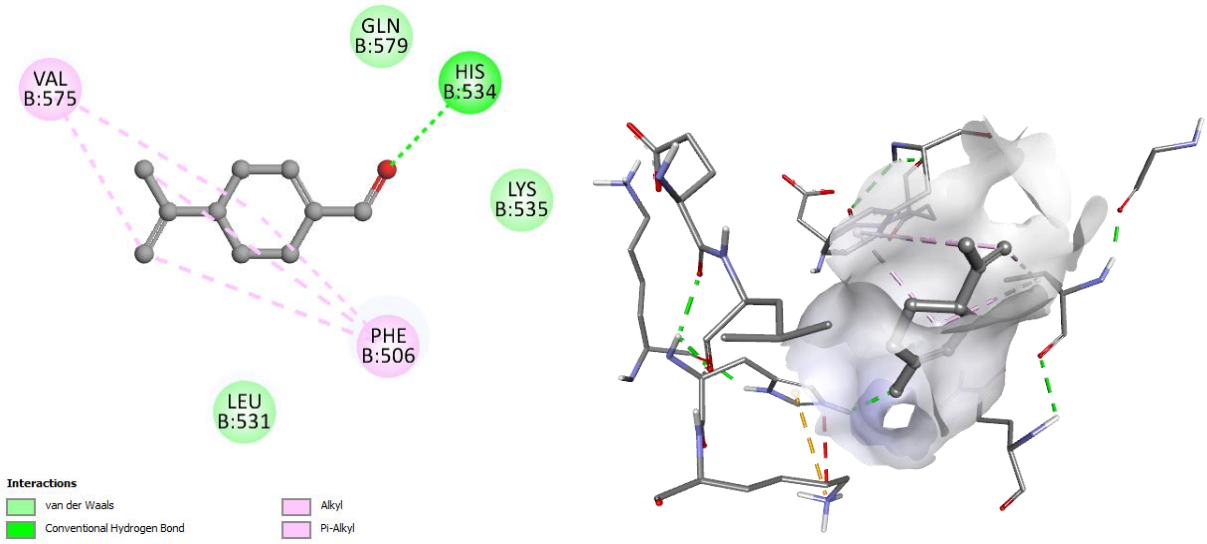


*Docking complex and interaction plot for compound Perilla aldehyde with BSA*

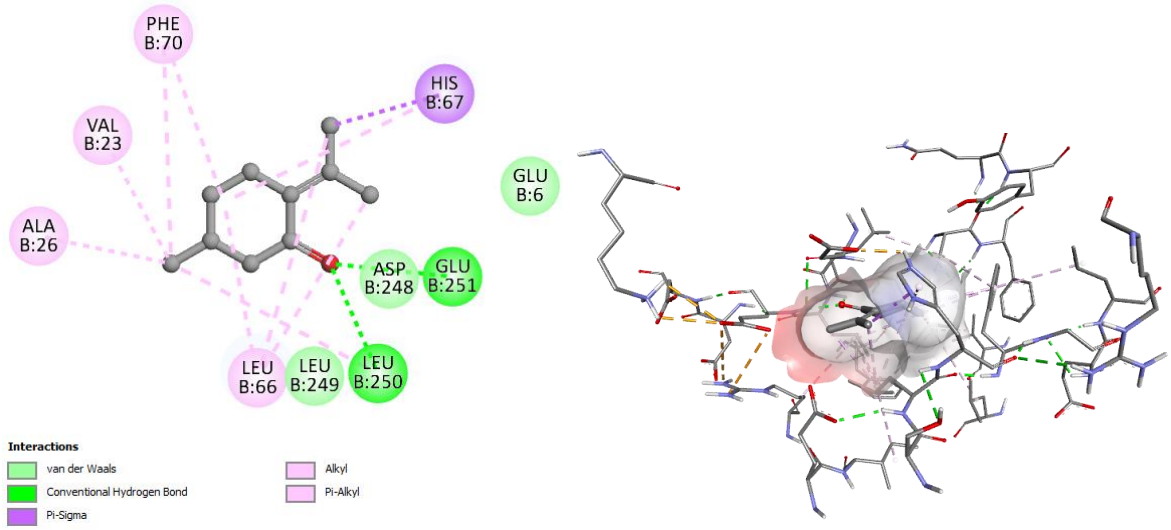


*Docking complex and interaction plot for compound Pulegone with BSA*

**Figure 22:** Molecular interactions of studied compounds with DNA and BSA

## 5. Assessment of Antibacterial Activity:

The *in vitro* assessment of the antimicrobial efficacy of *Ammudoucus leucotrichus* and *Mentha piperita* essential oils was conducted utilizing the disk diffusion technique against two prevalent bacterial strains associated with infections, *Escherichia coli* (*E. coli*), *Bacillus subtilis* (*B. subtilis*) and *Staphylococcus aureus* (*S. aureus*). Two distinct methodologies were employed to gauge the antibacterial activity: quantifying the zone of inhibition surrounding the EOs-impregnated disk and measuring the optical density of the bacterial suspension subsequent to treatment with varying concentrations of EOs. Comparative analysis was performed with amoxicillin, a widely utilized antibiotic. This study presents the findings derived from the

diverse methodologies employed to evaluate the antibacterial efficacy of the studied essential oils and juxtaposes these outcomes with those obtained with amoxicillin.

**5.1. Determination of the Diameter of the Inhibition Zone:**

Following a 24-hour incubation period at 37°C, the zones of inhibition surrounding the disks impregnated with *Ammudoucus leucotrichus* and *Mentha piperita* essential oils and amoxicillin were measured. The diameters of the inhibition zones obtained with EOs and amoxicillin against *E. coli*, *B. subtilis* and *S. aureus* are summarized below (Table 12). The inhibition zones are identified by clear areas devoid of bacterial growth surrounding the disks.

**Table 12:** Diameters of the inhibition zones of the studied essential oils and amoxicillin against *E. coli, B. subtilis* and *S. aureus*

| Antibiotics | Bacteria | Diameter of the inhibition zone (mm) |
|---|---|---|
| ***Ammudoucus leucotrichus*** | ***E. coli*** | 18.5 |
| | ***B. subtilis*** | 20.1 |
| | ***S. aureus*** | 10.9 |
| ***Mentha piperita*** | ***E. coli*** | 20.2 |
| | ***B. subtilis*** | 21.6 |
| | ***S. aureus*** | 13.8 |
| **Amoxicillin** | ***E. coli*** | 22.3 |
| | ***B. subtilis*** | 25.6 |
| | ***S. aureus*** | 24.6 |

The table provides a systematic examination of the antimicrobial efficacy of natural compounds, specifically *Ammudoucus leucotrichus* and *Mentha piperita* essential oils, alongside the conventional antibiotic Amoxicillin, against three bacterial strains: *Escherichia coli* (*E. coli*), *Bacillus subtilis (B. subtilis),* and *Staphylococcus aureus* (*S. aureus*). The diameter of the inhibition zones, measured in millimeters, serves as a quantitative indicator of antimicrobial activity (Cooper, 1963).

Analysis of the data reveals discernible trends in antimicrobial effectiveness across the tested antibiotics and bacterial strains. *Mentha piperita* and Amoxicillin consistently demonstrate larger inhibition zones compared to *Ammudoucus leucotrichus*, indicating superior antimicrobial potency. Furthermore, *B. subtilis* exhibits the largest inhibition zones among the

bacterial strains tested, suggesting varying susceptibility to the antibiotics among different bacterial species.

These findings underscore the importance of considering both the antimicrobial spectrum and potency of antibiotics when selecting appropriate treatment options for bacterial infections (Giurazza et al., 2021). Moreover, the observed efficacy of natural compounds like *Mentha piperita* highlights their potential as viable alternatives or adjuncts to conventional antibiotics

### 5.2. Electronic Spectroscopy Interaction Study:

#### 5.2.1. Bacterial inhibitory activities ($IC_{50}$):

The antibacterial activity of *Ammudoucus leucotrichus* and *Mentha piperita* was assessed using the absorbance measurement method to determine the $IC_{50}$. This methodology entails measuring bacterial growth in wells containing varying concentrations of EOs. The resulting data facilitated the determination of the minimum concentration of EOs required to inhibit bacterial growth by 50%.

To this end, cultures of *E. coli*, *B. subtilis* and *S. aureus* were incubated with different concentrations of EOs and amoxicillin, ranging from 1 to 10 mg/ml, for 24 hours at 37°C. Subsequently, the optical density of each sample was measured at 620 nm using a spectrophotometer. The findings obtained are summarized in the following Table 13.

**Table 13:** Absorbance values sorted from the antibacterial assays

| C (mg/ml) | *Ammudoucus leucotrichus* | | | *Mentha piperita* | | | Amoxicillin | | |
|---|---|---|---|---|---|---|---|---|---|
| | *E. coli* | *B. subtilis* | *S. aureus* | *E. coli* | *B. subtilis* | *S. aureus* | *E. coli* | *B. subtilis* | *S. aureus* |
| **0** | 2.571 | 2.571 | 2.571 | 2.571 | 2.571 | 2.571 | 2.117 | 2.209 | 1.954 |
| **1** | 1.587 | 1.21 | 1.752 | 1.461 | 1.089 | 1.576 | 1.718 | 2.191 | 1.816 |
| **2** | 1.438 | 1.207 | 1.634 | 1.309 | 0.965 | 1.42 | 1.658 | 2.183 | 1.626 |
| **3** | 1.196 | 1.12 | 1.481 | 0.944 | 0.822 | 1.2 | 1.103 | 2.176 | 1.389 |
| **4** | 1.081 | 0.845 | 1.232 | 0.905 | 0.788 | 0.97 | 0.828 | 2.169 | 1.344 |
| **5** | 0.689 | 0.779 | 1.099 | 0.718 | 0.673 | 0.843 | 0.677 | 2.153 | 0.868 |
| **6** | 0.547 | 0.572 | 0.94 | 0.704 | 0.55 | 0.652 | 0.638 | 2.144 | 0.71 |
| **7** | 0.478 | 0.514 | 0.732 | 0.478 | 0.5 | 0.526 | 0.395 | 2.133 | 0.697 |
| **8** | 0.468 | 0.421 | 0.53 | 0.389 | 0.398 | 0.419 | 0.198 | 2.103 | 0.587 |
| **9** | 0.294 | 0.352 | 0.418 | 0.353 | 0.317 | 0.317 | 0.127 | 2.098 | 0.477 |
| **10** | 0.246 | 0.313 | 0.406 | 0.172 | 0.222 | 0.268 | | | |

This table presents the outcomes of the investigation into the antibacterial efficacy of *Ammudoucus leucotrichus* and *Mentha piperita* essential oils and amoxicillin against *E. coli*, *B.*

*subtilis* and *S. aureus*, employing the absorbance measurement technique. The results depict a gradual decline in optical densities alongside escalating concentrations of EOs or amoxicillin, indicative of diminished bacterial proliferation. Subsequently, $IC_{50}$ values, delineating the concentration of EOs or amoxicillin necessary to impede 50% of bacterial growth, were derived from these observations by plotting the inhibition percentage against the compound concentrations (refer to Figure 23). The resultant of $IC_{50}$ values is meticulously documented in Table 14.

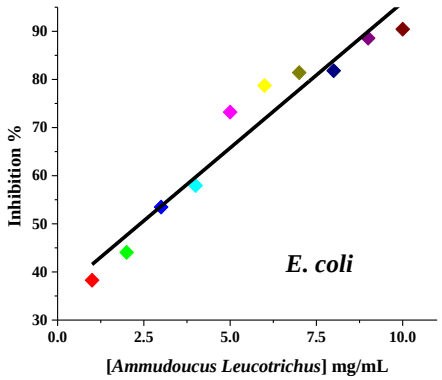


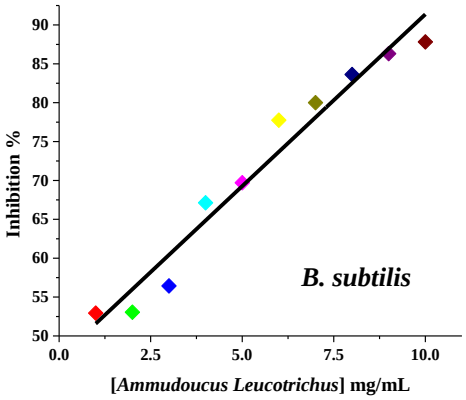


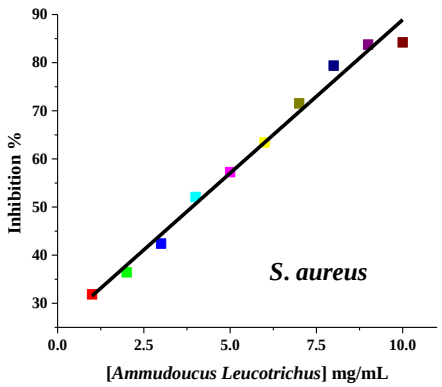


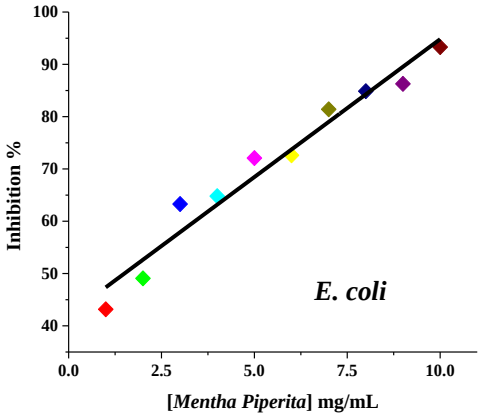


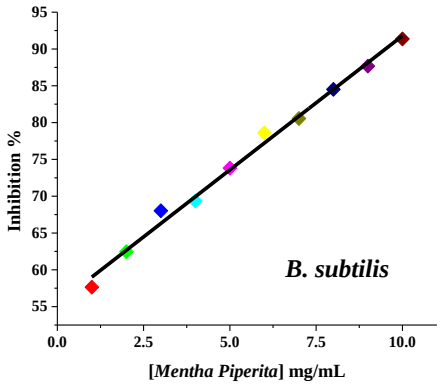


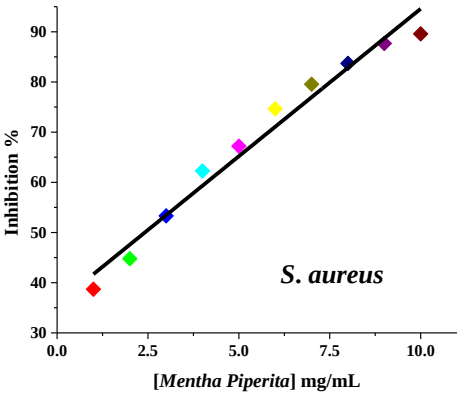

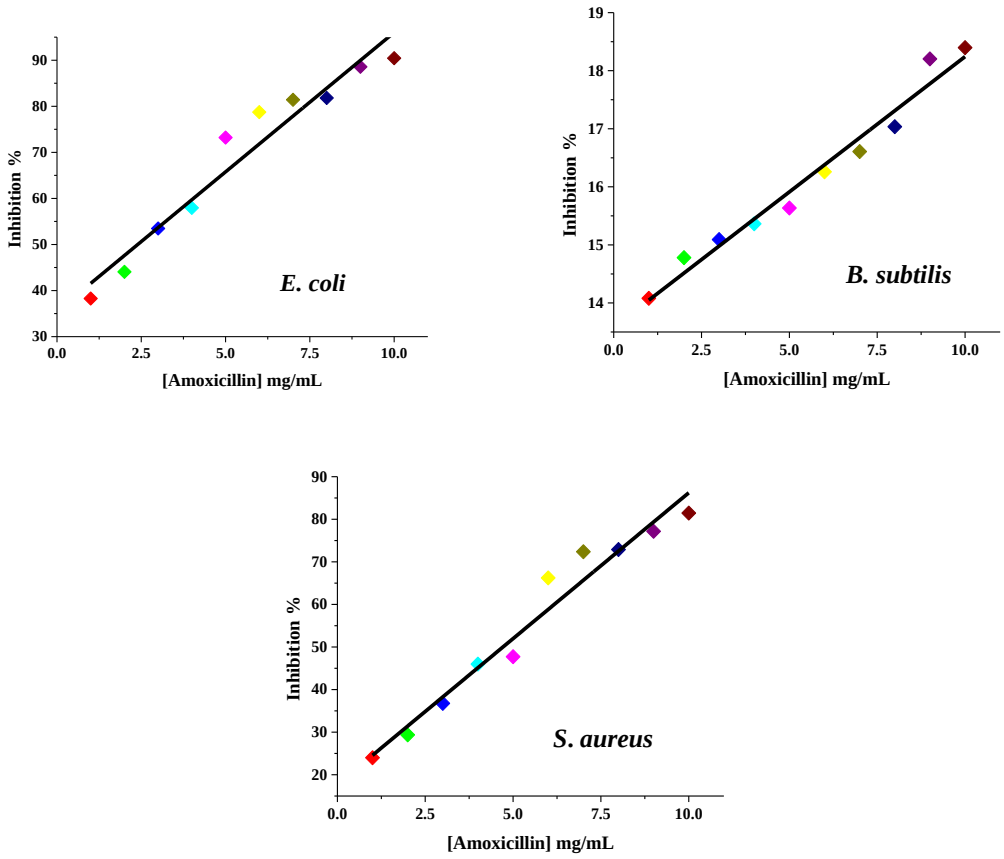


**Figure 23:** The linear regression curves depicting the percentage inhibition of bacteria versus The concentration of *Ammudoucus leucotrichus and Mentha piperita* essential oils and Amoxicilli

**Table 14:** The antibacterial activity of *Ammudoucus leucotrichus and Mentha piperita* essential oils and amoxicillin through the inhibition test against *E. coli*, *B. subtilis and S. aureus*

| ***Ammudoucus leucotrichus*** | | | ***Mentha piperita*** | | | **Amoxicillin** | | |
|---|---|---|---|---|---|---|---|---|
| ***E. coli*** | ***B. subtilis*** | ***S. aureus*** | ***E. coli*** | ***B. subtilis*** | ***S. aureus*** | ***E. coli*** | ***B. subtilis*** | ***S. aureus*** |
| 38.273 | 52.937 | 31.855 | 43.174 | 57.643 | 38.701 | 17.658 | 14.080 | 23.998 |
| 44.068 | 53.053 | 36.445 | 49.086 | 62.466 | 44.769 | 33.178 | 14.780 | 29.366 |
| 53.481 | 56.437 | 42.396 | 63.283 | 68.028 | 53.326 | 35.511 | 15.091 | 36.756 |
| 57.954 | 67.133 | 52.081 | 64.800 | 69.350 | 62.271 | 57.098 | 15.364 | 45.974 |
| 73.201 | 69.701 | 57.254 | 72.073 | 73.823 | 67.211 | 67.795 | 15.636 | 47.725 |
| 78.724 | 77.752 | 63.438 | 72.618 | 78.608 | 74.640 | 73.668 | 16.258 | 66.239 |
| 81.408 | 80.008 | 71.529 | 81.408 | 80.552 | 79.541 | 75.185 | 16.608 | 72.384 |
| 81.797 | 83.625 | 79.385 | 84.870 | 84.520 | 83.703 | 84.636 | 17.036 | 72.890 |
| 88.565 | 86.309 | 83.742 | 86.270 | 87.670 | 87.670 | 92.299 | 18.203 | 77.168 |

| | | | | | | | | |
|---|---|---|---|---|---|---|---|---|
| 90.432 | 87.826 | 84.208 | 93.310 | 91.365 | 89.576 | 95.060 | 18.398 | 81.447 |
| **$IC_{50}$ = 2.935 mg/ml** | **$IC_{50}$ = 0.641 mg/ml** | **$IC_{50}$ = 3.895 mg/ml** | **$IC_{50}$ = 1.500 mg/ml** | **$IC_{50}$ = 1.477 mg/ml** | **$IC_{50}$ = 2.412 mg/ml** | **$IC_{50}$ = 3.961 mg/ml** | **$IC_{50}$ = 8.154 mg/ml** | **$IC_{50}$ = 4.712 mg/ml** |

The findings reveal the growth inhibitions of *E. coli*, *B. subtilis*, and *S. aureus* bacteria in the presence of *Ammudoucus leucotrichus and Mentha piperita* essential oils, alongside amoxicillin. The results demonstrate a notably potent efficacy of *Ammudoucus leucotrichus and Mentha piperita* compared to amoxicillin, with $IC_{50}$ values of 3.961 mg/ml, 8.154 mg/ml, and 4.712 mg/ml, respectively.

Concerning *Ammudoucus leucotrichus*, the outcomes indicate bacterial growth inhibition of up to 90% for E. coli, 87% for B. subtilis, and 84% for S. aureus at the highest tested concentration (10 mg/ml). This suggests that *Ammudoucus leucotrichus* may possess antimicrobial activity, albeit at relatively elevated concentrations.

In contrast, *Mentha piperita* results in bacterial growth inhibition of up to 93% for *E. coli*, 81% for *B. subtilis*, and 89% for *S. aureus* at the highest tested concentration (10 mg/ml). This underscores the superior efficacy of this essential oil as an antibiotic against bacterial infections.

In conclusion, the findings of this study highlight the notable antibacterial effects exhibited by the two essential oils under investigation, *Ammudoucus leucotrichus* and *Mentha piperita*, surpassing those of amoxicillin. This suggests their potential as promising alternatives or adjuncts in combating bacterial infections.

### 5.2.2. Binding constants:

The spectrophotometric absorption method was employed to assess the binding constant ($K_b$) of *Ammudoucus leucotrichus* and *Mentha piperita* essential oils with the three types of bacteria under investigation. This constant was expressed in $M^{-1}$. Decreasing concentrations of EOs and amoxicillin resulted in a gradual decrease in the absorption of the solution containing the bacteria. By plotting $A_0/(A-A_0)$ against 1/C (Figure 23) (Tyagi et al., 2015), the slope was calculated as $\varepsilon/(\varepsilon_0-\varepsilon).Kb$, where $\varepsilon$ represents the absorbance of the solution containing the compound, and $\varepsilon_0$ denotes the absorbance of the control solution. The "y" intercept was also calculated as $\varepsilon/ (\varepsilon_0-\varepsilon)$. Subsequently, the binding constant was determined by dividing the slope by the intercept ($K_b$ = slope/intercept).

### 5.2.3. Binding free energy:

Utilizing Equation 10, the variation in binding free energy was calculated. Negative values of $\Delta G$ signify the spontaneity of the interaction between the specified bacteria and the studied compounds, with their magnitude indicative of a robust binding affinity between the protein

and the ligands. The binding constants alongside their corresponding binding free energies are succinctly presented in Table 15.

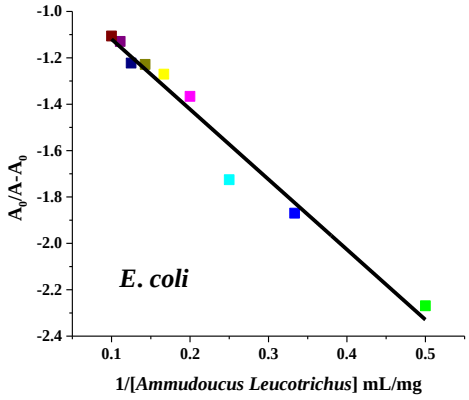


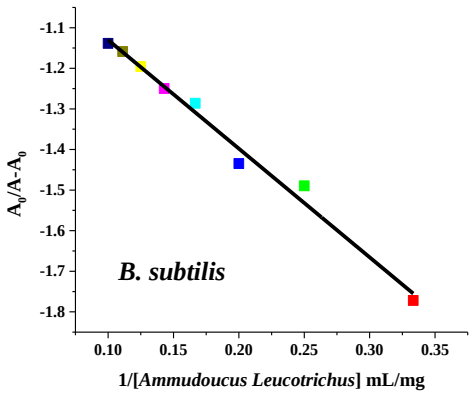


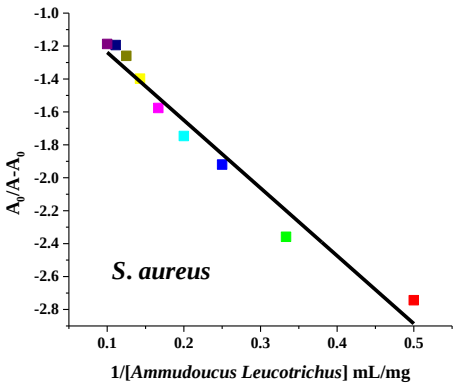


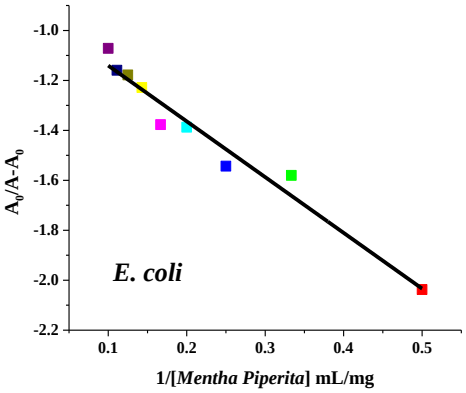


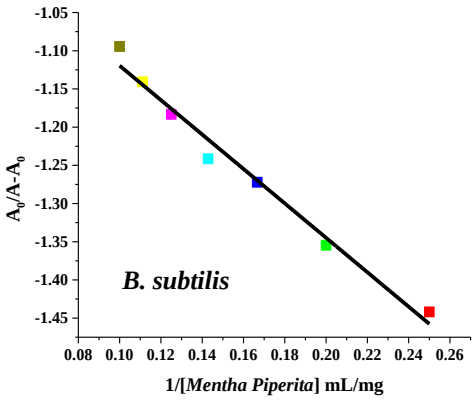


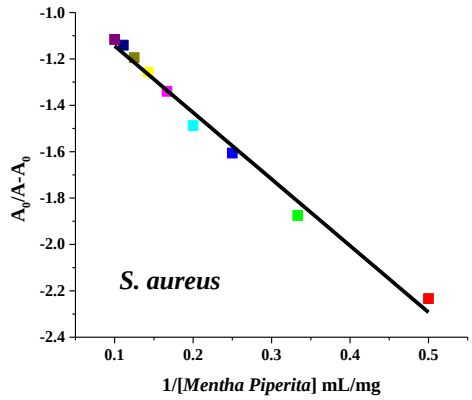

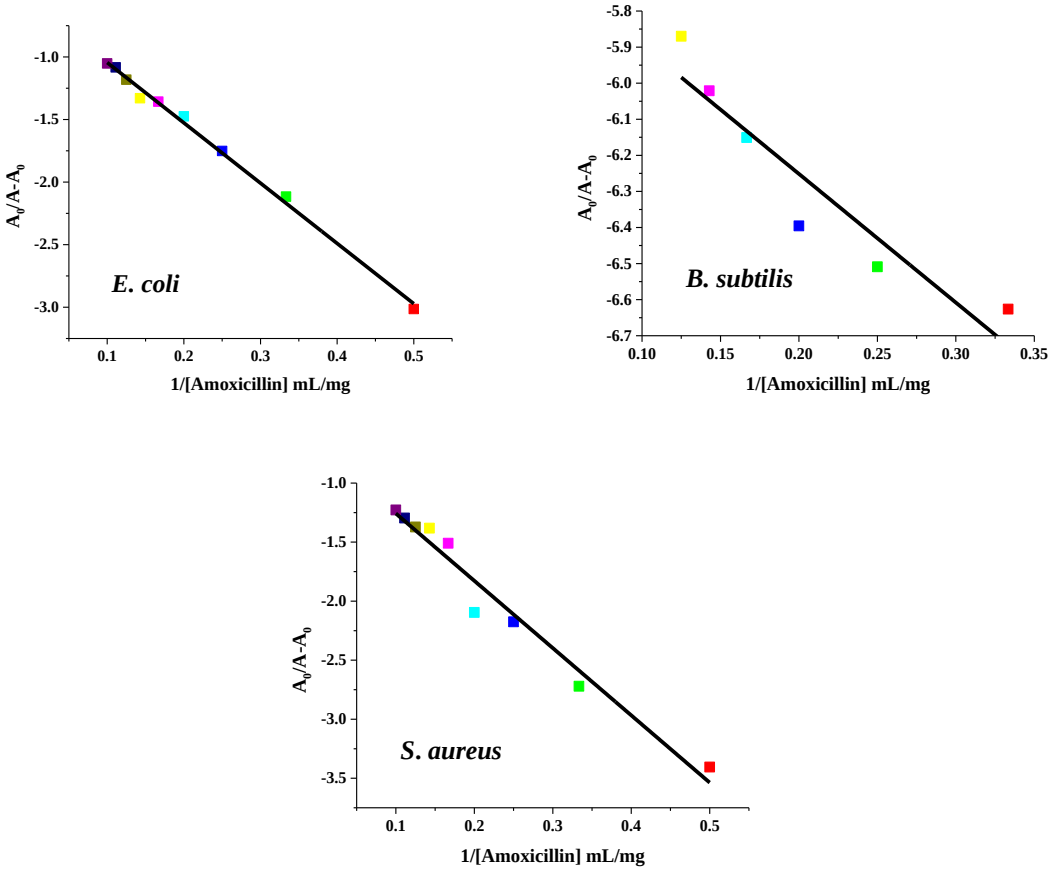


**Figure 24:** Plots of $A_0/(A - A_0)$ against 1/ [*Ammudoucus leucotrichus*], 1/ [*Mentha piperita*] and 1/ [Amoxicillin] were constructed to calculate the binding constants

**Table 15:** Binding constants and binding free energies of the studied compounds with bacterial strains

| Compounds | Bacteria's | Equations | $R^2$ | K ($M^{-1}$) | -ΔG ($KJ.mol^{-1}$) |
|---|---|---|---|---|---|
| ***Ammudoucus leucotrichus*** | *E. coli* | y = -3.024x – 0.817 | 0.968 | $2.70 \times 10^5$ | 31.01 |
| | *B. subtilis* | y = -2.677x – 0.862 | 0.985 | $3.22 \times 10^5$ | 31.45 |
| | *S. aureus* | y = -4.118x – 0.827 | 0.962 | $2.00 \times 10^5$ | 30.27 |
| ***Mentha piperita*** | *E. coli* | y = -2.232x – 0.917 | 0.960 | $4.11 \times 10^5$ | 32.05 |
| | *B. subtilis* | y = -2.254x – 0.894 | 0.977 | $3.97 \times 10^5$ | 31.96 |
| | *S. aureus* | y = -2.871x – 0.857 | 0.986 | $2.98 \times 10^5$ | 31.26 |
| **Amoxicillin** | *E. coli* | y = -4.817x – 0.563 | 0.995 | $1.17 \times 10^5$ | 28.93 |
| | *B. subtilis* | y = -3.566x – 5.538 | 0.853 | $1.55 \times 10^5$ | 35.35 |
| | *S. aureus* | y = -5.697x – 0.688 | 0.964 | $1.21 \times 10^5$ | 29.01 |

The table provides a comprehensive overview of the binding interactions between various compounds, including *Ammudoucus leucotrichus*, *Mentha piperita*, and amoxicillin, with

different bacterial strains, namely *E. coli, B. subtilis,* and *S. aureus*. Each entry includes the equation of the linear regression line obtained from the plots of $A/(A_0 - A)$ against 1/[EOs], the coefficient of determination ($R^2$) indicating the goodness of fit of the regression model, the binding constant (K) expressed in $M^{-1}$, and the corresponding negative change in Gibbs free energy ($-\Delta G$) in kJ/mol (Ozer, 1985).

The high values of $R^2$ across all entries indicate a strong correlation between the experimental data and the fitted regression lines, suggesting the reliability of the models in describing the binding behavior (Plonsky & Ghanbar, 2018). Additionally, the binding constants (K) provide quantitative measures of the strength of interaction between the compounds and the bacterial strains, with higher values indicating stronger binding affinities (T. Lanez et al., 2018).

The negative values of $\Delta G$ underscore the spontaneity of the binding interactions, with larger magnitudes indicating more favorable and energetically stable associations between the compounds and the bacteria (Kedadra et al., 2022). Notably, Amoxicillin exhibits relatively lower binding constants and $\Delta G$ values compared to the essential oils, suggesting potentially weaker interactions with the bacterial strains studied.

In the context of this study, higher values of K indicate stronger binding affinities between the compounds and the bacterial strains (Adaika et al., 2019). *Ammudoucus leucotrichus* and *Mentha piperita* essential oils exhibit notably higher K values compared to amoxicillin across all bacterial strains tested. This suggests that the essential oils have a greater propensity to bind to the bacterial receptors, potentially leading to enhanced antimicrobial efficacy. Conversely, amoxicillin demonstrates relatively lower K values, indicating comparatively weaker binding interactions with the bacterial strains. This observation aligns with the known mechanism of action of amoxicillin, which primarily targets specific bacterial cell wall components rather than interacting directly with bacterial receptors.

### 5.3. Molecular Docking Interaction Study:

In order to validate the experimentally measured antibacterial activity against E. *coli, B. subtilis*, and *S. aureus*, an in-silico molecular docking study was conducted on the proteins of the respective bacteria. The objective of this study was to predict the molecular interactions between the compound of interest and the studied bacteria, and to assess their antibacterial potential using Maestro version 11.7 user interface of the Schrödinger suite (Small-Molecule Drug Discovery Suite 2021-4, Schrödinger, LLC, New York, NY, 2021) (Schrödinger, 2015). Additionally, a comparison of the results obtained with amoxicillin, a commonly used

antibiotic, was performed. The results obtained after the docking assays are presented in the Table 16.

**Table 16:** Rigid and induced fit docking scores of the studied compounds against *E. coli*, *B. subtilis*, and *S. aureus*

| Compound | *E. coli* | | *B. subtilis* | | *S. aureus* | |
|---|---|---|---|---|---|---|
| | Rigid Docking Score (Kcal/mol) | IFD scores (Kcal/mol) | Rigid Docking Score (Kcal/mol) | IFD scores (Kcal/mol) | Rigid Docking Score (Kcal/mol) | IFD scores (Kcal/mol) |
| **Perilla aldehyde** | -7.728 | -8.228 | -6.894 | -7.394 | -5.828 | -7.128 |
| **D-Limonene** | -7.694 | -8.194 | -9.551 | -10.051 | -5.794 | -7.094 |
| **alpha-Pinene** | -6.894 | -7.394 | -8.969 | -9.469 | -4.994 | -6.294 |
| **Pulegone** | -9.551 | -10.051 | -8.569 | -9.069 | -7.651 | -8.951 |
| **Menthone** | -8.969 | -9.469 | -8.062 | -8.562 | -7.069 | -8.369 |
| **trans-Sabinene hydrate** | -8.569 | -9.069 | -7.536 | -8.036 | -6.669 | -7.969 |
| **alpha-Terpineol** | -8.062 | -8.562 | -8.062 | -8.562 | -6.162 | -7.462 |
| **Borneol** | -7.536 | -8.036 | -5.636 | -6.936 | -5.636 | -6.936 |
| **Linalool acetate** | -6.994 | -7.494 | -5.094 | -6.394 | -5.094 | -6.394 |
| **1,8-Cineole** | -6.716 | -7.216 | -4.816 | -6.116 | -4.816 | -6.116 |

The table presents the results of rigid docking scores and induced fit docking (IFD) scores for various compounds against three bacterial strains: Escherichia coli, Bacillus subtilis, and Staphylococcus aureus. These scores provide insights into the potential antibacterial activity of each compound by indicating the strength of interaction with the target proteins or receptors within the bacteria.

Observing the rigid docking scores, it is evident that compounds such as Pulegone and D-Limonene exhibit the most favorable scores across all three bacterial strains, suggesting strong binding affinities towards their respective targets. Conversely, Linalool acetate and 1, 8-Cineole demonstrate comparatively weaker rigid docking scores, indicating potentially weaker interactions with the bacterial proteins.

The induced fit docking (IFD) scores further validate the binding affinities of the compounds by considering the flexibility of both the ligands and the target proteins during the docking

process. Notably, compounds like Pulegone and D-Limonene maintain their favorable IFD scores, affirming their potential as promising antibacterial agents.

Comparing the results obtained for each compound across the three bacterial strains, variations in docking scores are observed, suggesting potential differences in the binding interactions with the specific target proteins or receptors present in each strain. This highlights the importance of considering the target specificity of antibacterial agents in rational drug design.

The photographs depicting the interaction of the best compound in each essential oil with the studied bacteria are presented in Figures 25 below:

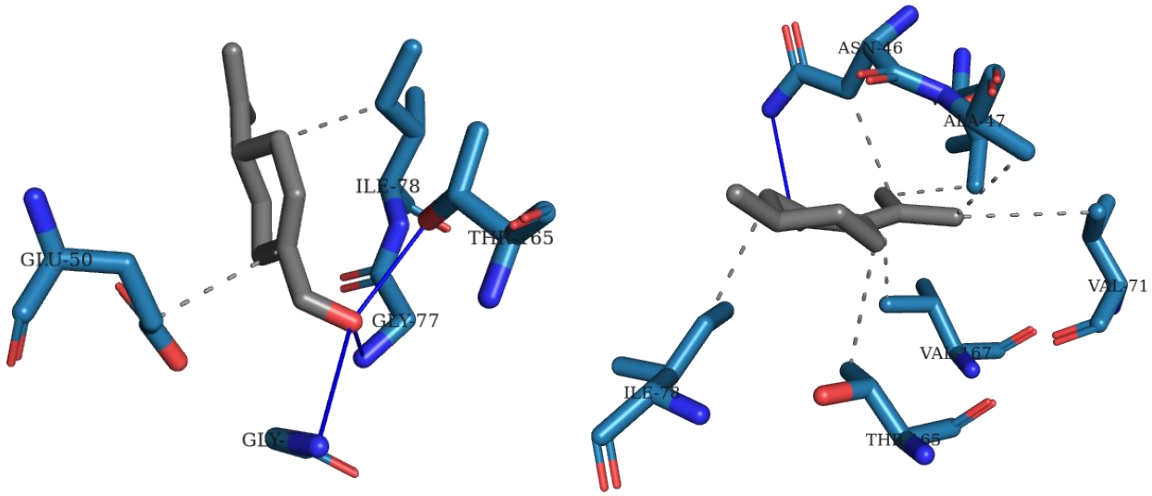


*Docking complex and interaction plot for compound Perilla aldehyde and Pulegone with E. coli*

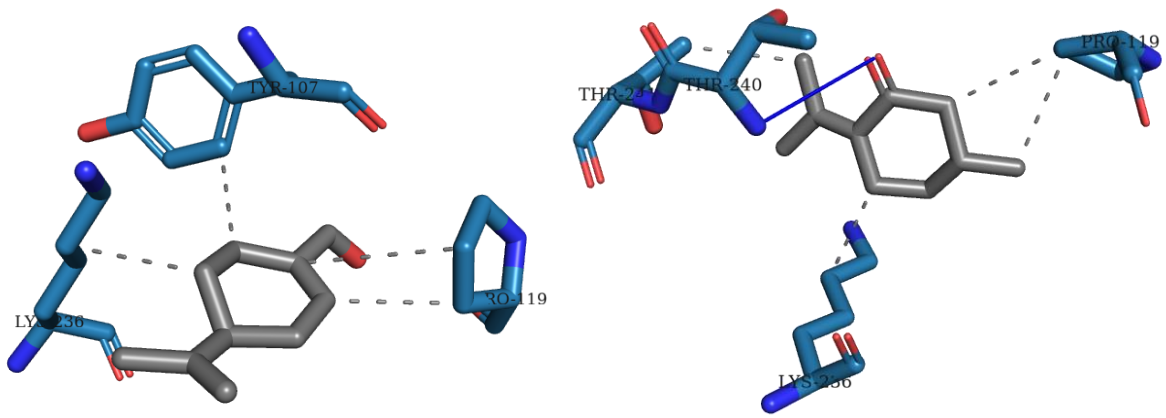


*Docking complex and interaction plot for compound Perilla aldehyde and Pulegone with B. subtilis*

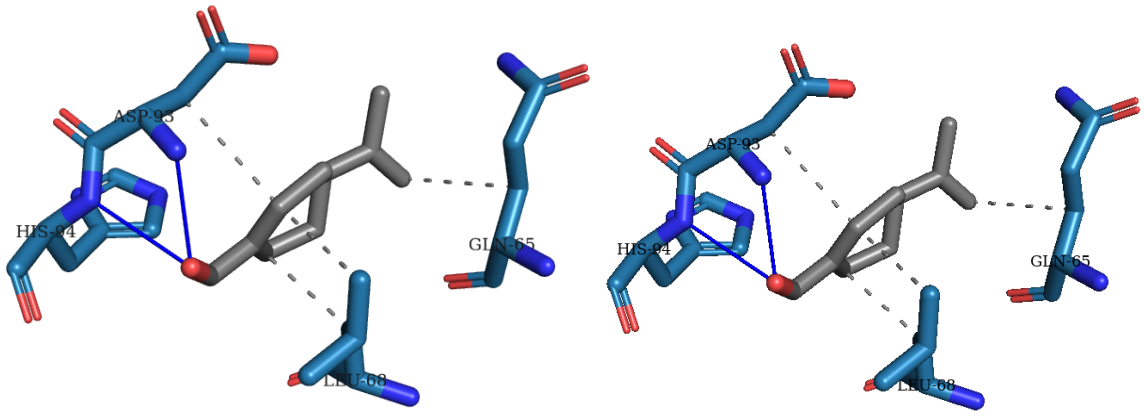


*Docking complex and interaction plot for compound Perilla aldehyde and Pulegone with S. aureus*

**Figure 25 :** Molecular interactions of studied compounds with *E. coli, B. subtilis* and *S. aureus*

## 6. ADMET and drug-likeness prediction:

Modern drug discovery involves assessment of competence of the dynamic molecules and their strength to reach target site in bioactive form, which involves cellular, animal and human clinical trials which are highly priced and encumbered with risks (Ranjith & Ravikumar, 2019; Ranjith D & Viswanath S, 2019). Presently computer aided drug development encouraged the estimate of absorption, distribution, metabolism and excretion of drugs (ADME), they postulate anticipatory and dependable data very quickly and compliment for experimental approaches (Ranjith & Ravikumar, 2019; Sliwoski et al., 2014). It has been determined that the initial appraisal of ADME properties in the discovery period diminishes remarkably the fraction of pharmacokinetics related failures in the clinical phase (Hay et al., 2014; Ranjith & Ravikumar, 2019).

In the present study we evaluated the ADME properties of the major compounds present in both essential oils using SwissADME web tool. A total of 4 potent phytoconstituents were analysed to study general characteristics (Table 17), Physicochemical properties (Table 18), lipophilicity and water solubility characteristics (Table 19 & 20), pharmacokinetic parameters (Table 21), drug likeness rule and bioavailability score (Table 22) and medicinal chemistry properties (Table 23), respectively. General characteristics of the studied compounds revealed all the compounds having molecular weight less than 500 Da, which is a good prime property to be called as drug likeness of the small molecules.

**Table 17:** General characteristics of the phytoconstituents of essential oils

| SI. No | Compounds | Molecular formula | Canonical SMILES | Molecular weight (g/mol) |
|---|---|---|---|---|
| **1** | **trans-Sabinene hydrate** | $C_{10}H_{18}O$ | CC(C12CCC(C2C1)(C)O)C | 154.25 |
| **2** | **Linalool acetate** | $C_{12}H_{20}O_2$ | C=CC(OC(=O)C)(CCC=C(C)C)C | 196.29 |
| **3** | **Perilla aldehyde** | $C_{10}H_{14}O$ | O=CC1=CCC(CC1)C(=C)C | 150.22 |
| **4** | **D-Limonene** | $C_{10}H_{16}$ | CC1=CCC(CC1)C(=C)C | 136.23 |

**Table 18:** Physicochemical properties of the phytoconstituents of essential oils

| Properties | trans-Sabinene hydrate | Linalool acetate | Perilla aldehyde | D-Limonene |
|---|---|---|---|---|
| **Num. heavy atoms** | 11 | 14 | 11 | 10 |
| **Num. arom. heavy atoms** | 0 | 0 | 0 | 0 |
| **Fraction Csp3** | 1.00 | 0.58 | 0.50 | 0.60 |
| **Num. rotatable bonds** | 1 | 6 | 2 | 1 |
| **Num. H-bond acceptors** | 1 | 2 | 1 | 0 |
| **Num. H-bond donors** | 1 | 0 | 0 | 0 |
| **Molar refractivity** | 46.90 | 60.17 | 47.32 | 47.12 |
| **TPSA (Å²)** | 20.23 | 26.30 | 17.07 | 0.00 |

**Table 19:** Lipophilicity characteristics of the phytoconstituents of essential oils

| Properties | trans-Sabinene hydrate | Linalool acetate | Perilla aldehyde | D-Limonene |
|---|---|---|---|---|
| **iLOGP** | 2.47 | 3.08 | 2.16 | 2.72 |
| **XLOGP3** | 2.12 | 3.93 | 3.13 | 4.57 |
| **WLOGP** | 2.19 | 3.24 | 2.49 | 3.31 |
| **MLOGP** | 2.45 | 2.95 | 2.10 | 3.27 |
| **SILICOS-IT** | 2.44 | 2.98 | 2.64 | 2.97 |
| **Consensus Log Po/w** | 2.33 | 3.24 | 2.50 | 3.37 |

**Table 20:** Water Solubility characteristics of the phytoconstituents of essential oils

| Small molecules | ESOL | | | | Ali | | | | SILICOS-IT | | | |
|---|---|---|---|---|---|---|---|---|---|---|---|---|
| | Log S (ESOL) | Solubility | | Class | Log S (Ali) | Solubility | | Class | Log S (SILICOS-IT) | Solubility | | Class |
| | | mg/ml | mol/L | | | mg/ml | mol/L | | | mg/ml | mol/L | |
| **trans-Sabinene hydrate** | -2.07 | 1.33e-0 | 8.59e-3 | **S** | -2.18 | 1.03e-0 | 6.67e-3 | **S** | -1.91 | 1.92e-0 | 1.24e-2 | **S** |
| **Linalool acetate** | -3.14 | 1.43e-1 | 7.30e-4 | **S** | -4.18 | 1.29e-2 | 6.58e-5 | **MS** | -2.52 | 5.97e-1 | 3.04e-3 | **S** |
| **Perilla aldehyde** | -2.61 | 3.68e-1 | 2.45e-3 | **S** | -3.16 | 1.04e-1 | 6.96e-4 | **S** | -1.83 | 2.22e-0 | 1.48e-2 | **S** |
| **D-Limonene** | -3.50 | 4.33e-2 | 3.18e-4 | **S** | -4.29 | 6.93e-3 | 5.09e-5 | **MS** | -2.26 | 7.54e-1 | 5.53e-3 | **S** |

**Table 21:** Pharmacokinetics parameters of the phytoconstituents of essential oils

| Proprieties | trans-Sabinene hydrate | Linalool acetate | Perilla aldehyde | D-Limonene |
|---|---|---|---|---|
| **GI absorption** | High | High | High | Low |
| **BBB permeant** | Yes | Yes | Yes | Yes |
| **P-gp substrate** | No | No | No | No |
| **CYP1A2 inhibitor** | No | No | No | No |
| **CYP2C19 inhibitor** | No | No | No | No |
| **CYP2C9 inhibitor** | No | No | No | Yes |
| **CYP2D6 inhibitor** | No | No | No | No |
| **CYP3A4 inhibitor** | No | No | No | No |
| **Log Kp (Skin Permeation) (cm/s)** | -5.74 | -4.71 | -4.99 | -3.89 |

**Table 22:** Druglikeness rule and bioavailability score of the phytoconstituents of essential oils

| Proprieties | trans-Sabinene hydrate | Linalool acetate | Perilla aldehyde | D-Limonene |
|---|---|---|---|---|
| **Lipinski** | Yes; 0 violations | Yes; 0 violations | Yes; 0 violations | Yes; 0 violations |
| **Ghose** | No; 1 violation: MW<160 | Yes | No; 1 violation: MW<160 | No; 1 violation: MW<160 |
| **Veber** | Yes | Yes | Yes | Yes |
| **Egan** | Yes | Yes | Yes | Yes |
| **Muegge** | No; 2 violations: MW<200, XLOGP3>3.5 | No; 1 violation: MW<200 | No; 2 violations: MW<200, Heteroatoms<2 | No; 2 violations: MW<200, Heteroatoms<2 |
| **Bioavailability score** | 0.55 | 0.55 | 0.55 | 0.55 |

**Table 23:** Medicinal Chemistry properties of the Phytoconstituents of essential oils

| Proprieties | trans-Sabinene hydrate | Linalool acetate | Perilla aldehyde | D-Limonene |
|---|---|---|---|---|
| **PAINS** | 0 alert | 0 alert | 0 alert | 0 alert |
| **Brenk** | 0 alert | 1 alert: isolated_alkene | 1 alert: isolated_alkene | 1 alert: isolated_alkene |
| **Leadlikeness** | No; 1 violation: MW<250 | No; 2 violations: MW<250, XLOGP3>3.5 | No; 1 violation: MW<250 | No; 2 violations: MW<250, XLOGP3>3.5 |
| **Synthetic accessibility** | 2.82 | 2.75 | 3.19 | 3.46 |

Lipophilicity property of the compounds portrays an important role for molecular discovery activities in multifarious domains. The quantitative descriptor of the lipophilicity is the partition coefficient P of a given molecule between *n*-octanol and water system (Daina et al., 2014). Because of its amphiphilic nature, *n*-octanol is considered a good mimic of phospholipid membrane characteristics (Liu et al., 2011). Multifarious algorithms are accessible to compute log Po/w, which rely on factual methodologies. The classic log P predictors branched in to two division, first ones split molecular structures into molecular fragments includes fragmental approach e.g. KLOGP (Klopman et al., 1993), KOWWNIN (Meylan & Howard, 2000) or atomic approach e.g. ALOGP (Ghose et al., 1998; R. Wang et al., 1997), XLOGP (Cheng et al., 2007; Moriguchi et al., 1994). The second division gathers the topological methods in which, the molecules description is related to its topology being as count or flags for specific atoms, groups or structural properties e.g. MLOGP (Brenk et al., 2008; Moriguchi et al., 1992), the prediction attained by manifold linear regression trained on large molecular data sets. The SILICOS-IT is a hybrid technique which combines both molecular fragments and topological parameters, which confide on 27 fragments and 7 topological descriptors, it was disciplined on 23,455 molecules with experimental *n*-octanol/water partition values (Daina et al., 2014). The version three of the XLOGP atomic model is established on a system of 87 fragments and two corrective factors. If the input structures are similar to a reference compound, the fragments differentiating them are treated and the corresponding log P contributions added to the reference structure log P value (Cheng et al., 2007). Lipophilicity estimated as consensus Log P, which is the average value of all Log P evaluated with various lipophilicity criteria, determined Perilla aldehyde as most lipophilic whereas trans-Sabinene hydrate as least lipophilic and water solubility of the small molecules ranged from highly water soluble (Perilla aldehyde) to water soluble (trans-Sabinene hydrate).

The SwissADME model returns “Yes” or “No” if the compound under examination has greater probability to be a substrate or non-substrate of P-gp or inhibitor or non-inhibitor of Cytochrome P450 isoenzymes (CYP1A2, CYP2C9, CYP2C19, CYP2D6 and CYP3A4).

The pharmacokinetics and drug likeness performed using SwissADME showed a low level of GI absorption and BBB permeant with D-Limonene while a high absorption detected with trans-Sabinene hydrate and Linalool acetate. All the compounds present in the essential oils are not the substrates for P-gp except (Table 21), so they are not susceptible to the efflux mechanism performed by this transporter which is used by many tumours cell lines as a drug-resistance mechanism (Ranjith & Ravikumar, 2019) .

All of the small molecules returned as non-inhibitors for inactivation for CYP isoenzymes. The skin permeability coefficient (Log Kp), a multiple linear regression, the more negative the log KP (with KP in cm/s), the less skin permeant is the molecule. Among the phytoconstituents, trans-Sabinene hydrate (-5.74) is the least permeant and D-Limonene (-4.13) is highly permeant respectively. This SwissADME section gives access to five different rule-based filters, with diverse ranges of properties inside of which the molecule is defined as drug-like. The Lipinski (Pfizer) filter is the pioneer rule-of-five implemented and with the Ghose (Amgen), Veber (GSK), Egan (Pharmacia) and Muegge (Bayer) methods. Multiple estimations allow consensus views or selection of methods best fitting the end-user's specific needs in terms of chemical space or project-related demands. Any violation of any rule described here appears explicitly in the output panel. All the four compounds followed the filtered rule invoked in the SwissADME; the violation shown by the molecules are minimal.

SwissADME interpretation posts 0 PAINS alert of the 4 studied compounds. Brenk considered compounds that are smaller and less hydrophobic and not those defined by "Lipinski's rule of 5" to widen opportunities for lead optimization. This was after exclusion of compounds with potentially mutagenic, reactive and unfavourable groups such as nitro groups, sulphates, phosphates, 2-halopyridines and thiols (Brenk et al., 2008). All the compounds examined flouted Brenk's rule with only one alert, all the compounds failed Lead-likeness criteria due to their molar weight.

In silico toxicity study aims to help in optimizing compounds regarding their toxicity proprieties. The study could offer an important improvement to the awareness of the full perspective of virtual screening for the identification of target compounds with negligible or no toxicity, which may open a path for the selection of novel nontoxic phytoconstituents present in *Ammudoucus leucotrichus* and *Mentha piperita* essential oils with high antidiabetic activity. In silico toxicity study of the chosen compounds was performed using the ProTox-II web server (Drwal et al., 2014). It aims to predict hepatotoxicity (Dili), carcinogenicity (Carcino), immunotoxicity (Immuno), mutagenicity (Mutagen), cytotoxicity (Cyto), median lethal dose ($LD_{50}$), and toxicity class (TC).

According to in silico toxicity profiles presented in Table 24, the toxicity class of all the phytoconstituents was detected to be equal to 5 except the Linalool acetate which predicted to be 6. Also, all the compounds were nontoxic in all the type of toxicities.

**Table 24:** In silico toxicity profiles of the studied compounds

| Molecule | Dili | Carcino | Immuno | Mutagen | Cyto | $LD_{50}$ ($mg.Kg^{-1}$) | TC |
|---|---|---|---|---|---|---|---|
| **trans-Sabinene hydrate** | Inactive | Inactive | Inactive | Inactive | Inactive | 2000 | 4 |
| **Linalool acetate** | Inactive | Inactive | Inactive | Inactive | Inactive | 12000 | 6 |
| **Perilla aldehyde** | Inactive | Inactive | Inactive | Inactive | Inactive | 1720 | 4 |
| **D-Limonene** | Inactive | Inactive | Inactive | Inactive | Inactive | 4400 | 5 |

## 7. Molecular Dynamics Simulation:

Molecular Dynamics Simulation (MDS) investigations were conducted for the premier compound show the best IFD score, Pulegone, in complex with E. coli. The principal objective of these MDS endeavours was to subject the ligand-receptor complex to physiological conditions, a feat unattainable through the confines of molecular docking (Dumitrică & James, 2007). Throughout the MDS protocol, a trajectory frame was generated at intervals of 100 picoseconds (Tu et al., 2008), accumulating a total of 1000 frames over the course of a 100-nanosecond simulation. Analysis encompassed metrics such as 'Root Mean Square Deviation (RMSD), and 'Root Mean Square Fluctuation (RMSF). Specifically, RMSD values were computed by aligning the frames of the protein and ligand-protein complex with the reference frame, respectively. These analytical approaches provide a detailed understanding of the structural stability and dynamic fluctuations exhibited by the Pulegone_*E.coli* complex throughout the simulation period (Schreiner et al., 2012).

The Root Mean Square Deviation (RMSD) values for the complex consistently fall within the acceptable range of 0 – 2 Å. Examination of the analysed complex revealed no significant conformational alterations; however, an initial minor deviation was discerned in the vicinity of 8 – 20 nanoseconds, and a subtle drift was observed approximately between 45 – 55 nanoseconds. Beyond these periods, the complex demonstrated marked stability throughout the entirety of the simulation process, with no notable occurrence of major conformational changes. (Figure 26).

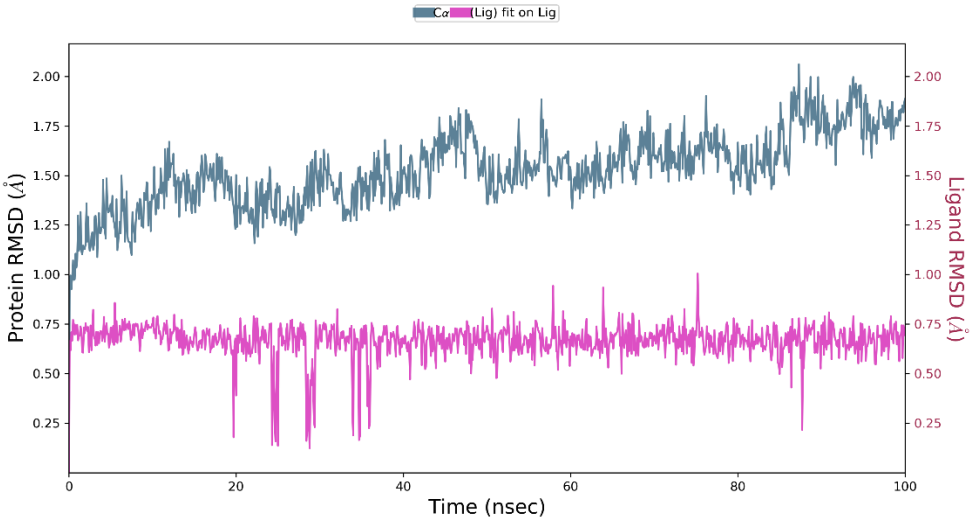


**Figure 26:** RMSD plot of Pulegone and *E. coli* complex

The Root Mean Square Fluctuation (RMSF) analysis provides insights into local variations along the protein chain, facilitating the identification of residues contributing to structural fluctuations within the complex (Dey et al., 2021). In the examined complex, the observed fluctuation variation remained below 3 Å. Major Fluctuations (2.20-2.63 and 1.81-2.96Å) were observed in the C-terminal and loop regions (223-225 and 363-366), respectively, which are positioned away from the binding pocket of alpha amylase. Except for the loop regions, the RMSF values of most residues are less than 1.5 Å, indicating that the residue conformation is relatively stable during the simulation. A graphical representation of the RMSF plot depicting the specific ligand interactions with amino acid residues in the protein is presented in Figure 27.

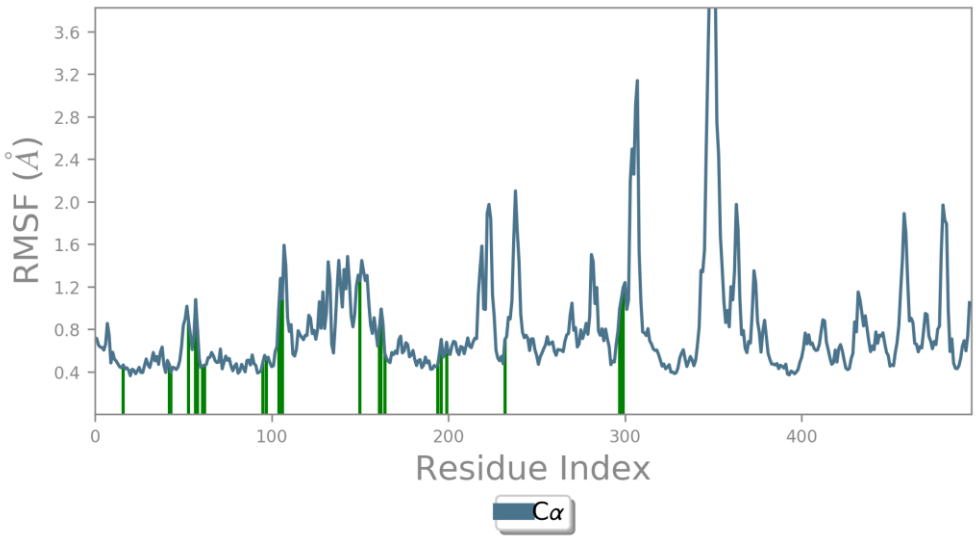


**Figure 27:** RMSF plot of Pulegone and *E. coli* complex

Within the investigated complex, notable hydrogen bond interactions were observed involving HIS299, ASP197, and TRP58. Additionally, water-mediated hydrogen bond interactions were formed, encompassing the same residues, as visually depicted in Figure 28.

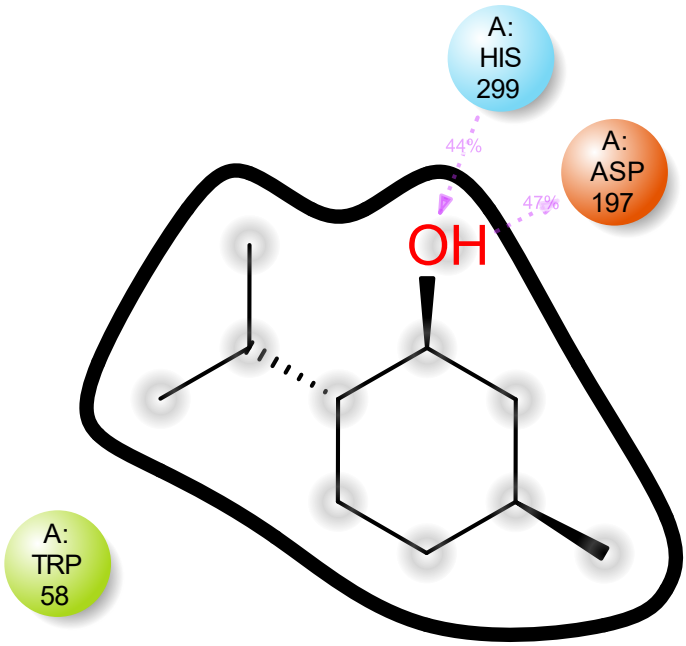


**Figure 28:** Interaction diagram of protein-ligand after MDS

The analysis of Protein-ligand contact serves to elucidate the temporal continuity of interactions between the ligand and protein amino acids throughout the simulation. A numerical representation is employed, where a value of 0.5 denotes that a specific interaction was sustained for 50% of the simulation duration. Conversely, a value exceeding 1 suggests that protein amino acids may establish multiple contacts of the same subtype with the ligand (Hatmal & Taha, 2017).

In the context of the investigated complex, the interaction values for the residues GLU240, HIS201, ASP197, GLN63, GLU233, and THR163 are recorded as 1.25, 1, 1.75, 1, 0.60, and 1.5, respectively. These values signify varying degrees of sustained interactions between the ligand and corresponding amino acid residues. The graphical representation of the protein-ligand contact histograms for the complex is depicted in Figure 29 for visual elucidation.

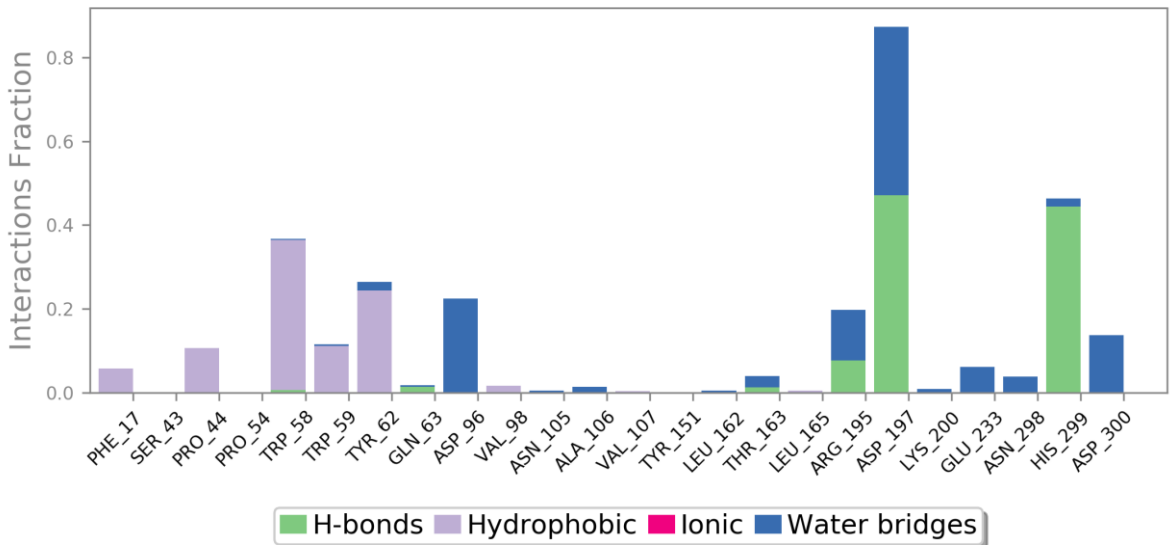


**Figure 29:** Histogram of protein-ligand complex

To comprehensively investigate the interactions between the ligand and alpha-amylase receptor, two supplementary panels were introduced by Schrödinger post Molecular Dynamics Simulation (MDS), as depicted in Figure 30. The upper panel provides insights into the total number of specific contacts established by the protein with the ligand throughout the trajectory. Conversely, the lower panel delineates the residues engaged in interactions with the ligand in each trajectory frame.

Notably, certain residues exhibit multiple specific contacts with the ligand, visualized through varying shades of orange on the plot, in accordance with the scale positioned to the right of the diagram. This nuanced representation captures the dynamic nature of the interactions, offering a detailed portrayal of the residues that consistently contribute to the ligand-receptor interface. The incorporation of these supplementary panels enhances the granularity of our understanding of the molecular dynamics and specific contacts governing the ligand-receptor interaction over the course of the simulation.

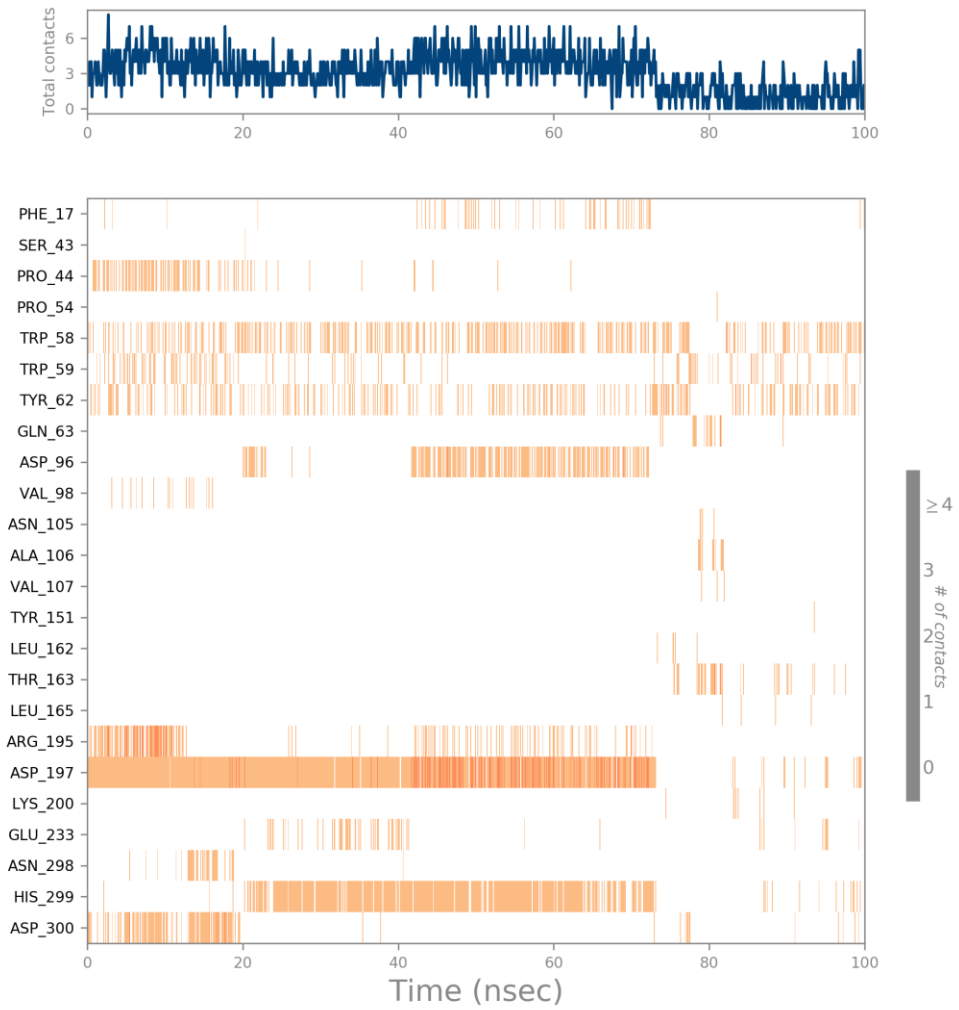


**Figure 30:** Details of the protein ligand contact

### 7.1. Free Energy (MM-GBSA) Calculation:

To evaluate the binding efficacy of the preeminent compound, Pulegone, with the E. coli protein, the Prime-MM-GBSA method was applied to compute the binding free energies. The establishment of stable complexes is evidenced by favourable binding interactions between the compound and the protein. The determination of binding free energy entails the consideration of various energy components, encompassing van der Waals (vdW), lipophilic (lipo), Generalized Born electrostatic solvation (Solv GB), Coulomb, and hydrogen-bonding (hbond) energies. The discrete contributions of these energy components to the overall binding free energy of the Pulegone and E. coli complex are delineated in Table 25.

**Table 25:** Energy components of the studied complex

| Component | Energy (kcal/mol) |
|---|---|
| **ΔG Bind** | -61.14 |
| **ΔG Bind Coulomb** | -30.03 |
| **ΔG Bind Solv GB** | 48.10 |
| **ΔG Bind vdW** | -54.91 |
| **ΔG Bind lipo** | -20.51 |
| **ΔG Bind hbond** | -3.79 |

Notably, ΔG Bind is calculated at -61.14 kcal/mol, indicating a robust favourable binding interaction. Individual positive contributions include Coulombic energy at -30.03 kcal/mol, van der Waals interactions at -54.91 kcal/mol, lipophilic energy at -20.51 kcal/mol, and hydrogen-bonding energy at -3.79 kcal/mol. However, solvation energy through Generalized Born model contributed negatively at 48.10 kcal/mol. This collective interplay of energy components underscores the strong binding affinity observed in the complex.

# *CONCLUSION*

## Conclusion:

This study, which examines the essential oils of the plants *Ammudoucus leucotrichus* and *Mentha piperita*, highlights their potential therapeutic capabilities, especially in the field of cancer and bacterial combat. The essential oils from these two plants contain biologically active compounds that can affect various biological pathways, making them candidates for the development of new drugs. In-vitro studies have confirmed the ability of these oils to exhibit anti-cancer activity by affecting enzymes involved in cancer development. Tests also revealed their effectiveness against bacteria such as *E.coli*, *S. aureus*, and *B. subtilis*, indicating their capacity to deal with various pathogens. Computer-based tests, including molecular docking and dynamics, provided insight into how these oils bind to active sites of certain enzymes associated with cancer. Simulations showed that the protein compounds were stable, enhancing our understanding of molecular-level interactions and potentially aiding in designing more effective compounds. An important aspect of searching for new therapeutic compounds is determining their toxicity level. The results predicting the toxicity of these oils were encouraging, as they showed low toxicity, supporting the possibility of their safer use as treatments. It is crucial to continue these studies to understand the precise mechanisms by which these essential oils operate and to evaluate their safety and efficacy in clinical contexts. Conducting clinical trials will be a critical step to verify the effectiveness of these oils in humans and their tolerability. Overall, this type of research can open doors to the development of new treatments that leverage the properties of natural plants, offering a potential alternative or supplement to currently available conventional treatments.

# *References*

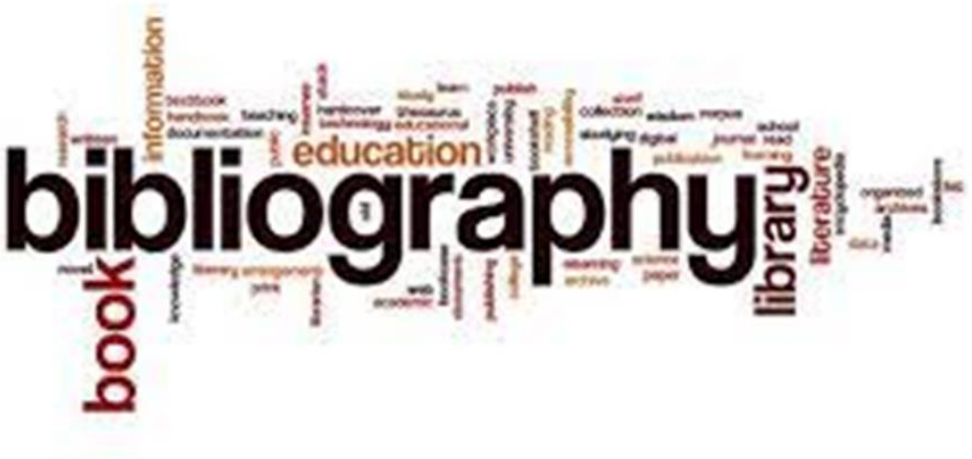
bibliography
education
information
book
library
literature

## References biblographic:

**A**

**Adaika, A., Adaika, A., Lanez, T., & Lanez, E. (2019).** in Vitro and in Silico Evaluation of Anticancer Activity of N,N-Dimethylaminomethylferrocene. *Journal of Fundamental and Applied Sciences*, *11*(2), 748–768. https://jfas.info/index.php/JFAS/article/view/289

**Afnor, Ø. (1982).** Recueil de normes françaises des produits dérivés des fruits et légumes jus de fruits. *AFNOR*, *325*.

**Ahmad, A., Khan, A., Samber, N., & Manzoor, N. (2014).** Antimicrobial activity of Mentha piperita essential oil in combination with silver ions. *Synergy*, *1*(2), 92–98.

**Akbar, S., Das, S., Iqubal, A., & Ahmed, B. (2022).** Synthesis, biological evaluation and molecular dynamics studies of oxadiazine derivatives as potential anti-hepatotoxic agents. *Journal of Biomolecular Structure and Dynamics*, *40*(20), 9974–9991. https://doi.org/10.1080/07391102.2021.1938233

**Alajtal, A. I., Sherami, F. E., & Elbagermi, M. A. (2018).** Acid, peroxide, ester and saponification values for some vegetable oils before and after frying. *AASCIT Journal of Materials*, *4*(2), 43–47.

**Atkins, P., & De Paula, J. (2010).** Physical Chemistry, Oxford University Press. In *Physical Chemistry, Oxford University Press: Vol. Ninth*.

**Atti-Santos, A. C., Rossato, M., Pauletti, G. F., Rota, L. D., Rech, J. C., Pansera, M. R., Agostini, F., Serafini, L. A., & Moyna, P. (2005).** Physico-chemical evaluation of Rosmarinus officinalis L. essential oils. *Brazilian Archives of Biology and Technology*, *48*, 1035–1039.

**Avwioroko, O. J., Oyetunde, T. T., Atanu, F. O., Otuechere, C. A., Anigboro, A. A., Dairo, O. F., Ejoh, A. S., Ajibade, S. O., & Omorogie, M. O. (2020).** Exploring the binding interactions of structurally diverse dichalcogenoimidodiphosphinate ligands with α-amylase: Spectroscopic approach coupled with molecular docking. *Biochemistry and Biophysics Reports*, *24*, 100837. https://doi.org/10.1016/j.bbrep.2020.100837

**B**

**Banerjee, P., Eckert, A. O., Schrey, A. K., & Preissner, R. (2018).** ProTox-II: A webserver for the prediction of toxicity of chemicals. *Nucleic Acids Research*, *46*(W1), W257–W263.

https://doi.org/10.1093/nar/gky318

**Baser, K. H. C., Özek, T., & Kirimer, N. (1993).** The essential oil of Laser trilobum fruit of Turkish origin. *Journal of Essential Oil Research*, *5*(4), 365–369.

**Biswa, M. S., Varsha, T., Abhishek, T., & Bimal, K. B. (2023).** Green Chemistry using Essential Oils as Synthons. *Journal of Indian Chemical Society*, *Mar2023*, 1–24. https://doi.org/10.5281/zenodo.7841465

**Bowers, K. J., Chow, E., Xu, H., Dror, R. O., Eastwood, M. P., Gregersen, B. A., Klepeis, J. L., Kolossvary, I., Moraes, M. A., & Sacerdoti, F. D. (2006).** Scalable algorithms for molecular dynamics simulations on commodity clusters. *Proceedings of the 2006 ACM/IEEE Conference on Supercomputing*, 84-es.

**Brenk, R., Schipani, A., James, D., Krasowski, A., Gilbert, I. H., Frearson, J., & Wyatt, P. G. (2008)**. Lessons learnt from assembling screening libraries for drug discovery for neglected diseases. *ChemMedChem*, *3*(3), 435–444. https://doi.org/10.1002/cmdc.200700139

**C**

**Castagna, R., Donini, S., Colnago, P., Serafini, A., Parisini, E., & Bertarelli, C. (2019).** Biohybrid Electrospun Membrane for the Filtration of Ketoprofen Drug from Water. *ACS Omega*, *4*(8), 13270–13278. https://doi.org/10.1021/acsomega.9b01442

**Cheng, T., Zhao, Y., Li, X., Lin, F., Xu, Y., Zhang, X., Li, Y., Wang, R., & Lai, L. (2007).** Computation of octanol-water partition coefficients by guiding an additive model with knowledge. *Journal of Chemical Information and Modeling*, *47*(6), 2140–2148. https://doi.org/10.1021/ci700257y

**Chiu, S. Y. C., Dobberstein, R. H., Fong, H. H. S., & Farnsworth, N. R. (1982).** Oxoaporphine alkaloids from Siparuna gilgiana. *Journal of Natural Products*, *45*(2), 229–230.

**Cooper, K. E. (1963).** The theory of antibiotic inhibition zones. In *Analytical microbiology* (pp. 1–86). Elsevier.

**Court, R., Chapman, L., Fairall, L., & Rhodes, D. (2005).** How the human telomeric proteins TRF1 and TRF2 recognize telomeric DNA: A view from high-resolution crystal structures. *EMBO Reports*, *6*(1), 39–45. https://doi.org/10.1038/sj.embor.7400314

**D**

**Daina, A., Michielin, O., & Zoete, V. (2014).** ILOGP: A simple, robust, and efficient description of n-octanol/water partition coefficient for drug design using the GB/SA approach. *Journal of Chemical Information and Modeling*, *54*(12), 3284–3301. https://doi.org/10.1021/ci500467k

**Daina, A., Michielin, O., & Zoete, V. (2017).** SwissADME: A free web tool to evaluate pharmacokinetics, drug-likeness and medicinal chemistry friendliness of small molecules. *Scientific Reports*, *7*(1), 1–13. https://doi.org/10.1038/srep42717

**Dey, D., Paul, P. K., Azad, S. Al, Mazid, M. F. Al, Khan, A. M., Sharif, M. A., & Rahman, M. H. (2021).** Molecular optimization, docking, and dynamic simulation profiling of selective aromatic phytochemical ligands in blocking the SARS-CoV-2 S protein attachment to ACE2 receptor: an in silico approach of targeted drug designing. *Journal of Advanced Veterinary and Animal Research*, *8*(1), 24–35. https://doi.org/10.5455/javar.2021.h481

**Drwal, M. N., Banerjee, P., Dunkel, M., Wettig, M. R., & Preissner, R. (2014).** ProTox: A web server for the in silico prediction of rodent oral toxicity. *Nucleic Acids Research*, *42*(W1), W53–W58. https://doi.org/10.1093/nar/gku401

**Dumitrică, T., & James, R. D. (2007).** Objective molecular dynamics. *Journal of the Mechanics and Physics of Solids*, *55*(10), 2206–2236. https://doi.org/10.1016/j.jmps.2007.03.001

**F**

**Filote, C., Lanez, E., Popa, V. I., Lanez, T., & Volf, I. (2022).** Characterization and Bioactivity of Polysaccharides Separated through a (Sequential) Biorefinery Process from Fucus spiralis Brown Macroalgae. *Polymers*, *14*(19), 4106. https://doi.org/10.3390/polym14194106

**Friesner, R. A., Murphy, R. B., Repasky, M. P., Frye, L. L., Greenwood, J. R., Halgren, T. A., Sanschagrin, P. C., & Mainz, D. T. (2006).** Extra precision glide: Docking and scoring incorporating a model of hydrophobic enclosure for protein− ligand complexes. *Journal of Medicinal Chemistry*, *49*(21), 6177–6196.

**G**

**Gaaib, J. N., Nassief, A. F., & Al-assi, A. H. (2011).** Simple salting – out method for genomic

DNA extraction from whole blood Abstract : Introduction : *Nucleic Acids Research*, *16*(2), 15–17.

**Gavahian, M., Farahnaky, A., Farhoosh, R., Javidnia, K., & Shahidi, F. (2015).** Extraction of essential oils from Mentha piperita using advanced techniques: Microwave versus ohmic assisted hydrodistillation. *Food and Bioproducts Processing*, *94*, 50–58.

**Ghose, A. K., Viswanadhan, V. N., & Wendoloski, J. J. (1998).** Prediction of hydrophobic (lipophilic) properties of small organic molecules using fragmental methods: An analysis of ALOGP and CLOGP methods. *Journal of Physical Chemistry A*, *102*(21), 3762–3772. https://doi.org/10.1021/jp980230o

**Giurazza, R., Mazza, M. C., Andini, R., Sansone, P., Pace, M. C., & Durante-Mangoni, E. (2021).** Emerging treatment options for multi-drug-resistant bacterial infections. *Life*, *11*(6), 519.

**Gorla, U. S., Gsn, K. R., Kulandaivelu, U., Alavala, R. R., Das, S., & Joseph, A. (2021).** Bioflavonoids as potential target inhibitors in covid-19: An in silico analysis. *Journal of Research in Pharmacy*, *25*(6), 982–997. https://doi.org/10.29228/jrp.94

**Griffiths, L., & Chacon-Cortes, D. (2014).** Methods for extracting genomic DNA from whole blood samples: current perspectives. *Journal of Biorepository Science for Applied Medicine*, *2014*(2), 1. https://doi.org/10.2147/bsam.s46573

**Guinaudeau, H., Leboeuf, M., & Cave, A. (1975).** *Aporphine alkaloids.*

**H**

**Halder, D., Das, S., Joseph, A., & Jeyaprakash, R. S. (2023).** Molecular docking and dynamics approach to in silico drug repurposing for inflammatory bowels disease by targeting TNF alpha. *Journal of Biomolecular Structure and Dynamics*, *41*(8), 3462–3475. https://doi.org/10.1080/07391102.2022.2050948

**Hatmal, M. M., & Taha, M. O. (2017).** Simulated annealing molecular dynamics and ligand-receptor contacts analysis for pharmacophore modeling. *Future Medicinal Chemistry*, *9*(11), 1141–1159. https://doi.org/10.4155/fmc-2017-0061

**Hay, M., Thomas, D. W., Craighead, J. L., Economides, C., & Rosenthal, J. (2014).** Clinical development success rates for investigational drugs. *Nature Biotechnology*, *32*(1), 40–51. https://doi.org/10.1038/nbt.2786

**Heckel, R., Shomorony, I., Ramchandran, K., & Tse, D. N. C. (2017).** Fundamental limits of DNA storage systems. *IEEE International Symposium on Information Theory* -

*Proceedings*, 3130–3134. https://doi.org/10.1109/ISIT.2017.8007106

**Horai, H., Arita, M., Kanaya, S., Nihei, Y., Ikeda, T., Suwa, K., Ojima, Y., Tanaka, K., Tanaka, S., & Aoshima, K. (2010).** MassBank: a public repository for sharing mass spectral data for life sciences. *Journal of Mass Spectrometry*, *45*(7), 703–714.

**Hossain, M. A., Al-Hdhrami, S. S., Weli, A. M., Al-Riyami, Q., & Al-Sabahi, J. N. (2014).** Isolation, fractionation and identification of chemical constituents from the leaves crude extracts of Mentha piperita L grown in Sultanate of Oman. *Asian Pacific Journal of Tropical Biomedicine*, *4*, S368–S372.

**Howe, J. R. (1997).** DNA extraction from paraffin-embedded tissues using a salting-out procedure: A reliable method for PCR amplification of archival material. *Histology and Histopathology*, *12*(3), 595–601.

**Isaac, C., Gibson, A., Horrocks, B., & Elsegood, M. J. (1999).** Synthesis, structure and redox properties of ferrocenylmethylnucleobases. *Journal of the Chemical Society, Dalton Transactions*, *18*, 3229–3234.

**J**

**Jamil, M., Altaf, A. A., Badshah, A., Ahmad, I., Zubair, M., Kemal, S., & Ali, M. I. (2013).** Naked Eye DNA detection: Synthesis, characterization and DNA binding studies of a novel azo-guanidine. *Spectrochimica Acta Part A: Molecular and Biomolecular Spectroscopy*, *105*, 165–170.

**Javanrouh, A., & Jelokhani-niaraki, S. (2020).** DNA extraction from chicken blood using a modified Salting-out method. *Applied Animal Science Research Journal*, *9*(34), 3–10.

**K**

**Kedadra, A., Lanez, T., Lanez, E., Hemmami, H., & Henni, M. (2022).** Synthesis and antioxidant activity of six novel N-ferrocenylmethyl-N-(nitrophenyl)and-N-(cyanophenyl)-acetamides: Cyclic voltammetry and molecular docking studies. *Journal of Electrochemical Science and Engineering*, *12*(2), 293–304. https://doi.org/10.5599/jese.1162

**Khelil, C. K. M., Amrouche, B., soufiane Benyoucef, A., Kara, K., & Chouder, A. (2020).** New Intelligent Fault Diagnosis (IFD) approach for grid-connected photovoltaic systems. *Energy*, *211*, 118591.

**Khennoufa, A., Bechki, L., Lanez, T., Lanez, E., & Zegheb, N. (2021).** Spectrophotometric,

voltammetric and molecular docking studies of binding interaction of N-ferrocenylmethylnitroanilines with bovine serum albumin. *Journal of Molecular Structure*, *1224*, 129052. https://doi.org/10.1016/j.molstruc.2020.129052

**Kim, S., Thiessen, P. A., Bolton, E. E., Chen, J., Fu, G., Gindulyte, A., Han, L., He, J., He, S., Shoemaker, B. A., Wang, J., Yu, B., Zhang, J., & Bryant, S. H. (2016).** PubChem substance and compound databases. *Nucleic Acids Research*, *44*(D1), D1202–D1213. https://doi.org/10.1093/nar/gkv951

**Kiryakov, H. G. (1968).** *Structure of dehydroglaucine: a new aporphine alkaloid.*

**Klančnik, A., Piskernik, S., Jeršek, B., & Možina, S. S. (2010).** Evaluation of diffusion and dilution methods to determine the antibacterial activity of plant extracts. *Journal of Microbiological Methods*, *81*(2), 121–126. https://doi.org/10.1016/j.mimet.2010.02.004

**Klopman, G., Li, J. Y., Wang, S., & Dimayuga, M. (1993).** Computer automated log P calculations based on an extended group contribution approach. *Journal of Chemical Information and Computer Sciences*, *33*(4), 752–781.

**Korb, O., Olsson, T. S. G., Bowden, S. J., Hall, R. J., Verdonk, M. L., Liebeschuetz, J. W., & Cole, J. C. (2012)**. Potential and limitations of ensemble docking. *Journal of Chemical Information and Modeling*, *52*(5), 1262–1274.

**L**

**Lanez, E., Bechki, L., & Lanez, T. (2019).** Computational molecular docking, voltammetric and spectroscopic DNA interaction studies of 9N-(Ferrocenylmethyl)adenine. *Chemistry and Chemical Technology*, *13*(1), 11–17. https://doi.org/10.23939/chcht13.01.011

**Lanez, T., Benaicha, H., Lanez, E., & Saidi, M. (2018).** Electrochemical, spectroscopic and molecular docking studies of 4-methyl-5-((phenylimino)methyl)-3H- and 5-(4-fluorophenyl)-3H-1,2-dithiole-3-thione interacting with DNA. *Journal of Sulfur Chemistry*, *39*(1), 76–88. https://doi.org/10.1080/17415993.2017.1391811

**Larbi, B. A. M., Naima, B., Elsharkawy, E. R., & Neghmouche, N. S. (2018).** Phytochemical characterization, in-vitro cytotoxic and antibacterial activity of Cotula cinerea (Delile) Vis essential oil. *Journal of Natural Remedies*, 107–112.

**Liu, X., Testa, B., & Fahr, A. (2011)**. Lipophilicity and its relationship with passive drug permeation. *Pharmaceutical Research*, *28*(5), 962–977. https://doi.org/10.1007/s11095-010-0303-7

**Louail, Z., Kameli, A., Benabdelkader, T., Bouti, K., Hamza, K., & Krimat, S. (2016).**

Antimicrobial and antioxidant activity of essential oil of Ammodaucus leucotrichus Coss. & Dur. seeds. *J. Mater. Environ. Sci*, *7*(7), 2328–2334.

**Lu, C., Wu, C., Ghoreishi, D., Chen, W., Wang, L., Damm, W., Ross, G. A., Dahlgren, M. K., Russell, E., & Von Bargen, C. D. (2021).** OPLS4: Improving force field accuracy on challenging regimes of chemical space. *Journal of Chemical Theory and Computation*, *17*(7), 4291–4300.

**M**

**Madhavi Sastry, G., Adzhigirey, M., Day, T., Annabhimoju, R., & Sherman, W. (2013).** Protein and ligand preparation: parameters, protocols, and influence on virtual screening enrichments. *Journal of Computer-Aided Molecular Design*, *27*, 221–234.

**Manssouri, M., Znini, M., & Majidi, L. (2020).** Studies on the antioxidant activity of essential oil and various extracts of Ammodaucus leucotrichus Coss. & Dur. Fruits from Morocco. *Journal of Taibah University for Science*, *14*(1), 124–130.

**Meylan, W. M., & Howard, P. H. (2000).** Estimating log P with atom/fragments and water solubility with log P. *Perspectives in Drug Discovery and Design*, *19*(1), 67–84. https://doi.org/10.1023/A:1008715521862

**Miller, S. A., Dykes, D. D., & Polesky, H. F. (1988).** A simple salting out procedure for extracting DNA from human nucleated cells. *Nucleic Acids Research*, *16*(3), 1215. https://doi.org/10.1093/nar/16.3.1215

**Mimica-Dukić, N., Božin, B., Soković, M., Mihajlović, B., & Matavulj, M. (2003).** Antimicrobial and antioxidant activities of three Mentha species essential oils. *Planta Medica*, *69*(05), 413–419.

**Moriguchi, I., Hirano, H., & Nakagome, I. (1994).** Comparison of Reliability of log P Values for Drugs Calculated by Several Methods. *Chemical and Pharmaceutical Bulletin*, *42*(4), 976–978. https://doi.org/10.1248/cpb.42.976

**Moriguchi, I., Hirono, S., Liu, Q., Nakagome, Izum., & Matsushita, Y. (1992).** Simple Method of Calculating Octanol/Water Partition Coefficient. *Chemical and Pharmaceutical Bulletin*, *40*(1), 127–130. https://doi.org/10.1248/cpb.40.127

**Mouada, H., Lanez, T., & Lanez, E. (2019).** Investigations of the binding parametres of the interaction of N'-ferrocenylmethyl-N'-phenylaceto-and propionohydrazide with DNA. *Journal of Fundamental and Applied Sciences*, *11*(2), 875–882.

**Moulay, A., Brahim, S., Satrani, B., Ghanmi, M., Aafi, A., Amusant, N., El Antry, S., &**

**Chaouch, A. (2014)**. *Bioactivity and chemical quality of Ammodaucus leucotrichus ssp. Leucotrichus Coss. & Durieu essential oils from Morocco*.

**N**

**Naima, B., Abdelkrim, R., Ouarda, B., Salah, N. N., & Larbi, B. A. M. (2019).** Chemical composition, antimicrobial, antioxidant and anticancer activities of essential oil from *Ammodaucus leucotrichus* Cosson & Durieu (Apiaceae) growing in South Algeria. *Bulletin of the Chemical Society of Ethiopia*, *33*(3), 541–549.

**Narramore, S., Stevenson, C. E. M., Maxwell, A., Lawson, D. M., & Fishwick, C. W. G. (2019).** New insights into the binding mode of pyridine-3-carboxamide inhibitors of E. coli DNA gyrase. *Bioorganic and Medicinal Chemistry*, *27*(16), 3546–3550. https://doi.org/10.1016/j.bmc.2019.06.015

**Nasiri, H., Forouzandeh, M., Rasaee, M. J., & Rahbarizadeh, F. (2005).** Modified salting-out method: High-yield, high-quality genomic DNA extraction from whole blood using laundry detergent. *Journal of Clinical Laboratory Analysis*, *19*(6), 229–232. https://doi.org/10.1002/jcla.20083

**Ni, M. Y., Wang, Y., & Li, H. L. (1997).** Electrochemical and spectral properties of phenylhydrazine in the presence of β-cyclodextrin. *Pol. J. Chem.*, *71*, 816–822.

**Ning, J., Liebich, J., Kästner, M., Zhou, J., Schäffer, A., & Burauel, P. (2009).** Different influences of DNA purity indices and quantity on PCR-based DGGE and functional gene microarray in soil microbial community study. *Applied Microbiology and Biotechnology*, *82*(5), 983–993. https://doi.org/10.1007/s00253-009-1912-0

**O**

**Ozer, D. J. (1985).** Correlation and the coefficient of determination. *Psychological Bulletin*, *97*(2), 307.

**P**

**Plonsky, L., & Ghanbar, H. (2018).** Multiple regression in L2 research: A methodological synthesis and guide to interpreting R2 values. *The Modern Language Journal*, *102*(4), 713–731.

**R**

**Rakesh, K. P., Shiva Prasad, K., & Shridhara Prasad, K. (2012).** Synthesis and characterization of chromium (III) complexes of 4 (3H)-quinazolinone derived schiff base:

antimicrobial and DNA interaction studies. *Int. J. Res. Chem. Environ*, *2*, 221–225.

**Ranjith, D., & Ravikumar, C. (2019).** SwissADME predictions of pharmacokinetics and drug-likeness properties of small molecules present in Ipomoea mauritiana Jacq. *Journal of Pharmacognosy and Phytochemistry*, *8*(5), 2063–2073.

**Ranjith D, & Viswanath S. (2019).** In silico antidiabetic activity of bioactive compounds in Ipomoea mauritiana Jacq. *~ 5 ~ The Pharma Innovation Journal*, *8*(10), 5–11. http://www.thepharmajournal.com

**Rivero, E. R. C., Neves, A. C., Silva-Valenzuela, M. G., Sousa, S. O. M., & Nunes, F. D. (2006).** Simple salting-out method for DNA extraction from formalin-fixed, paraffin-embedded tissues. *Pathology-Research and Practice*, *202*(7), 523–529.

**Riyadi, P. H., Romadhon, Sari, I. D., Kurniasih, R. A., Agustini, T. W., Swastawati, F., Herawati, V. E., & Tanod, W. A. (2021).** SwissADME predictions of pharmacokinetics and drug-likeness properties of small molecules present in Spirulina platensis. *IOP Conference Series: Earth and Environmental Science*, *890*(1), 2063–2073. https://doi.org/10.1088/1755-1315/890/1/012021

**Roos, K., Wu, C., Damm, W., Reboul, M., Stevenson, J. M., Lu, C., Dahlgren, M. K., Mondal, S., Chen, W., Wang, L., Abel, R., Friesner, R. A., & Harder, E. D. (2019).** OPLS3e: Extending Force Field Coverage for Drug-Like Small Molecules. *Journal of Chemical Theory and Computation*, *15*(3), 1863–1874. https://doi.org/10.1021/acs.jctc.8b01026

**S**

**Saab, Y. B., Kabbara, W., Chbib, C., & Gard, P. R. (2007).** Buccal cell DNA extraction: Yield, purity, and cost: A comparison of two methods. *Genetic Testing*, *11*(4), 413–416. https://doi.org/10.1089/gte.2007.0044

**Sahoo, P. K., Das, L. M., Babu, M. K. G., & Naik, S. N. (2007).** Biodiesel development from high acid value polanga seed oil and performance evaluation in a CI engine. *Fuel*, *86*(3), 448–454.

**Samber, N., Khan, A., Varma, A., & Manzoor, N. (2015).** Synergistic anti-candidal activity and mode of action of Mentha piperita essential oil and its major components. *Pharmaceutical Biology*, *53*(10), 1496–1504.

**Schöppler, F., Mann, C., Hain, T. C., Neubauer, F. M., Privitera, G., Bonaccorso, F., Chu, D., Ferrari, A. C., & Hertel, T. (2011).** Molar extinction coefficient of single-wall carbon

nanotubes. *Journal of Physical Chemistry C*, *115*(30), 14682–14686. https://doi.org/10.1021/jp205289h

**Schreiner, W., Karch, R., Knapp, B., & Ilieva, N. (2012).** Relaxation estimation of RMSD in molecular dynamics immunosimulations. *Computational and Mathematical Methods in Medicine*, *2012*. https://doi.org/10.1155/2012/173521

**Schrödinger. (2015).** Small-Molecule Drug Discovery Suite 2015-3: Schrödinger Suite 2015-3 Induced Fit Docking protocol; Glide version 6.8; Prime version 4.1. *Glide Version*, *6*.

**Schrödinger. (2024).** *Schrödinger Release 2024-1: LigPrep, Schrödinger, LLC.*

**Shah, A., Zaheer, M., Qureshi, R., Akhter, Z., & Nazar, M. F. (2010).** Voltammetric and spectroscopic investigations of 4-nitrophenylferrocene interacting with DNA. *Spectrochimica Acta Part A: Molecular and Biomolecular Spectroscopy*, *75*(3), 1082–1087.

**Shahabadi, N., Kashanian, S., Mahdavi, M., & Sourinejad, N. (2011).** DNA interaction and DNA cleavage studies of a new platinum (II) complex containing aliphatic and aromatic dinitrogen ligands. *Bioinorganic Chemistry and Applications*, *2011*.

**Shamma, M. (1972).** The Isoquinoline Alkaloids, New York and London. *Academic Press*, *81*, 335–341.

**Singh, S. (2002).** Refractive index measurement and its applications. *Physica Scripta*, *65*(2), 167.

**Sliwoski, G., Kothiwale, S., Meiler, J., & Lowe, E. W. (2014).** Computational methods in drug discovery. *Pharmacological Reviews*, *66*(1), 334–395.

**Smaoui, S., Hsouna, A. Ben, Lahmar, A., Ennouri, K., Mtibaa-Chakchouk, A., Sellem, I., Najah, S., Bouaziz, M., & Mellouli, L. (2016).** Bio-preservative effect of the essential oil of the endemic Mentha piperita used alone and in combination with BacTN635 in stored minced beef meat. *Meat Science*, *117*, 196–204.

**Sonboli, A., Gholipour, A., & Yousefzadi, M. (2012).** Antibacterial activity of the essential oil and main components of two Dracocephalum species from Iran. *Natural Product Research*, *26*(22), 2121–2125.

**T**

**Tandukar, S., Kwon, E., & Kim, D. Y. (2023).** Structural insights into the regulation of peptidoglycan DL-endopeptidases by inhibitory protein IseA. *Structure*, *31*(5), 619–628.

**Telfer, E., Graham, N., Stanbra, L., Manley, T., & Wilcox, P. (2013).** Extraction of high

purity genomic DNA from pine for use in a high-throughput genotyping platform. *New Zealand Journal of Forestry Science*, *43*(1), 1–8. https://doi.org/10.1186/1179-5395-43-3

**Tu, T., Rendleman, C. A., Borhani, D. W., Dror, R. O., Gullingsrud, J., Jensen, M. O., Klepeis, J. L., Maragakis, P., Miller, P., Stafford, K. A., & Shaw, D. E. (2008).** A scalable parallel framework for analyzing terascale molecular dynamics simulation trajectories. *2008 SC - International Conference for High Performance Computing, Networking, Storage and Analysis, SC 2008*, 1–12. https://doi.org/10.1109/SC.2008.5214715

**Tyagi, P., Singh, M., Kumari, H., Kumari, A., & Mukhopadhyay, K. (2015).** Bactericidal Activity of Curcumin I Is Associated with Damaging of Bacterial Membrane. *PLOS ONE*, *10*(3), 1–15. https://doi.org/10.1371/journal.pone.0121313.

**V**

**Valarezo, E., Rosales, J., Morocho, V., Cartuche, L., Guaya, D., Ojeda-Riascos, S., Armijos, C., & González, S. (2015).** Chemical composition and biological activity of the essential oil of Baccharis obtusifolia Kunth from Loja, Ecuador. *Journal of Essential Oil Research*, *27*(3), 212–216.

**W**

**W., A. P. (1998).** Physical Chemistry, 6th edition. Oxford University Press. *Chem. Soc. Rev.*, *41*(2), 753. http://xlink.rsc.org/?DOI=C1CS15191F.

**Wang, E., Fu, W., Jiang, D., Sun, H., Wang, J., Zhang, X., Weng, G., Liu, H., Tao, P., & Hou, T. (2021).** VAD-MM/GBSA: a variable atomic dielectric MM/GBSA model for improved accuracy in protein–ligand binding free energy calculations. *Journal of Chemical Information and Modeling*, *61*(6), 2844–2856.

**Wang, H. W., Bringans, C., Hickey, A. J. R., Windsor, J. A., Kilmartin, P. A., & Phillips, A. R. J. (2021).** Cyclic Voltammetry in Biological Samples: A Systematic Review of Methods and Techniques Applicable to Clinical Settings. *Signals*, *2*(1), 138–158. https://doi.org/10.3390/signals2010012

**Wang, M., Guo, Q., Zhu, K., Fang, B., Yang, Y., Teng, M., Li, X., & Tao, Y. (2020).** Interface switch mediates signal transmission in a two-component system. *Proceedings of the National Academy of Sciences of the United States of America*, *117*(48), 30433–30440. https://doi.org/10.1073/pnas.1912080117

**Wang, R., Fu, Y., & Lai, L. (1997).** A new atom-additive method for calculating partition

coefficients. *Journal of Chemical Information and Computer Sciences*, *37*(3), 615–621.

**Wang, S. Y., & Chen, C.-T. (2010).** Effect of allyl isothiocyanate on antioxidant enzyme activities, flavonoids and post-harvest fruit quality of blueberries (Vaccinium corymbosum L., cv. Duke). *Food Chemistry*, *122*(4), 1153–1158.

**Whitlock, R., Hipperson, H., Mannarelli, M., & Burke, T. (2008).** A high-throughput protocol for extracting high-purity genomic DNA from plants and animals. *Molecular Ecology Resources*, *8*(4), 736–741. https://doi.org/10.1111/j.1755-0998.2007.02074.x.

**Y**

**Yang, Y., Yao, K., Repasky, M. P., Leswing, K., Abel, R., Shoichet, B. K., & Jerome, S. V. (2021).** Efficient exploration of chemical space with docking and deep learning. *Journal of Chemical Theory and Computation*, *17*(11), 7106–7119.

**Z**

**Zhao, G.-C., Zhu, J.-J., Zhang, J.-J., & Chen, H.-Y. (1999).** Voltammetric studies of the interaction of methylene blue with DNA by means of β-cyclodextrin. *Analytica Chimica Acta*, *394*(2–3), 337–344.

# *Annexes*

**Annexes :**

- **Continue to Essential Oils Extraction :**




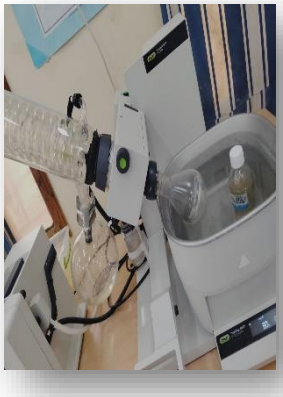

- **Continue to DNA Extraction :**